A Study on the Buckling Strength of Offshore Pipeline Subjected to Bending and External Pressure

ハルトノ, ユド

https://doi.org/10.15017/1470590

出版情報：九州大学, 2014, 博士（工学）, 課程博士
バージョン：

A Study on the Buckling Strength of Offshore Pipeline Subjected to Bending and External Pressure

Kyushu University
2014

Hartono Yudo

九州大学

Kyushu University

Graduate School of Engineering

Department of Marine System Engineering

A Study on the Buckling Strength of Offshore Pipeline Subjected to Bending and External Pressure

By:

Hartono Yudo

Under Supervision of:

Professor Takao YOSHIKAWA

A Thesis Submitted to the Graduate Studies Office in Fulfilment of the Requirements for the Degree of Doctor of Philosophy in Marine System Engineering at Kyushu University, Fukuoka, Japan

July 2014

Certificate

The undersigned reviewing committee members hereby certify that **Hartono Yudo** defended his thesis entitled "**A Study on the Buckling Strength of Offshore Pipeline Subjected to Bending and External Pressure**" on July 2014 and the thesis was accepted in fulfilment of the requirement for the degree of Doctor of Philosophy at Kyushu University.

Takao YOSHIKAWA

(Professor at Faculty of Engineering, Kyushu University)

Hiroyuki KAJIWARA

(Professor at Faculty of Engineering, Kyushu University)

Koji GOTOH

(Associate Professor at Faculty of Engineering, Kyushu University)

Acknowledgements

First of all, I am deeply grateful to the supervisor Prof. Takao YOSHIKAWA for all his support, patience, kindness advices, continuous encouragement and invaluable guidance throughout my doctoral study at Kyushu University. Indeed, I feel very happy and fortunate to know him and learn how to perform a good research.

I am also very grateful to Prof. Hiroyuki KAJIWARA and Associate Prof. Koji GOTOH for serving on my thesis committee and taking their time and energy to appraise my thesis.

I would also like to express my appreciation towards Associate Prof. Yukitaka YASUZAWA, Assistant Prof. Masahiro MAEDA, Mr. Koji MURAKAMI and all members at Structural Engineering Laboratory of Ships and Marine Systems, for their kind assistance, many interesting discussions, friendliness and availability. They make me really enjoy working on this PhD project.

I am gratefully acknowledges the support of the International Special Course on Environment Systems Engineering, sponsored by the Japanese Ministry of Education, Culture, Sports, Science and Technology.

I would like to thank the Indonesian Directorate General of Higher Education (DGHE), Ministry of National Education, for supporting my doctoral study through granting a scholarship.

Finally, I would like to dedicate this thesis to my wife, my children and my family in Indonesia. It was because of their everlasting love and encouragements that I could pursue my study at Kyushu University.

Abstract

Seabed pipelines are a part of the infrastructure of all offshore oil or gas fields. As well as straight pipes, curved ones are also used in an actual pipeline. In designing such a pipeline, it is important to know the buckling strength of the pipe under various kinds of loads. Buckling strength under axial compression has been investigated by many researchers and an accurate formula has been presented, but the accurate formula for the buckling strength under bending load has not been presented up to now.

It is well known that the buckling moment will be reduced by increasing the pipe's length. In the case of the long pipe, the cross sectional oval deformation takes place much and the buckling strength of pipe is reduced due to this deformation. However, comprehensive studies for the buckling strength of straight and curved pipe under bending are still limited. In this research, the previous research for the buckling strength of pipe under bending moments was firstly reviewed.

Secondly, the linear buckling strength for pipe under pure bending was investigated by linear *FEA*. The eigenvalue calculations under bending load was performed for various lengths, radiuses and thicknesses of pipe. The linear buckling strength was compared with the previously proposed formula which was derived from the buckling strength of pipe under axial compression.

Thirdly, the buckling phenomenon for a straight pipe under a pure bending moment was investigated by nonlinear *FEA,* considering the effect of a cross sectional oval deformation by changing the dimensions of the pipes, that is, the length-to-diameter ratio *(L/D)* varying from about 2.5 to 20 and the diameter-to-thickness ratio *(D/t)* varying from about 50 to 200. The buckling phenomenon for curved pipe (D/t = 200) was also investigated

by changing the *R/D* from 50 to 200, where, *R* is the curvature radius of curved pipe. From the results of the calculations for the straight pipe, the reduction rate of the buckling moment due to the oval deformation of pipe was clarified for various values of *L/D* and *D/t*, not only in elastic buckling, but also in elasto-plastic buckling. And for the curved pipe, it was explained that the buckling moment will be reduced by lowering the value of *R/D*. To investigate the yielding effect on the buckling strength of the pipe in bending, the non-dimensional parameter $\beta = ((D/t)\ (\sigma_Y/E))$ was considered. The parameter of β is possibly the parameter which represents the yielding effect on the buckling strength of pipe under bending.

Fourthly, the effect of initial imperfection on the buckling strength of a straight pipe under bending has been investigated by nonlinear *FEA*, considering the effect of a cross sectional oval deformation by changing the variables of pipes, that is, *L/D* varying from about 2.5 to 20 and *D/t* varying from about 50 to 200. Furthermore the buckling strength of curved pipes (*D/t* = 200) have also been investigated by changing *R/D* from 50 to 200. Not only elastic buckling but also elasto-plastic buckling was investigated. From the numerical results, the following was found. The buckling strength reduced more in longer pipes than shorter pipes due to pre-buckling oval deformation. But, the reduction of buckling strength due to imperfection is greater in shorter pipes than in longer pipes. Moreover, buckling strength reduces more by the imperfection of buckling mode than by that of oval mode. The effect of imperfection on buckling strength in the plastic region was smaller than in the elastic region. The buckling moment of curved pipes reduces more when the curvature of pipe increases in both original and imperfect pipes, especially for longer pipes. Similarly for a perfect pipe, to investigate the yielding effect on the buckling strength of an imperfect pipe in bending, the non-dimensional parameter (β) was considered.

Finally, the buckling strength of pipe under pure bending and external pressure has been investigated by nonlinear *FEA*. Not only elastic buckling but also elasto-plastic buckling was investigated. From the numerical results, the following was found. The reductions of buckling strength due to external pressure will decrease with increasing *L/D* and become constant on the long pipe. For a straight pipe with $D/t \geqq 35$ and $\sigma_Y = 621$MPa under external pressure, the buckling strength occurs in the elastic region. Therefore, although the ratio of linear buckling pressure to initial yielding pressure, $\alpha = (P_{cr}/P_Y)$ is proportionate to $(D/t)^2(\sigma_Y/E)$, the non-dimensional parameter (β), which is proportionate to $(D/t)(\sigma_Y/E)$ is considered to investigate the yielding effect on the buckling strength of pipe under combined loading of bending and external pressure as well as under bending. Using the non-dimensional parameter (β), the yielding effect on the buckling strength of pipe subjected to bending and external pressure was investigated. The interaction curves of the buckling strength of pipe with various *D/t* under combination loads of external pressure and bending moment were obtained. Straight pipes, with length-to-diameter ratio *(L/D)* varying from 2.5 to 40, diameter ranging from 1000 to 4000 mm, and with diameter-to-thickness ratio *(D/t)* varying from about 50 to 200, and curved pipes (D/t = 200 , L/D varying 2.5 to 30) have been investigated by changing *R/D* from 50 to 200, respectively.

Table of Contents

Acknowledgements………………………………………………………………….. i

Abstract….……………………………………………………………………… ii

Table of Contents……………………………………………………………….. v

List of Figures ………………………………………………………………….. ix

List of Tables………. ………………………………………………………….. xiv

Nomenclature………………………………………………………………….. xv

Chapter I. Introduction

1.1 Overview…….……………………………………………………………. 1

1.1.1 Geography of Indonesia……..……….…………………………….. 1

1.1.2 Offshore pipelines……..…………………………………………… 3

1.2 Literature Review………………………………………………………. 7

1.2.1 The theoretical moment-curvature relationship (M-Φ relation)..... 7

1.2.2 The buckling strength of pipe under bending………………….... 14

1.2.3 The buckling strength of pipe under external pressure..………..... 19

1.2.4 The buckling strength of pipe under combined loading ………... 20

1.3 Research Scope and Objective….………………………………………… 21

1.4 Outline of Dissertation….………………………………………………… 22

Chapter II. The Linear Buckling Strength of Pipe under Pure Bending

2.1 Introduction……..……………………………………………………….. 24

2.2 Procedures of Calculation for Estimating Linear Buckling Strength of Pipe under Bending………………………………………………………… 25

2.2.1 Model for calculation……………………………………….. 25

2.2.2 Program name….………………………………………………. 25

2.2.3 Element mesh for analysis……..………………………………….. 25

2.2.4 Boundary conditions…………………………………………… 26

2.2.5 The loading conditions..……………………………………… 27

2.3 The Numerical Results on Linier Buckling Strength of Pipe under Bending 28

2.4 Discussion……..…………………………………………………….. 29

2.5 Conclusions……...………………………………………………….. 32

Chapter III. The Nonlinear Buckling Strength of Straight and Curved Pipe under Pure Bending

3.1 Introduction……...………………………………………………….. 34

3.2 Procedures of Calculation for Estimating Nonlinear Buckling Strength of Pipe under Bending …..……………………..………………………. 36

3.2.1 Parameters for calculation………………………………………. 36

3.2.2 Model for calculation and calculation program…………………. 37

3.2.3 Boundary conditions and loading conditions..…………………. 38

3.2.4 Method to obtain bifurcation moment in nonlinear calculation…. 39

3.3 Numerical Results……..……………………………………………………. 40

3.3.1 The numerical results on nonlinear buckling strength of straight pipe under pure bending………………………………………. 42

3.3.2 The numerical results on nonlinear buckling strength of curved pipe under pure bending…………………………………………. 54

3.4 Conclusions……...………………………………………………………. 64

Chapter IV. The Effect of Initial Imperfection on Buckling Strength for Straight and Curved Pipe under Pure Bending Load

4.1 Introduction………………………………………………………………. 66

4.2 Procedures of Calculation for Estimating Nonlinear Buckling Strength of Imperfect Pipe under Bending ….………………………..………... 67

4.2.1 Parameters for calculation……..…………………………….……. 67

4.2.2 Model for calculation and calculation program………..………. 68

4.2.3 Boundary conditions and loading conditions.…………………. 69

4.2.4 Method to obtain bifurcation moment in nonlinear calculation… 69

4.3 The Numerical Results on Nonlinear Buckling Strength of Imperfect Straight Pipe under Pure Bending……..…………………………………. 70

4.4 The Numerical Results on Nonlinear Buckling Strength of Imperfect Curved Pipe under Pure Bending……..…………………………………. 84

4.5 Conclusions……….……………………………………………………. 95

Chapter V. Buckling Strength of Pipe under Bending and External Pressure

5.1 Introduction………………………………………………………………. 97

5.2 Procedure of Calculation for Estimating Nonlinear Buckling Strength of Pipe under Bending and External Pressure….…………………………. 98

5.2.1 Parameters for calculation…….……………………………………. 98

5.2.2 Model for calculation and calculation program…………………. 98

5.2.3 Boundary conditions and loading conditions….…………………. 99

5.3 The Numerical Results on Nonlinear Buckling Strength of Straight Pipe under Bending and External Pressure….……………………..…………... 100

5.4 The Numerical Results on Nonlinear Buckling Strength of Curved Pipe under Bending and External Pressure……………………………………. 105

5.5 Conclusions……..…………………………………………..…………. 107

Chapter VI. Conclusions

6.1 Summary………………………………………………………………. 109

6.2 Recommendation for Future Work………………………………………. 112

References.....……………………………………………………………………….. 114

List of Figures

Figure	Title	Page
Figure 1-1	Geography of Indonesia……………………………………………………….	1
Figure 1-2	The map of Natuna gas field map………………………………………..	2
Figure 1-3	Uses of offshore pipelines………..…………………………..…………	3
Figure 1-4	S-Lay method…..…………………………………………………………	5
Figure 1-5	J-Lay method…..…………………………………………………………	6
Figure 1-6	Reel-Lay method…………………………………………………………	6
Figure 1-7	Pipe in operating condition subjected a combination of functional and environmental loads…….……………………………………………………	7
Figure 1-8	Pure bending of a thin – walled tubular beam segment..…………………	7
Figure 1-9	Thin-walled tubular section under pure bending…………………….......	8
Figure 1-10	Elastic - plastic state of section..………………………………………	9
Figure 1-11	Moment - curvature relationship for perfect thin-walled tubular section..	13
Figure 1-12	Moment-curvature response and deformation process of pipe subjected to bending….………………………………………………………………….	14
Figure 2-1	The schematic view of a pipe under bending moment……………...…	25
Figure 2-2	Boundary condition at mid span of cylinder……………………………..	27
Figure 2-3	*FEA* model for full pipe in linear analysis……………………………......	27
Figure 2-4	Buckling modes of pipe under pure bending in linear analysis….……….	28
Figure 3-1	Schematic view of a pipe in bending and the oval deformation which takes place at mid span…….………………………………………………	35
Figure 3-2	The geometry of a curved pipe….……………………………………….	37
Figure 3-3	Finite element model for straight pipe in non-linear analysis. ………….	38
Figure 3-4	Geometry for (a) straight pipe and (b) curved pipe……….……………....	39

Figure 3-5 Schematic diagram for estimation of bifurcation moment……………… 40

Figure 3-6 Buckling modes of pipe (*D/t* = 200, *L/D* = 2.5) under pure bending:
(a) the straight pipe and (b) the curved pipe *R/D* = 50………………..… 41

Figure 3-7 Relationship between buckling moment and *L/D* for pipe under pure
bending in elastic analysis………………..……………........................... 42

Figure 3-8 Ovalization at the mid span for straight pipe (*D/t* = 200) in elastic analysis 44

Figure 3-9 Ovalization at the mid span for straight pipe (*D/t* = 200)………………… 44

Figure 3-10 Relationships between ovalization and position from pipe end
(for cylinder with *L/D* = 20, at just before buckling)……………………… 46

Figure 3-11 Relationship between Buckling moment and *L/D* for straight pipe
σ_Y = 621 MPa………..……………………………………………………. 48

Figure 3-12 Relationship between Buckling moment and *D/t* for straight pipe
σ_Y = 621 MPa….……………………………………………………….. 51

Figure 3-13 Relationship between Buckling moment and *L/D* for straight pipe
in elasto-plastic analysis…………………………………………………. 53

Figure 3-14 Distribution of oval deformation along the pipe length for curved pipe
(*L/D* = 20, *D/t* = 200), σ_Y = 621 MPa ………………………………….. 55

Figure 3-15 The mechanism of oval deformation due to axial stresses in curved pipe
under bending……………………………………………………………. 56

Figure 3-16 Ovalization at the mid span for curved pipe
(*L/D* = 20, *D/t* = 200) in elastic analysis…………………………………. 56

Figure 3-17 Ovalization at the mid span for curved pipe
(*L/D* = 20, *D/t* = 200, σ_Y = 621 MPa)……………………………………. 57

Figure 3-18 Relationship between buckling moment and *L/D* for curved pipe
(*D/t* = 200, σ_Y = 621 MPa)……………………………………………… 59

Figure 3-19 Relationship between buckling moment and *R/D* for curved pipe
(D/t = 200, σ_Y = 621 MPa)…………………………………………………. 62

Figure 3-20 Relationship between Buckling moment and *L/D* for curved pipe
in elasto-plastic analysis (R/D = 200)……………………………………. 63

Figure 4-1 Finite element modelling for full imperfect Pipe
(a) the straight pipe, (b) the curved pipe…………………………………. 68

Figure 4-2 Mid span section & *RBE* at both end section…..………………………… 69

Figure 4-3 Relationships between the applied moment and oval deformation at the mid span for the perfect pipe and the imperfect pipe *in* elastic analysis
(imperfection of buckling mode δ_o/t = 0.05, D/t = 200)………………... 71

Figure 4-4 Deformation just before buckling at the mid span for original straight pipe, (a) L/D = 2.5, (b) L/D = 20 (in elastic analysis, D/t = 200)….……… 71

Figure 4-5. Deformation just before buckling at the mid span for straight pipe with imperfection of buckling mode, δ_o/t = 0.05 (a) L/D = 2.5, (b) L/D = 20
(in elastic analysis, D/t = 200)…..…………………………………….. 72

Figure 4-6 Relationships between the buckling moment and *L/D* for original straight pipe and pipe with imperfection of buckling mode
δ_o/t = 0.05 σ_Y = 621 MPa ……………………………………………….. 74

Figure 4-7 Relationship between the maximum buckling moment and the imperfection of buckling mode for straight pipe
(in elastic analysis, D/t = 200) …………………………………………… 75

Figure 4-8 Relationship between the maximum buckling moment and the imperfection of buckling mode for straight pipe
(in elastic analysis, L/D = 2.5)……………………………………………. 77

Figure 4-9 Ovalization at the mid span for straight pipe

(L/D = 2.5 and D/t = 50 ~ 200) in elastic analysis………………………... 78

Figure 4-10 Relationship between the maximum buckling moment and the imperfection of buckling mode for straight pipes (L/D = 2.5) in elasto-plastic analysis ………………………………………………… 80

Figure 4-11 Relationship between the maximum buckling moment and the imperfection of buckling mode for straight pipes (L/D = 20) in elasto-plastic analysis…………………………………………………... 81

Figure 4-12 Relationships between the buckling moment and L/D by changing the mode of imperfection for straight pipe (D/t = 200, δ_o/t = 0.2 σ_Y = 621 MPa) …………………………………... 83

Figure 4-13 Relationships between the applied moment and oval deformation at the mid span for the perfect pipe and the imperfect pipe in elastic analysis (imperfection of buckling mode δ_o/t = 0.05, D/t = 200 , R/D = 200) …… 85

Figure 4-14 Oval deformation at the mid span for original pipe, (a) L/D = 2.5, (b) L/D = 20 (in elastic analysis, curved pipe, D/t = 200, R/D = 200)…… 85

Figure 4-15 Oval deformation at the mid span for pipe with imperfection of buckling mode δ_o/t = 0.05 (a) L/D = 2.5, (b) L/D = 20 (in elastic analysis, curved pipe D/t = 200, R/D = 200)……………………. 86

Figure 4-16 Relationship between buckling moment and L/D for original curved pipe and pipe with imperfection of buckling mode δ_o/t = 0.05 (in elastic analysis, D/t = 200)………….……………………………………. 89

Figure 4-17 Relationship between buckling moment and L/D for curved pipe with imperfection of buckling mode δ_o/t = 0.05 (σ_Y = 621 MPa, D/t = 200)…….…………………………………………. 90

Figure 4-18 Relationship between maximum buckling moment and imperfection of buckling mode for curved pipe (in elastic analysis, *D/t* = 200, *R/D* = 200) 91

Figure 4-19 Relationship between maximum buckling moment and imperfection of buckling mode for curved pipe (in elastic analysis, *D/t* = 200, L*/D* = 2.5) 92

Figure 4-20 Relationship between maximum buckling moment and imperfection for curved pipe (*R/D* = 200, *L/D* = 2.5) in elasto-plastic analysis ………. 93

Figure 4-21 Relationship between maximum buckling moment and imperfection for curved pipe (*D/t* = 200, *L/D* = 20) in elasto-plastic analysis, ………… 94

Figure 5-1 Boundary conditions of pipe under combined loading of bending and external pressure………………………………………. 99

Figure 5-2 The applied load vector of uniform external pressure …………………… 100

Figure 5-3 Relationship between non-dimensional pressure and *L/D* for straight pipe (*D/t* = 50~200) in elastic analysis ………………………………………. 101

Figure 5-4 Moment - pressure interaction stability for straight pipe in elastic analysis (*L/D* = 30)……….……………………………………..……………… 102

Figure 5-5 Moment - pressure interaction stability for straight pipe in elasto-plastic analysis (*L/D* = 30)…….…………………………………… 103

Figure 5-6 Moment - pressure interaction stability for straight pipe in elasto-plastic analysis by using parameter β (*L/D* = 30) …………..... 104

Figure 5-7 Relationship between non-dimensional pressure and *L/D* for curved pipe (*D/t* = 200) in elastic analysis……………………………………………. 105

Figure 5-8 Moment - pressure interaction stability for curved pipe in elastic analysis (*L/D* = 30)……………………………………………………………… 106

Figure 5-9 Moment - pressure interaction stability for curved pipe in elasto-plastic analysis (*L/D* = 30)……………………………………… 107

List of Tables

Table	Title	Page
Table 2-1	The parameters of calculation on linear buckling strength of pipe under pure bending…………………………………………………………………	26
Table 2-2	The numerical results of linear buckling strength by MSC Nastran……….	30
Table 2-3	The numerical results of linear buckling strength by MSC Nastran for pipe *D/t* = 200, *L/D* = 20……….…..	31
Table 3-1	The parameters for calculating the nonlinear buckling strength of straight pipe under pure bending…… ………………………………….	36
Table 3-2	The parameters for calculating the nonlinear buckling strength of a curved pipe under pure bending……..………………………………..	37
Table 3-3	The mesh convergence study in MSC Marc……………………………….	41
Table 3-4	The nonlinear buckling moment in elastic and elasto-plastic analysis…….	49

Nomenclature

A : Area of the cross section of the tube

D : Pipe diameter.

E : Young's modulus.

$$E' = \frac{E}{(1-v^2)}$$

$I_{x\text{-}el}$: Moment of inertia of the elastic part about the bending axis (x-axis).

L : Length of pipe.

M : Applied moment.

M_b : Buckling moment obtained by nonlinear calculation in elastic analysis.

M_{cr} : Critical bending moment.

M_{cr1} : Critical bending moment, when the critical buckling stress of a cylinder under bending is same as the buckling stress of a cylinder under axial compression.

M_{cr2} : Critical bending moment, results from MSC Nastran

M_{cr3} : Critical bending moment by Timoshenko

M_o : Maximum moment in elastic analysis without imperfection.

M_p : Ultimate (plastic) moment.

M_u : Ultimate moment in elasto-plastic analysis.

M_Y : Initial yield moment.

M_{max} : Maximum bending moment

P : Applied pressure.

P_{cr} : Critical pressure.

P_Y : Initial yield pressure

r : Pipe radius.

R, ρ : Radius of curvature in curved pipe.

t : Wall thickness.

$y_{0.I}$: Distance from the centroid of Zone I to the x-axis

x,y,z : Cartesian coordinat

$\overline{m}$: M/Mp

α : Parameter $\alpha = (D/t)^2(\sigma_Y/E)$

β : Parameter $\beta = (D/t)(\sigma_Y/E)$

ϕ	: Curvature normalized by the yield curvature of the cross section
Φ	: Curvature
Φ_Y	: Initial yield curvature
Θ, Ψ	: Angle
ϵ	: Strain
ϵ_Y	: Initial yield strain
δ	: Amplitude of oval deformation.
δ_o	: Maximum amplitude of imperfection.
ν	: Poisson’s ratio.
σ_{cr}	: Critical buckling stress under axial compression.
σ_Y	: Yield stress.
M_b/M_{cr1}	: Non-dimensional buckling moment in elastic analysis.
M_u/M_Y	: Non-dimensional buckling moment in elasto-plastic analysis.

Chapter I

Introduction

1.1 Overview

1.1.1 Geography of Indonesia

Indonesia is an archipelago in the region of Southeast Asia. It lies between latitudes 11°S and 6°N and longitudes 95°E and 141°E and has 17,508 islands scattered over both sides of the equator. The largest islands are Sumatra, Java, Bali, Kalimantan (Indonesia's part of Borneo), Sulawesi, the Nusa Tenggara islands, the Moluccas Islands, and Irian Jaya (the western part of New Guinea).

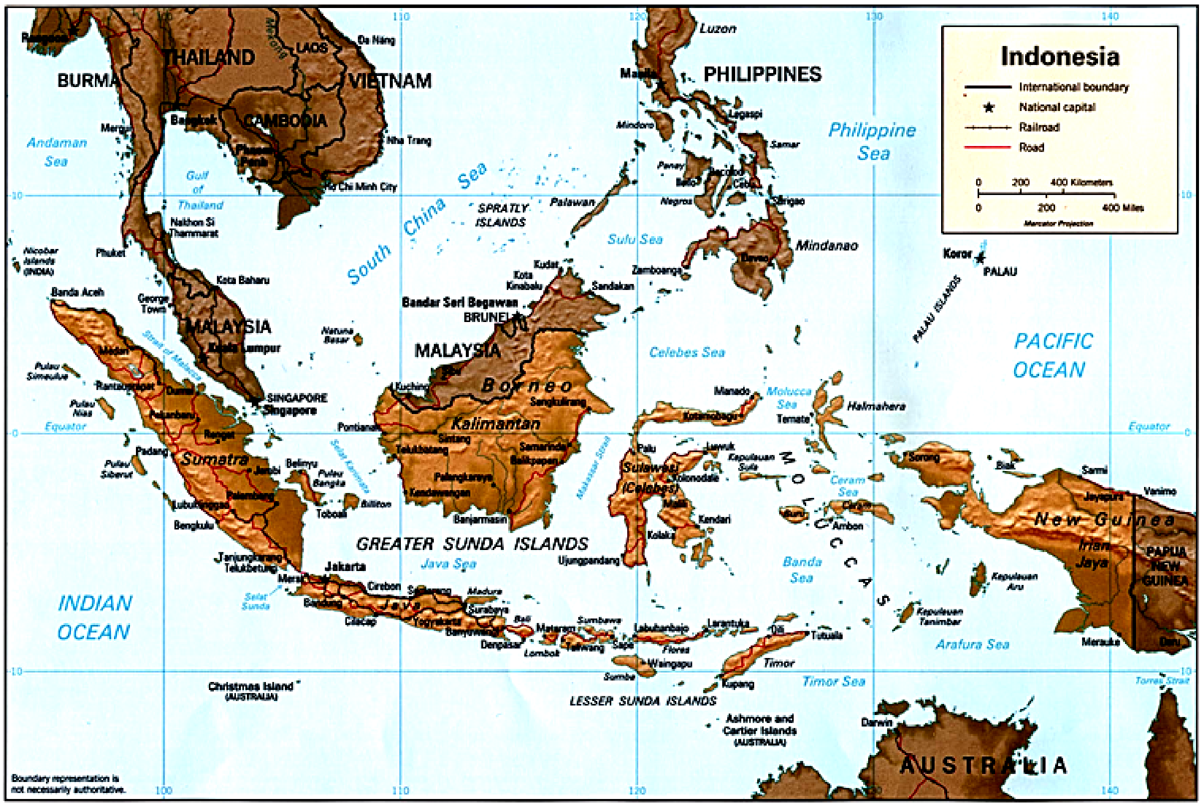

Figure 1-1. Geography of Indonesia

(www.lib.utexas.edu/maps/indonesia.html)

Figure 1-1 shows that Indonesia shares land borders with Malaysia on Borneo, Papua New Guinea on the island of New Guinea, and East Timor on the island of Timor. Moreover, Indonesia also shares maritime borders with Singapore, Malaysia, Philippines, and Palau to the north and Australia to the south. Indonesia is the world's 16th-largest country in terms of land area with 1,919,440 square kilometres of land, and world's 7th-largest country in terms of combined sea and land area.

Indonesia is rich in mineral resources such as natural gas and petroleum. Therefore, it has been one of the world’s leading exporters of Liquefied Natural Gas (LNG) after Qatar, the majority of which is derived from the seabed. One of the biggest sources is the Natuna gas field as shown in Figure 1-2.

Figure 1-2. The map of Natuna gas field map
(http://www.offshore-technology.com/projects/natuna/)

The Natuna gas fields deliver gas to Singapore via a pipeline. This transportation system is one of the world's longest subsea gas pipelines, delivering 3.4 billion cubic metres annually. Furthermore, Malaysia began importing gas from the Natuna Sea in mid-2003 however, unfortunately a pipeline linking East Natuna with Sarawak and the Philippines is unlikely to be built in the near future due to concerns about expense and security. Other possibilities include linking gas grids from Thailand to China via an offshore pipeline from a hub at the Natuna gas field. The alternative version would only link Indonesia and China.

1.1.2 Offshore pipelines

In their article Guo, Song, Chacko and Ghalambor (2005) described offshore pipelines, which are a part of the infrastructure of any offshore oil or gas field. The pipelines seem to be the most suitable long-term solution for transporting fluids when the offshore hydrocarbon exploration and production activities expand into deep water. Figure 1-3 shows a pipeline built for applications such as support of oil and gas transportation that is:

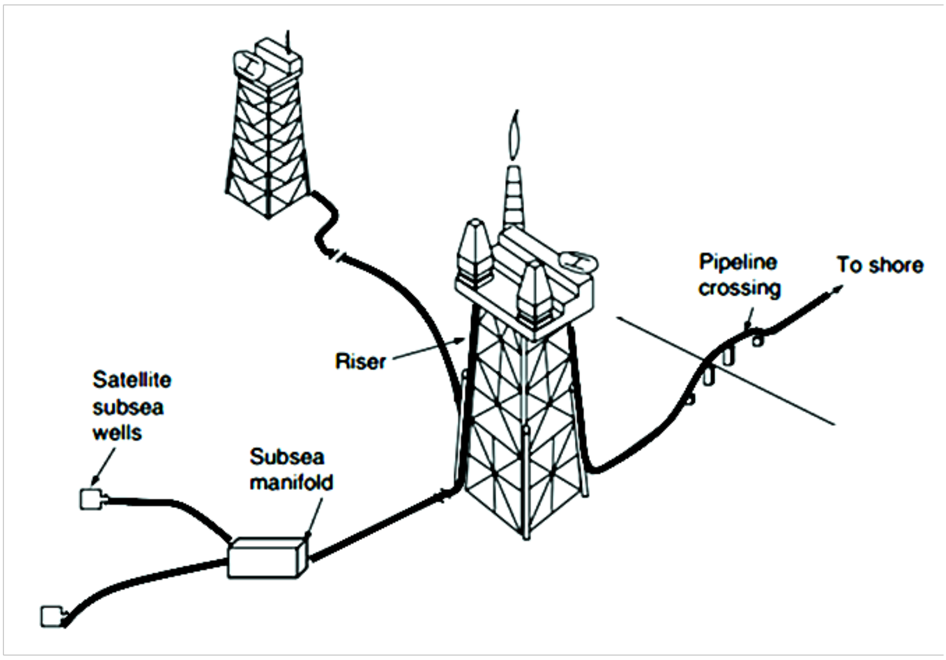

Figure 1-3. Uses of offshore pipelines

(Guo, B.et al. 2005)

- Transporting oil or gas from satellite subsea wells to subsea manifolds;
- Transporting oil or gas from subsea manifolds to production facility platforms;
- Transporting oil or gas between production facility platforms;
- Transporting oil or gas from production facility platforms to shore;
- Transporting water or chemicals from production facility platforms, through subsea injection manifolds, to injection wellheads.

On the installation of pipeline, a wide range of loads and environmental conditions should be considered. Marine pipelines are constructed by different methods. Kyriakides & Corona (2007) described the various methods for pipe laying as shown in Figures 1-4, 1-5 and 1-6, that are: S-lay, J-lay and reeling techniques, respectively. The name S-lay is taken from the suspended shape of the pipe at the end of the barge, which lays in an elongated "S" from the stringer to the seabed, while J-lay takes its name from the shape of the suspended pipe, which forms a "J" from the vessel to the seabed and then regarding reel-lay method, the pipe is assembled onshore and wound onto a large reel on the vessel. Furthermore, before being 'J-laid' in its final location it has to be unwound and straightened.

Buckling and collapse are one of important failure modes not only for laying condition but also for operating condition in a subsea position as shown in Figures 1-4 ~ 1-7. The pipeline will experience a combination of functional and environmental loads. Pipes should be safely operated. When a water pipeline suffers a leak, it can be a problem but it usually doesn't harm the environment. However, if a petroleum or gas pipeline leaks, it can cause an environmental disaster.

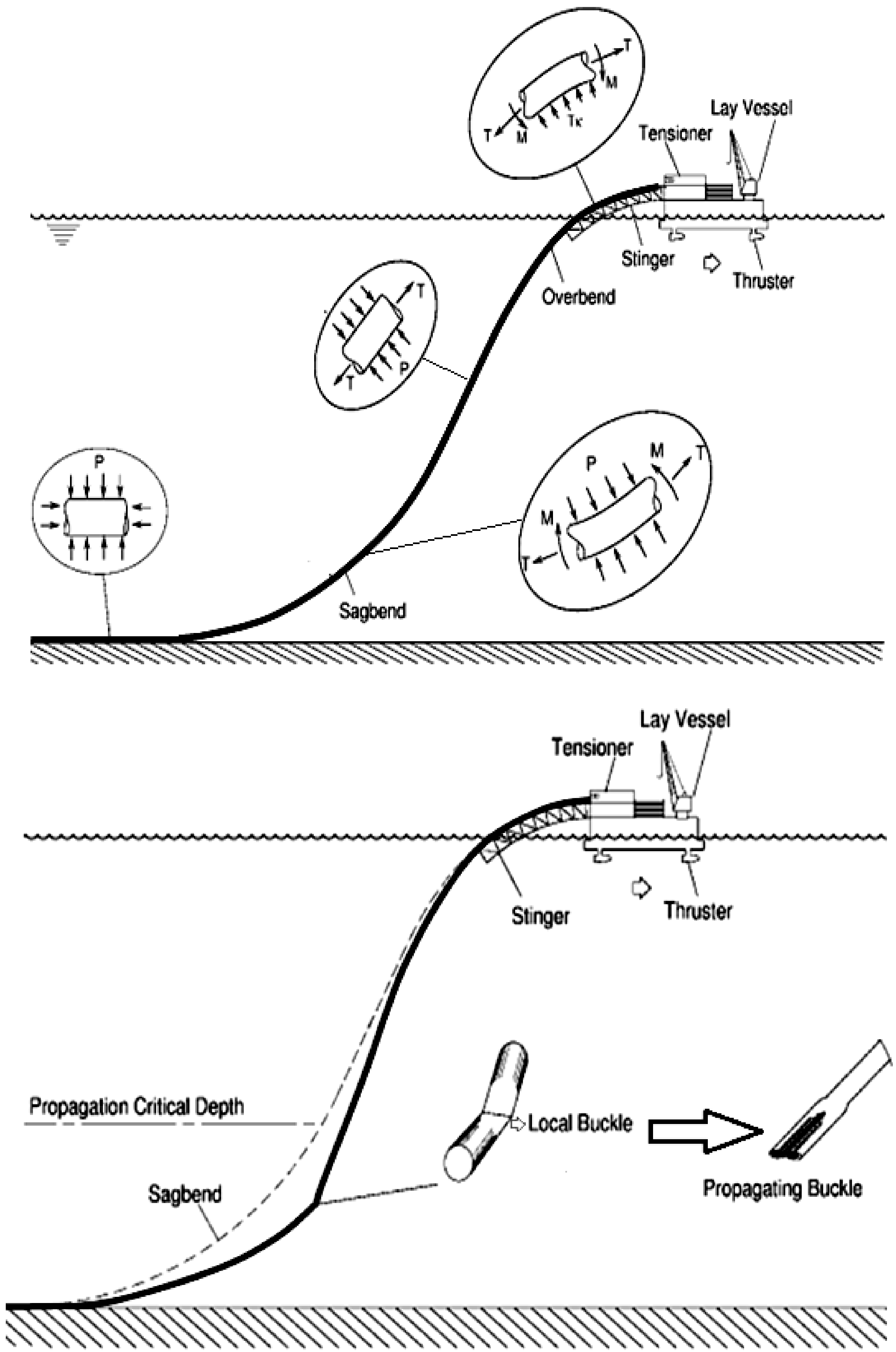

Figure 1-4. S-Lay method

(Mina, K. 2012)

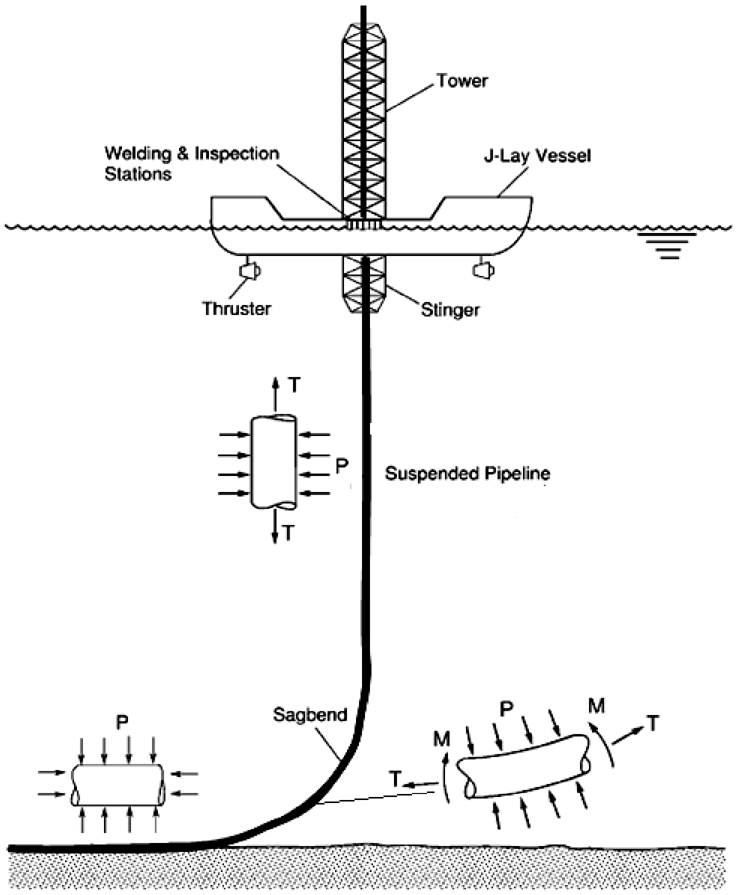

Figure 1-5. J-Lay method

(Mina, K. 2012)

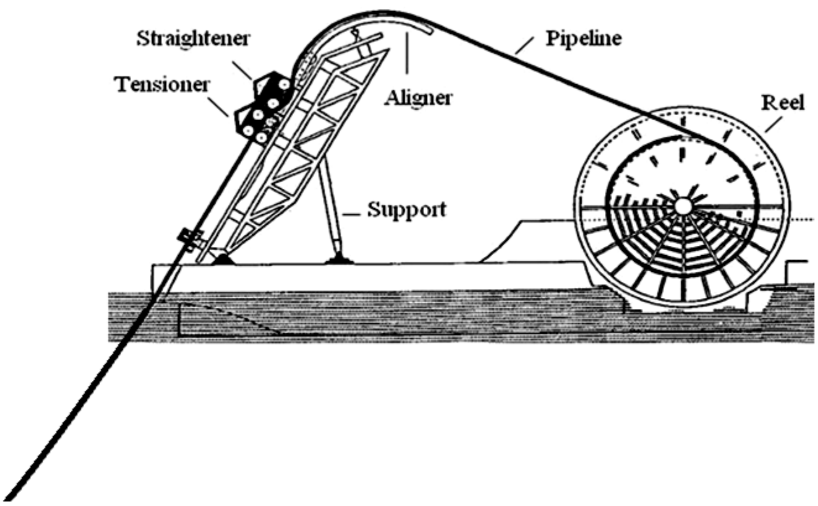

Figure 1-6. Reel-Lay method

(http://file.scirp.org)

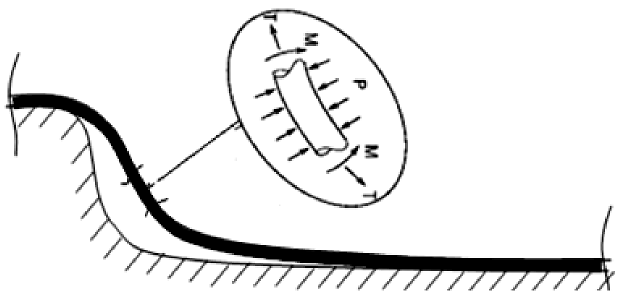

Figure 1-7. Pipe in operating condition subjected a combination of functional and environmental loads

1.2 Literature Review

1.2.1 The theoretical moment – curvature relationships (M – Φ relation)

Chen (1988) explained the analytical equations for the 'moment' - curvature relationships of a perfect circular tubular section are derived without considering the oval deformation.

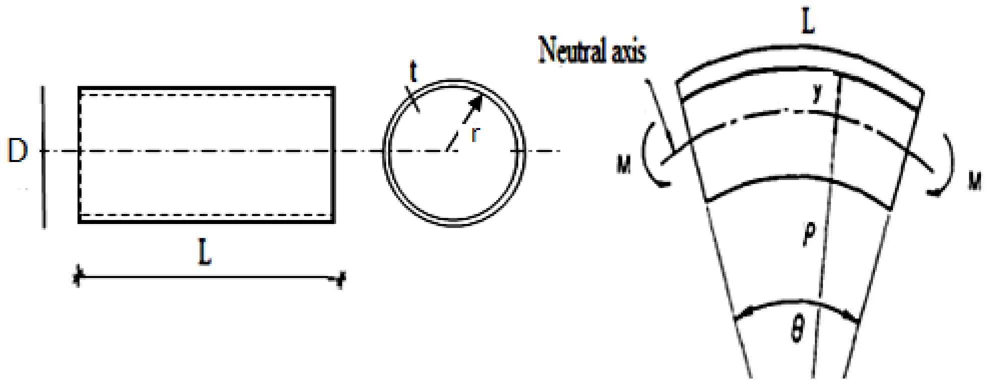

(a) (b)

Figure 1-8. Pure bending of a thin walled tubular beam segment
(Chen, et. al. 1988)

Figure 1-8 (a) shows the thin-walled tubular beam segment. *L* is length of thin-walled tubular beam, mean radius of cross section *r* and wall thickness *t*. When this beam segment is subjected to bending moment *M* at its ends, it will bend into an arc of radius ρ shown in Figure 1-8 (b). The central angle *Θ* and curvature *Φ* are related to *ρ* by the following relationships.

$$\theta = \frac{L}{\rho} \tag{1. 1}$$

$$\Phi = \frac{1}{\rho} \tag{1. 2}$$

Using assumption that after the deformation, the plane section would remain plane, furthermore, follows on from the assumption that shear deformation is negligible. Then, the length in longitudinal direction at a distance *y* from the neutral axis will be $(\rho+y)\Theta$; and the bending strain at this location will be given in the following equation:

$$\epsilon_Z = \frac{(\rho+y)\theta-\rho\theta}{\rho\theta} = \frac{y}{\rho} = \Phi y \tag{1. 3}$$

The initial yield curvature (the curvature at which $y = \pm r$ begins to yield) can be written as:

$$\Phi_Y = \frac{\epsilon_Y}{r} \tag{1. 4}$$

Where, ϵ_Y is the yield strain of the material.

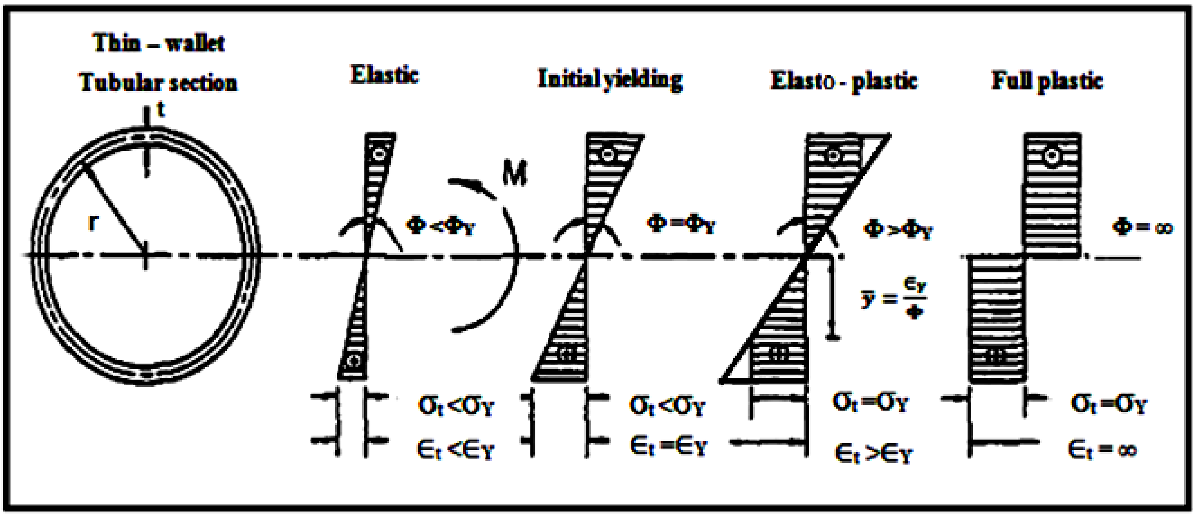

Figure 1-9. Thin-walled tubular section under pure bending
(Chen, et. al. 1988)

Under pure bending, the cylindrical tubular section can have two states shown in Figure 1-9 : the elastic state for $\Phi \leq \Phi_Y$, and then the elasto-plastic state for $\Phi > \Phi_Y$.

For the elasto-plastic state, the section is divided into the yielded zone and the elastic zone by the boundary defined by the angle Θ_0 as shown in Figure 1-10.

$$\Theta_0 = cos^{-1}\frac{\bar{y}}{r} \tag{1. 5}$$

Where, $\bar{y}$ = is given by:

$$\bar{y} = \pm\frac{\epsilon_Y}{\Phi} \tag{1. 6}$$

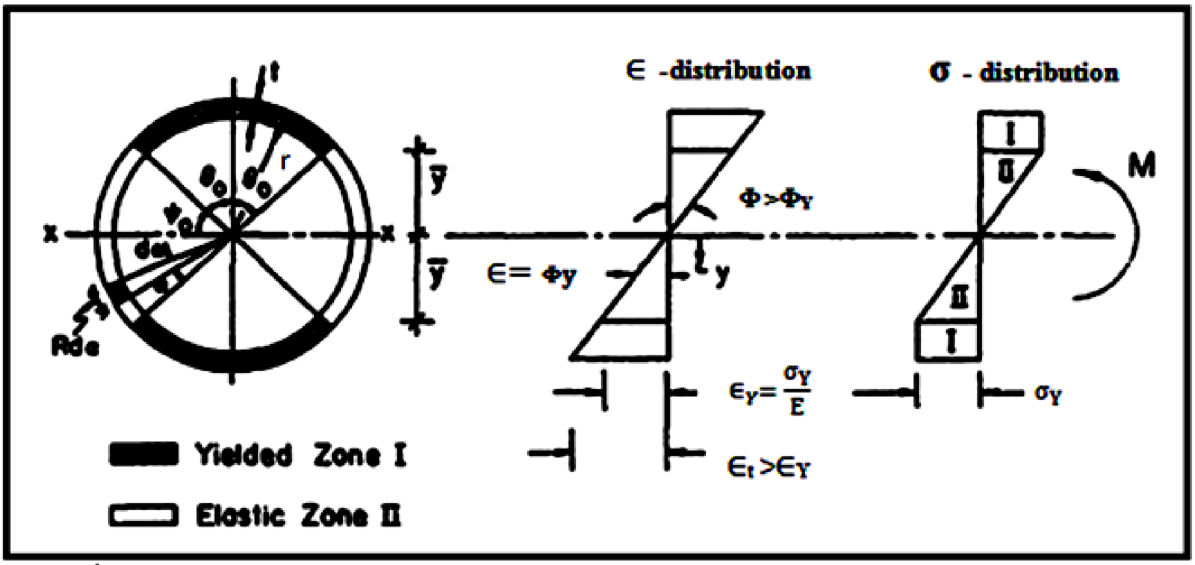

Figure 1-10. Elasto- plastic state of section
(Chen, et. al. 1988)

Substituting $\bar{y}$ from Eq. (1. 6), in Eq. (1. 5) and using Eq. (1. 4), we obtain:

$$\theta_0 = \cos^{-1}\frac{\Phi_Y}{\Phi} \tag{1. 7}$$

Assumed that the material is elastic-perfectly plastic and yield stress σ_Y, the stresses in the section are obtained from:

$$\begin{aligned} \sigma &= -\sigma_Y && (y \leq -\bar{y}) \\ \sigma &= E\Phi y && (-\bar{y} \leq y \leq \bar{y}) \\ \sigma &= \sigma_Y && (\bar{y} \leq y) \end{aligned} \tag{1. 8}$$

The bending moment in plastic zone (Zone I) is:

$$M_I = 2\sigma_Y [A_I y_{0.I}] \tag{1. 9}$$

Where A_I is area of Zone I = $2r\Theta_0 t$.

$y_{0.I}$ = distance from the centroid of Zone I to the x-axis, therefore sin $(90 - \Psi_0) = \cos \Psi_0$, then $y_{0.I}$ can be expressed as Eq. (1.10)

$$y_{0.I} = \frac{r sin\theta_0}{\theta_0} = \frac{r cos\Psi_0}{\theta_0} \tag{1. 10}$$

From Eq. (1. 10) substituting to Eq. (1. 9), we obtain:

$$M_I = 4\sigma_Y\, t\, r^2\, cos\Psi_0 \tag{1. 11}$$

The bending moment in elastic zone (Zone II) is:

$$M_{II} = \sigma_Y \frac{I_{x-el}}{\bar{y}} \tag{1. 12}$$

Where, I_{x-el} = moment of inertia of the elastic part about the bending axis (x-axis). For the thin-walled tubular section, the value of I_{x-el} can be approximated by the expression.

$$I_{x-el} = 2\int_0^{2\Psi_0} tr^2 sin^2(\Psi_0 - \alpha) r d\alpha \tag{1. 13}$$

Where α and Ψ_0 are defined in Figure 1-10, moreover I_{x-el} can be expressed as:

$$I_{x-el} = tr^3(2\Psi_0 - \ sin2\Psi_0) \tag{1. 14}$$

Substituting $\bar{y}$ = *r sin* Ψ_0 and I_{x-el} from Eq. (1. 14) into Eq. (1. 12), we obtain:

$$M_{II} = \sigma_Y tr^2 \frac{(2\Psi_0 - \ sin2\Psi_0)}{sin\Psi_0} \tag{1. 15}$$

Finally, the total bending moment *M*, which is the sum of M_I and M_{II}, can be expressed as:

$$M = \sigma_Y tr^2 \frac{(2\Psi_0 + sin2\Psi_0)}{sin\Psi_0} \tag{1. 16}$$

When, in the elastic state, σ_Y in Eq. (1. 16) becomes σ, and Ψ_0 must be equal to *π/2*. Therefore Eq. (1. 16) reduces to the following equation.

$$M = \pi\sigma t\mathrm{r}^2 \tag{1. 17}$$

Furthermore, Eq. (1. 16) can be non-dimensionalzed by defining:

$$\bar{m} = \frac{M}{M_p} \tag{1. 18}$$

$$\phi = \frac{\Phi}{\Phi_Y} \tag{1. 18'}$$

Where, Φ_Y has been already defined by Eq. (1. 4). M_p is the fully plastic moment capacity of the cross section and is given by:

$$M_p = 4\sigma_Y tr^2 \tag{1. 19}$$

Substituting Eq. (1. 7) in ' $\cos\theta_0 = \sin\Psi_0$', and using Eq. (1. 18), Ψ_0 can be shown as follow.

$$\Psi_0 = sin^{-1}(\cos\theta_0)$$

$$= sin^{-1}(\frac{\Phi_y}{\Phi})$$

$$= sin^{-1}\frac{1}{\phi} \tag{1. 20}$$

By combining Eq. (1. 17) with Eq. (1. 18) and (1. 19), and using $\sigma/\ \sigma_Y = Er\ \Phi/\ Er\ \Phi_Y = \phi$, the relationship between the non-dimensional moment and the curvature of the section in the elastic state ($\phi \leq 1$) can be expressed as;

$$\bar{m} = \frac{\pi}{4}\,\phi \tag{1. 21}$$

Substituting Ψ_0 to Eq. (1. 16), the relationships between the non-dimensional moment and the curvature for the elasto - plastic regime ($\phi \geq 1$) can be expressed as;

$$\bar{m} = \frac{\phi}{4}\left[2sin^{-1}\left(\frac{1}{\phi}\right) + \frac{2}{\phi^2}\sqrt{(\phi^2 - 1)}\right] \tag{1. 22}$$

Figure 1-11 shows the moment - curvature curve in both elastic and elasto- plastic region of a perfect thin walled tubular section, which is plotted using Eq. (1. 21) and (1. 22). All of which have been clearly explained by Chen (1988).

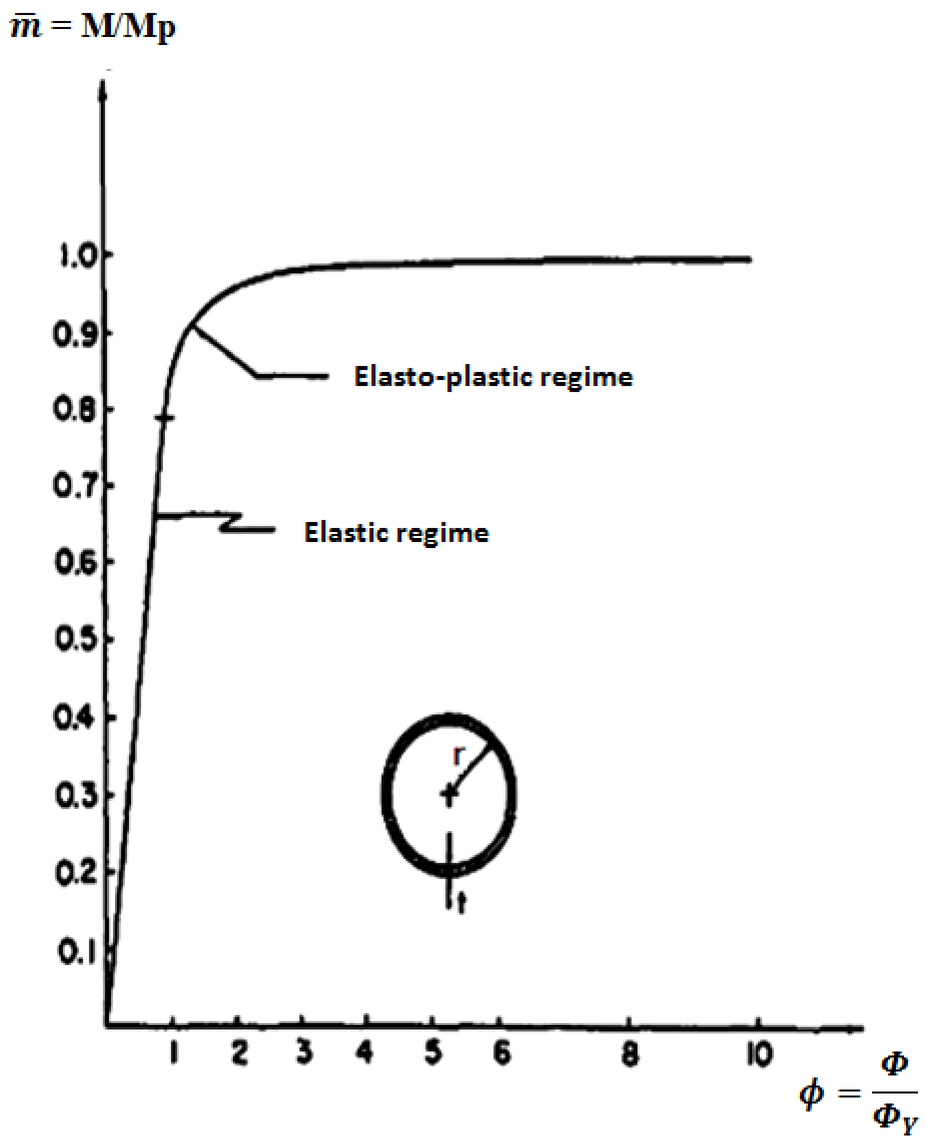

Figure 1-11. Moment - curvature relationship for perfect thin-walled tubular section (Chen, et. al. 1988)

Jialing & Reaid (1997) explained the theoretical of a pipe under pure bending as shown in Figure 1-12, where, the deformation process of pipe under pure bending and moment – curvature response was divided into 3 stages, that is, elastic bending, uniform ovalization and local collapse.

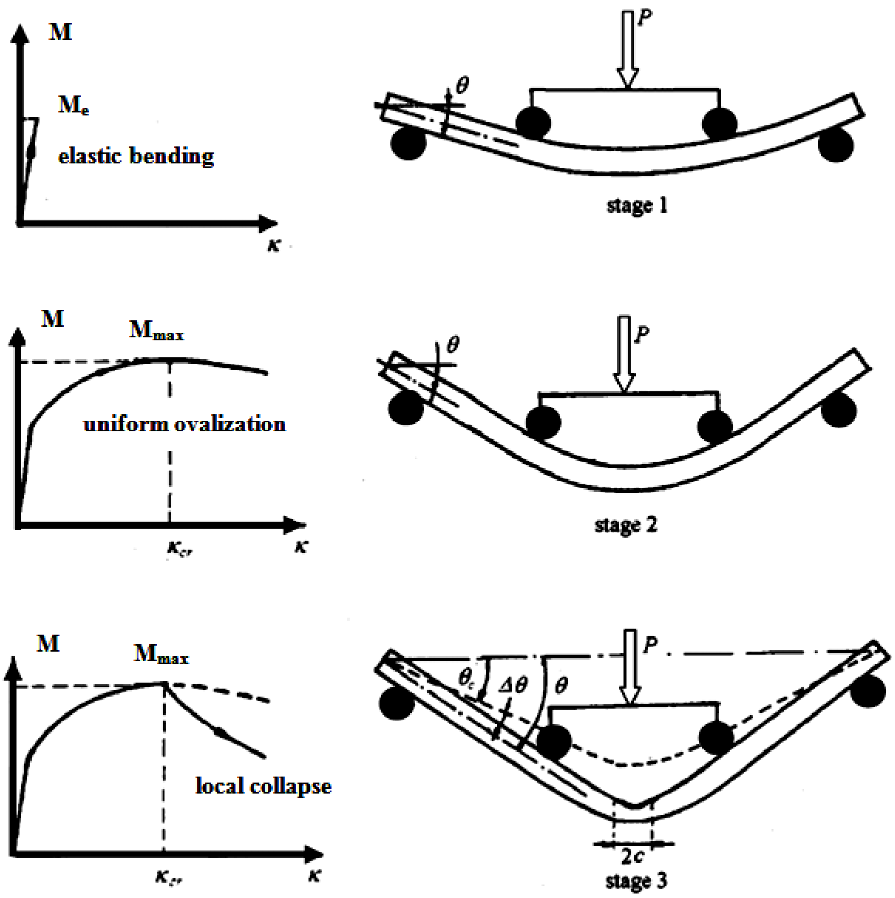

Figure 1-12. Moment-curvature response and deformation process of pipe subjected to bending. (Jialing, et. al. 1997)

1.2.2 The buckling strength of pipe under bending

The formulas for estimating the buckling stress and the buckling moment of cylinder under bending are now to be briefly explained. And also the previous researches will be presented.

If the critical buckling stress of a cylinder under bending is same as the buckling stress of a cylinder under axial compression, then the critical stress can be expressed by Eq. (1. 23).

$$\sigma_{cr} = \frac{E}{\sqrt{3(1-\nu^2)}}\left(\frac{t}{r}\right) \tag{1. 23}$$

The maximum bending stress of a cylinder under the critical (buckling) moment M_{cr} can be expressed by Eq. (1. 24).

$$\sigma_{cr} = \frac{M_{cr}}{\pi r^2 t} \tag{1. 24}$$

Where, r is the pipe radius, and t is the wall thickness.

From Eq. (1. 23) ~ (1. 24), the critical moment can be estimated as follow.

$$\begin{aligned} M_{cr1} &= \sigma_{cr} . \pi r^2 t \\ &= 0.605 \pi E r t^2 \end{aligned} \tag{1. 25}$$

Donnell (1934) found that the elastic buckling stress in bending is somewhat higher than the critical stress for axial compression.

Timoshenko and Gere (1961) gave the statement that the maximum compressive stress at critical buckling moment is about 30 % higher than the stress obtained from Eq. (1. 24). Then, the buckling moment is given by Eq. (1. 26).

$$\begin{aligned} M_{cr3} &= 1.3 \times M_{cr1} \\ &= 0.787 \pi E r t^2 \end{aligned} \tag{1. 26}$$

One of the earliest efforts in nonlinear structural analysis was performed by Brazier (1927). He had investigated the stability of long cylindrical shells under bending. If a long cylinder is subjected to bending, its cross section flatters. Consequently, its bending stiffness deteriorates with increasing bending moment as a function of applied curvature, and the bending moment exhibits a maximum. Brazier performed a somewhat approximate analysis and found that the buckling moment is given by Eq. (1. 27) with ν = 0.3.

$$M_{\max} = (2\sqrt{2}/9)\pi E r t^2 / \sqrt{1-\nu^2} = 0.329 \pi E r t^2 \tag{1. 27}$$

The maximum stress caused by this moment is computed as follow.

$$\sigma_{\max} = 0.33 E t / r \tag{1. 28}$$

Chwalla (1933) derived the equation (1. 29) as the maximum moment, considering the oval deformation of section by the energy method. And, he also showed that the maximum stress occurs at another bending curvature and it can be expressed by Eq. (1. 30).

$$M_{\max} = M_k = 0.378\pi Ert^2 \tag{1. 29}$$

$$\sigma_{\max} = 0.51Et / r \tag{1. 30}$$

Seide & Weingarten (1961) solved this as a bifurcation buckling problem. Assuming that the pre-buckling behaviour can be defined with sufficient accuracy by a linear membrane solution, they found that the critical buckling stress is only 1.5% higher than Eq. (1. 24), for a cylinder with r/t = 100. For thinner cylinders the difference is even smaller.

Odland (1978) calculated that the collapse moment of cylinder with R/t=100 and showed that the collapse moment of cylinder with L/D=5, 10, and infinity is ab.70, 60, and 50% of M_{cr1}, respectively, because of oval deformation of a section.

Ju & Kyriakides (1992) mentioned that oval deformation reduces the bending rigidity and leads to a limited load instability associated with local collapse.

The initial yield moment of a pipe under bending is shown below.

$$M_Y = \sigma_Y \pi \cdot r^2 \cdot t \tag{1. 31}$$

Where, σ_Y is the yield stress.

SUPERB (1996) outlined the geometrical imperfections (excluding corrosion) that are normally allowed in pipeline design will not exert a significant influence on the maximum strength of the pipe, and the buckling moment in the plastic region can be calculated as:

$$M_p = \left(1.05 - 0.003 \cdot \frac{r}{t}\right) \cdot \sigma_Y \cdot D^2 \cdot t \tag{1. 32}$$

If r/t equals to 50, Eq. (1. 32) becomes

$$M_p = 1.14 \cdot \sigma_Y \pi \cdot r^2 \cdot t \tag{1. 33}$$

The ultimate moment in Eq. (1.32) is only 15% higher than the initial yielding moment.

Zhang and Li (1999) had already develop a set of new governing equations to solve the nonlinear bending and the instability of imperfect cylindrical tubes, furthermore formulating the effects of initial out-of-roundness on the bending and stability.

Gellin (1980) has investigated the effect of nonlinear material behaviour on the buckling of an infinitely long cylindrical shell under pure bending. The maximum moment and associated curvature is determined as a function of material and geometric parameters. The curvature at which short wave length bifurcations occur is also determined.

Zhang (1987) investigated the Brazier effect of originally straight cylindrical tubes under pure elasto - plastic bending by the deformation theory, based on some deformation assumptions agreeing with numerous experiments. The results concerning the variations of flattening ratio and bending moment obtained by the present method are in good accordance with those reported by experiments. Zhang said that the phenomenon of the flattening of elastic tubes under bending called the Brazier effect.

Hauch and Bai (1999) had obtained a set of equations for calculating the maximum allowable bending moment including proposed safety factors for different targeted safety levels. The applied safety factor methodology ensures that the target safety levels are uniformly maintained for all load combinations.

Elchalakani, Zhao and Grzebieta (2002) presented a theoretical treatment to predict the moment rotation response of circular hollow steel tubes of varying *D/t* ratios under pure bending. In extensional deformation and rigid plastic material certain behaviour was assumed in the derivation of the deformation energy. The plasticity observed in the tests was assumed to spread linearly along the length of the tube. Two local plastic mechanisms (Star and Diamond shapes) were studied to model the behaviour observed in the tests especially during the unloading stage.

In previous researches, the buckling strength of a straight pipe under pure bending has been investigated and some formulas have presented, not only for the elastic buckling, but also for the elasto-plastic buckling. But, it seems that the accuracy of proposed formulas have not yet confirmed sufficiently, and the comprehensive study of buckling and collapse analysis, changing length-to-diameter ratio (*L/D*), the diameter-to-thickness ratio (*D/t*), and yield stress, have not been carried out.

As for curved pipe, Bantlin (1910) had found experimentally, that a curved tube is much more flexible in bending compared to curved beams of the same configuration but solid cross section.

Axelrad (1978) explained that flexible shells, designed to sustain elastic displacements, have a "semi membrane" type of deformation, described by simplified equations. In what follows, flexible shell equations are derived and used to analyse the bending of curved tubes and buckling of tubes and toroidal shells under external pressure.

Boyle (1981) presented using a thin shell theory developed by Reissner (1949), a nonlinear model to describe the in-plane bending of a curved pipe. The classical thin shell models can be deduced by making certain simplifying assumptions concerning the mode of deformation. The buckling of the curved pipe in pure bending is examined using numerical nonlinear analysis, and then compared to the previous simplified solutions.

Boussaa (1996) explained an original treatment for the finite bending of curved pipe with an arbitrary cross section. The original formulation for the in plane bending of curved tubes including geometrical nonlinearities has been proposed for each model.

S.V. Levyakov (2013) discussed nonlinear equations of in-plane bending of curved tubes formulated by Reissner (1981). The accuracy of the equations is evaluated by comparing the numerical results with predictions obtained by a special shell finite element.

In the previous research, experiments to ascertain the buckling strength of curved pipe under bending were performed. Furthermore, the geometrical nonlinear theories for describing the pre-buckling deformation were investigated, and using these theories the buckling of a curved shell was investigated. But, the calculated geometrical parameters of shell were limited. Therefore, the buckling strength of pipe with arbitrary geometrical parameters, such as *L/D*, *D/t*, and *R/D*, cannot be predicted using the results of previous studies.

1.2.3 The buckling strength of pipe under external pressure.

When a pipe is subjected to uniform external pressure, the compressive stress will be developed in pipe and increases with the increase of external pressure. And when the compressive stress reaches a limit value, the pipe is not able to maintain its initial circular shape, and distorts unstably in buckling. For an infinite long free pipe the buckling has been discussed by Von. Mises (1914), Donnel (1976), Southwell (1913), Timoshenko (1961), Flügge (1960), Tokugawa (1929), the buckling equation can be derived using the Euler buckling theory, by assumed as a ring with the second moment of inertia (I). The buckling equation is expressed as follows,

$$P_{cr} = \frac{(n^2-1)EI}{R^3} = \frac{(n^2-1)E}{12}\left(\frac{t}{R}\right)^3 \tag{1. 34}$$

However, if the pipe is longitudinal restrained, Eq. (1. 34) should be modified by considering the Poisson's effect. The equation given by the following,

$$P_{cr} = \frac{(n^2-1)EI}{12(1-\mathrm{v}^2)}\left(\frac{t}{R}\right)^3 = \frac{(n^2-1)E'}{12}\left(\frac{t}{R}\right)^3 \tag{1. 35}$$

Where, $E' = \frac{E}{(1-\mathrm{v}^2)}$ (1. 36)

Where *n* is wave number in circumferential direction.

As for a long free pipe, the number of waves is commonly given 2. Thus the buckling equation of a long pipe can be expressed by Eq. (1. 37).

$$P_{cr} = \frac{E'}{4}\left(\frac{t}{R}\right)^3 \tag{1. 37}$$

And then, the analytical solution using Eq. (1. 37) is only valid for hydrostatic pressure with the acting direction normal to pipe surface.

In previous researches, the buckling strength of pipes under external pressure has not been clarified for various values of (*L/D*) and (*D/t*).

1.2.4 The buckling strength of pipe under combined loading.

Igland, R.T & Moan, T (2000) investigated the ultimate strength of tubes under combined loading. Furthermore, they applied the reliability theory for estimating the buckling strength of pipelines with different geometry and load conditions during laying in order to achieve a more uniform and consistent safety level for semi-probabilistic design criteria.

Reddy (1979) presented experimental investigation into the plastic buckling of cylindrical tubes subjected to bending moments. And, these results are compared with analytical results for the collapse of cylinders under pure bending and uniform axial compression. The mode of deformation of the cylinders is discussed and the experimental strains are compared with those of others for tests on axially compressed cylinders as well as cylinders in pure bending.

Corona and Kyriakides (1988) presented the response and stability of long and relatively thick-walled metal tubes under combined bending and external pressure through combined experimental and numerical efforts. In experiments, they used the stainless steel 304 tubes with nominal diameter to thickness ratios of 34.7 and 24.5.

Gerard and Becker (1957) presented interaction formulas of buckling strength with experimental verification for several conditions of combined non pressure loading, that is, (1) axial compression and bending; (2) axial compression and torsion; (3) axial compression, bending and torsion; and (4) bending and torsion.

Lo et al. (1951); Fung and Sechler (1957); Gerard (1957); Baker et al. (1968) ; Mungan (1974) have already done the test, and have shown that the internal pressure increases the axial buckling stress as long as the failure stress remains elastic.

Ghazijahani, T.G, et al (2013) presented experimental study. In this study, the buckling behaviour of long cylindrical steel shells was investigated under combined bending and uniform peripheral pressure.

In previous study, the comprehensive study for the buckling strength of pipes under combined bending and external pressure still limited and the effect of imperfection on buckling and the discrepancy to straight pipe have not been discussed carefully.

1.3 Research Scope and Objective

Not only for the laying condition but also for operating condition on subsea shown in Figures 1-4 ~ 1-7, the pipe will be subjected to various kinds of loads, i.e., bending moment, external pressure and tension. In this study, the buckling strength of pipe under bending and external pressure is the focus. In the designing of offshore pipelines, it is very important to know the buckling strength for steel pipes subjected to bending and external pressure.

Under the bending loads, it is well known that the oval deformation of section takes place and this deformation will be reducing the buckling strength. Therefore, to investigate the buckling strength of pipe, nonlinear *FE* analysis taking into account of cross sectional oval deformation before buckling are performed. It is also required to be able to quantify the effect of shape imperfections, such as oval modes and buckle modes on the buckling strength. Furthermore, the buckling strength of pipe under combination loads, that is, bending and external pressure, must been investigated.

The buckling strength for a straight pipe under a pure bending moment was investigated by nonlinear *FEA*, considering the effect of a cross sectional oval deformation by changing the varying of pipes, that is, the length-to-diameter ratio *(L/D)* varying from about 2.5 to 20 and the diameter-to-thickness ratio *(D/t)* varying from about 50 to 200, respectively.

In addition, the buckling strength for a curved pipe was investigated by changing the *R/D* from 50 to 200. Where, *R* is the curvature radius of curved pipe.

1.4 Outline of Dissertation

This dissertation consists of six chapters. Chapter I introduces the overview of offshore pipelines and the previous studies on the buckling strength of pipe under bending and external pressure. Moreover, the purpose and method of this research was explained in this chapter.

In Chapter II, the linear buckling strength for pipe under pure bending will be investigated by linear *FEA*. At first, the eigenvalue calculations under bending load are performed for various length, radius and thickness of the pipe. The linear buckling strength is then compared with previously proposed formula which was derived from the buckling strength of pipe under axial compression.

In Chapter III, the buckling phenomenon for straight and curved pipe under pure bending will be investigated by nonlinear *FEA* considering the effect of cross sectional oval deformation. For the straight pipe, the reduction rate of the buckling moment due to the oval deformation of pipe is clarified for various values of *L/D* and *D/t*, not only in elastic buckling, but also in elasto-plastic buckling. Moreover, for the curved pipe, the reduction rate of the buckling moment due to the oval deformation of pipe is clarified for various values of *R/D*.

In Chapter IV, we explain the effect of initial imperfection on buckling strength for straight and curved pipe under pure bending. As well as for perfect pipe, the buckling strength for imperfect pipe will be investigated by nonlinear *FEA* considering the effect of cross sectional oval deformation. For imperfect straight pipe, the reduction rate of the buckling moment due to the oval deformation of pipe is clarified for various values of *L/D, D/t* and $\delta o/t$, not only in elastic buckling, but also in elasto-plastic buckling. Moreover, for imperfect curved pipe, the reduction rate of the buckling moment due to the oval deformation of pipe is clarified for various values of *R/D* and *δo/t*. The effect of buckling mode and oval mode of imperfection are also investigated in this chapter.

In Chapter V, the buckling strength of pipe under bending and external pressure will be investigated by nonlinear *FEA*. The relationships between non-dimensional pressure and non-dimensional moment will be shown in this chapter.

Finally, Chapter VI is devoted to drawing conclusions and summarising findings concerning pipes under bending and external pressures for application on offshore pipelines.

Chapter II

The Linear Buckling Strength of Pipe under Pure Bending

2.1 Introduction

Fluids such as oil and natural gas are often transported over long distances from subsea wells to a process facility offshore or onshore via pipelines. At the time of operation, the pipeline will be subjected to a wide range of loads. The buckling of structural components under various types of loading is a common cause of structural failure. In the designing of pipelines, it is therefore, important to know the buckling strength of pipe under various kinds of loads. Many researchers have already investigated the buckling strength under axial compression and an accurate formula was presented, but the accurate formula for the buckling strength of pipe under bending load seems not to have been presented up to now.

In this Chapter, the buckling strength of pipe under pure bending load will be investigated by linear *FEA*. At first, the eigenvalue calculations under bending load are performed for various length, radius and thickness of the pipe. Secondly, the linear buckling strength is compared with the previously proposed formula which was derived from the buckling strength of pipe under axial compression.

In linear buckling strength calculation, the parametric study is performed. That is, for the pipes with ratio between length and diameter *(L/D)* varying from about 2.5 to 20, diameter ranging from 1000 to 4000 mm, and with ratio between diameter and thickness *(D/t)* varying from about 50 to 200, the linear buckling strength is investigated.

In this study, the series of calculations on linear buckling strength of pipe under bending are performed by utilizing linear *FE* software.

2.2 Procedures of Calculation for Estimating Linear Buckling Strength of Pipe under Bending

2.2.1 Model for calculation

The calculations for linear buckling strength of pipe under pure bending are performed. Figure 2-1 shows the schematic view of pipe under bending moment. The full length models of pipe are used in *FEA*.

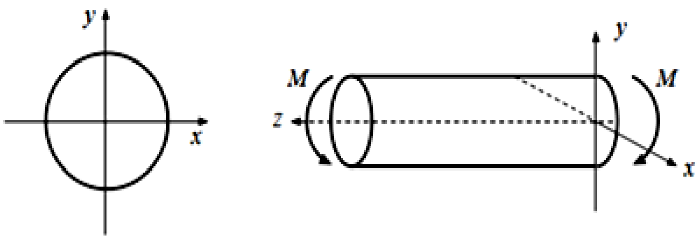

Figure 2-1. The schematic view of a pipe under bending moment

2.2.2 Program name

For linier buckling analysis, the finite element software MSC Nastran is used. The finite element analysis *(FEA)* model can be generated in any available pre-process software. In this study, the models are generated by MSC Patran.

2.2.3 Element mesh for analysis

The Linear eigenvalue analysis using MSC Nastran is performed by using a quadrilateral 4 node element with 36 elements in circumference. The element number is basically 120 elements in length and more elements are used to maintain the calculation accuracy in the case of long cylinder as shown in Table 2-1. Cases I - III are changing *D/t* from 50 to 200. For each case, *L/D* are varying from 2.5 to 20.

Table 2-1. The parameters of calculation on linear buckling strength of pipe under pure bending

CASES	D (mm)	D/t	L/D	Element Number in Length (in circumferential direction, and in axial direction)
Cases I	1,000	50	2.5	36 elements 120 elements
			5.0	36 elements 240 elements
			7.5	36 element 360 elements
			10	36 elements 480 elements
			15	36 elements 720 elements
			20	36 element 960 elements
Cases II	2,000	100	2.5	36 element 120 elements
			5.0	36 elements 240 elements
			7.5	36 elements 360 elements
			10	36 elements 480 elements
			15	36 elements 720 elements
			20	36 elements 960 elements
Cases III	4,000	200	2.5	36 elements 120 elements
			5.0	36 elements 240 elements
			7.5	36 elements 360 elements
			10	36 elements 480 elements
			15	36 elements 720 elements
			20	36 elements 960 elements

2.2.4 Boundary conditions

The Cylindrical coordinates are used. The following boundary conditions are given at the mid span of cylinder shown in Eq. (2.1), and $U_\Theta = 0$ at four points as shown in Figure 2-2.

$$U_Z = 0 \tag{2. 1}$$

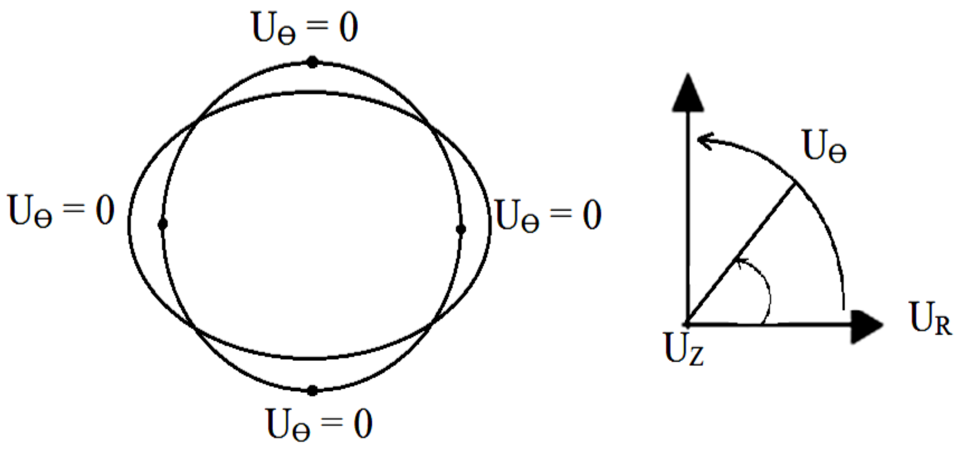

Figure 2-2. Boundary condition at mid span of cylinder

2.2.5 The loading conditions

The bending moment is applied at the centre of the circle at both ends as shown in Figure 2-3. The rigid body elements *(RBE)* are inserted at both ends of sections in order to connect the centre of a circle and the points on a circle. *RBE* prevents the oval deformation of both end sections, and keeps the section in plane under rotational deformation by a bending moment.

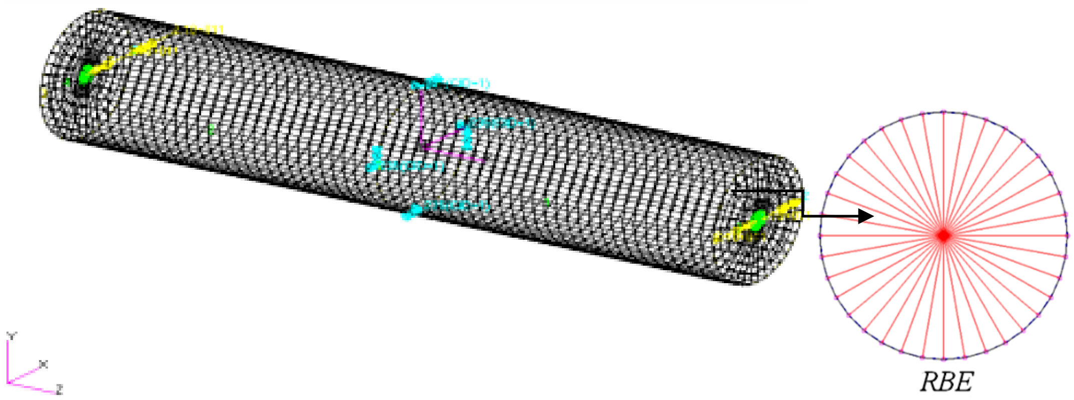

Figure 2-3. *FEA* model for full pipe in linear analysis

2.3 The Numerical Results on Linier Buckling Strength of Pipe under Bending

The typical buckling mode which is obtained from numerical calculation is shown in Figure 2-4. The stress at the lower side of cylinder is compression, and at the upper side is tension under bending moment. Therefore, the region of buckling is limited in the vicinity of bottom.

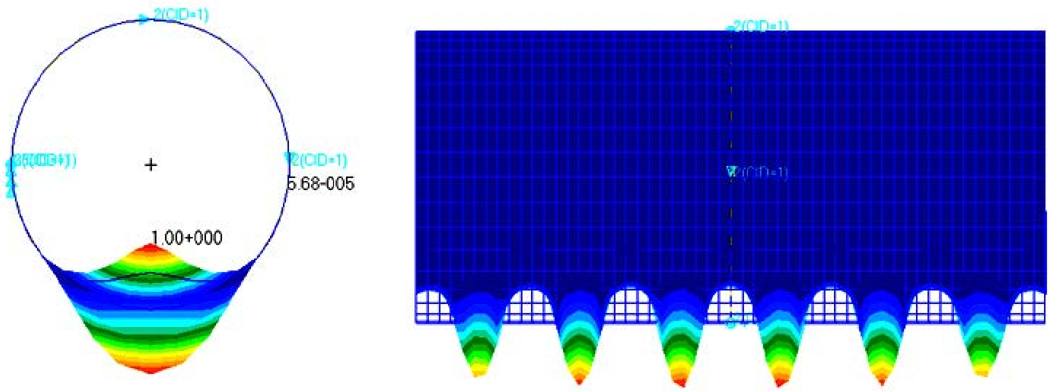

Figure 2-4. Buckling mode of pipe under pure bending in linear analysis

The buckling moments obtained by linear eigenvalue calculation are shown in Table 2-2. For the cylinder with same *D/t*, the buckling moments are almost same for all length of cylinder.

In Table 2-2 also shows the critical bending moment, M_{cr1}, when the critical buckling stress of a cylinder under bending is same as the buckling stress of a cylinder under axial compression. The numerical result M_{cr2} is 10% higher than M_{cr1}. From the numerical results, the critical bending moment in linear calculation can be expressed by Eq. (2. 2).

$$M_{cr2} = 1.1 \times \frac{E}{\sqrt{3(1-\nu^2)}} \left(\frac{t}{r}\right) \times \pi r^2 t \tag{2. 2}$$

As mention before, the critical moment proposed by Timoshenko is 30% higher than M_{cr1}. Therefore the critical moment proposed by Timoshenko seems to give a considerably unsafe estimation on the buckling moment.

Table 2-3 shows the calculated linier buckling strength for pipe of D/t = 200, L/D = 20, using 10, 12 and 16 elements for one wave length. When the number of elements for one wave length increases, the value of ($Mcr2/Mcr1$) will approach to 1.0 as shown in Table 2-3. Thus, 18 elements for one wave offer a more accurate result.

2.4 Discussion

The numerical results were shown in Tables 2-2 ~ 2-3 changing the element size, in other words, the element number. It is well known that both elements of smaller dimensions and a greater number of elements will result in smaller errors and the numerical results will be more precise. However, a numerical calculation with a greater number of elements requires a longer computation time. The point at which the computational time increases is when using more than 18 elements for one wave. In this case, 10 elements for one wave length had a small error. Therefore, we used 10 elements for next calculation.

In the linear buckling analysis, the effect of value L/D is not as much as shown in Table 2-2 in the last column. The ratio of linear buckling strength of longer pipe to that of short pipe is almost 100% for every case.

Table 2-2.The numerical results of linear buckling strength by MSC Nastran

Cases	L/D	$Z = \sqrt{(1-v^2)}\frac{L^2}{Rt}$	Buckling Moment Pure Bending *Mcr1 (N mm)*	From *FEM* Buckling Moment *Mcr2 (N mm)*	*Mcr2/Mcr1*	Element every one wave	Length for one wave *(mm)*	Ratio to first calculation
Cases I **D/t = 50**	2.5	6.0E+2	8.0E+10	8.3E+10	1.034 ≈ 1.03	18	375	
	5	2.4E+3	8.0E+10	8.3E+10	1.033 ≈ 1.03	18	375	100%
	7.5	5.4E+3	8.0E+10	8.3E+10	1.032 ≈ 1.03	18	375	100%
	10	9.6E+3	8.0E+10	8.3E+10	1.032 ≈ 1.03	18	375	100%
	15	2.15E+4	8.0E+10	8.3E+10	1.032 ≈ 1.03	18	375	100%
	20	3.82E+4	8.0E+10	8.3E+10	1.032 ≈ 1.03	18	375	100%
Cases II **D/t = 100**	2.5	1.2E+3	1.6E+11	1.68E+11	1.047 ≈ 1.05	12	500	
	5	4.8E+3	1.6E+11	1.67E+11	1.043 ≈ 1.04	12	500	100%
	7.5	1.08E+4	1.6E+11	1.67E+11	1.043 ≈ 1.04	12	500	100%
	10	1.91E+4	1.6E+11	1.67E+11	1.042 ≈ 1.04	12	500	100%
	15	4.3E+4	1.6E+11	1.67E+11	1.042 ≈ 1.04	12	500	100%
	20	7.63E+4	1.6E+11	1.67E+11	1.042 ≈ 1.04	12	500	100%
Cases III **D/t = 200**	2.5	2.4E+3	3.2E+11	3.4E+11	1.06 ≈ 1.06	10	833	
	5	9.5E+3	3.2E+11	3.39E+11	1.058 ≈ 1.06	10	833	100%
	7.5	2.15E+4	3.2E+11	3.39E+11	1.058 ≈ 1.06	10	833	100%
	10	3.82E+4	3.2E+11	3.39E+11	1.058 ≈ 1.06	10	833	100%
	15	8.6E+4	3.2E+11	3.39E+11	1.058 ≈ 1.06	10	833	100%
	20	1.53E+5	3.2E+11	3.39E+11	1.058 ≈ 1.06	10	833	100%

Table 2-3.The numerical results of linear buckling strength by MSC Nastran for pipe $D/t = 200$, $L/D = 20$

Cases	L/D	$Z = \sqrt{(1-\nu^2)}\frac{L^2}{Rt}$	Buckling Moment Pure Bending Mcr1 (N mm)	From FEM Buckling Moment Mcr2 (N mm)	Mcr2/Mcr1	Element every one wave	Length for one wave (mm)	Ratio to first calculation
D/t = 200	20	1.53E+5	3.2E+11	3.39E+11	1.058 ≈ 1.06	10	833	100%
			3.2E+11	3.36E+11	1.05 ≈ 1.05	12	800	100%
			3.2E+11	3.36E+11	1.049 ≈ 1.05	16	667	100%

2.5 Conclusions

In this study, the series calculations on the linear buckling strength of pipe under bending are performed by utilizing linear *FE* software. The typical buckling mode which is obtained from numerical calculation is shown in Figure 2-4. Under the bending moment, the region of buckling is limited to the vicinity of the bottom, because the stress at the lower side of cylinder is compression, and at the upper side is tension.

As shown in Tables 2-2 ~ 2-3, the linear buckling moment M_{cr2} calculated by finite element software MSC NASTRAN is 10% higher than M_{cr1}. Where M_{cr1} is the critical bending moment when the critical buckling stress of a cylinder under bending is same as the buckling stress of a cylinder under axial compression. From the numerical results, the critical bending moment, M_{cr2}, in linear calculation can be expressed as follows,

$$M_{cr2} = 1.1 \times \frac{E}{\sqrt{3(1-\nu^2)}} \left(\frac{t}{r}\right) \times \pi r^2 t$$

The critical moment proposed by Timoshenko is 30% higher than M_{cr1}, and it seems to be considerably on the unsafe side in terms of an estimation of the buckling moment.

Numerical error can be avoided when the total number of elements in every one wave length of buckling mode is more than 18 elements as shown in Tables 2-2 ~ 2-3, but this would need much more computation time. By using 10 elements in every one wave length of buckling mode, the errors were not so large, with a limited amount of extra computation time. Therefore, it is recommended that the number of elements for one wave length is 10.

In the linear buckling analysis, the effect of value *L/D* is insignificant. The cylinder with same *D/t*, the linear buckling moments are almost same for all length of cylinder.

In this chapter, the linear buckling moment, M_{cr2}, of pipe was obtained for various dimension of pipe utilizing *FEA*. It was shown that M_{cr2} is approximately 1.1 times M_{cr1}, Where, M_{cr1} is the critical bending moment when the critical buckling stress of a cylinder under bending is same as the buckling stress of a cylinder under axial compression.

In actual pipe, the oval deformation of cross section will take place before buckling, and the buckling moment will be reduced due to this deformation. Therefore, the linear buckling moment will not present the exact strength of pipe under bending. But, it can be the rough standard of the buckling moment of the pipe.

In the following chapter, the exact buckling moments will be examined by considering pre-buckling oval deformation, and will be compared with the linear buckling moment, M_{cr2}, or the buckling moment, M_{cr1}, to clarify the effect of pre-buckling oval deformation on the buckling moment.

Chapter III

The Nonlinear Buckling Strength of Straight and Curved Pipe under Pure Bending

3.1 Introduction

The numerical results on the linear buckling strength of pipe under pure bending were explained in Chapter II. The parameters of the calculations involved using pipes with *L/D* varying from 2.5 to 20, and *D/t* from 50 to 200. The linear *FE* software was used in this study. Through such methods the linear buckling strength was obtained. The linear buckling strength is compared with the previously proposed formula, which was derived from the buckling strength of pipe under axial compression. Therefore, the critical bending moment in the linear calculation can be expressed by M_{cr2} as shown in Eq. (3. 1).

$$\begin{aligned} M_{cr2} &= 1.1 \times M_{cr1} \\ &= 0.666 \pi E r t^2 \end{aligned} \tag{3. 1}$$

Where M_{cr1} is the critical bending moment, when the critical buckling stress of a cylinder under bending is same as the buckling stress of a cylinder under axial compression.

Not only straight pipes, but also curved ones are utilised in an actual pipeline. In designing such a pipeline, it is important to know the buckling strength of the pipe under various kinds of loads; especially as it is established that the buckling moment will be reduced by increasing the pipe's length.

It is well known that cross sectional oval deformation takes place and the buckling strength of pipe is reduced due to this deformation. This oval deformation occurs at the mid span of a pipe, as shown in Figure 3-1.

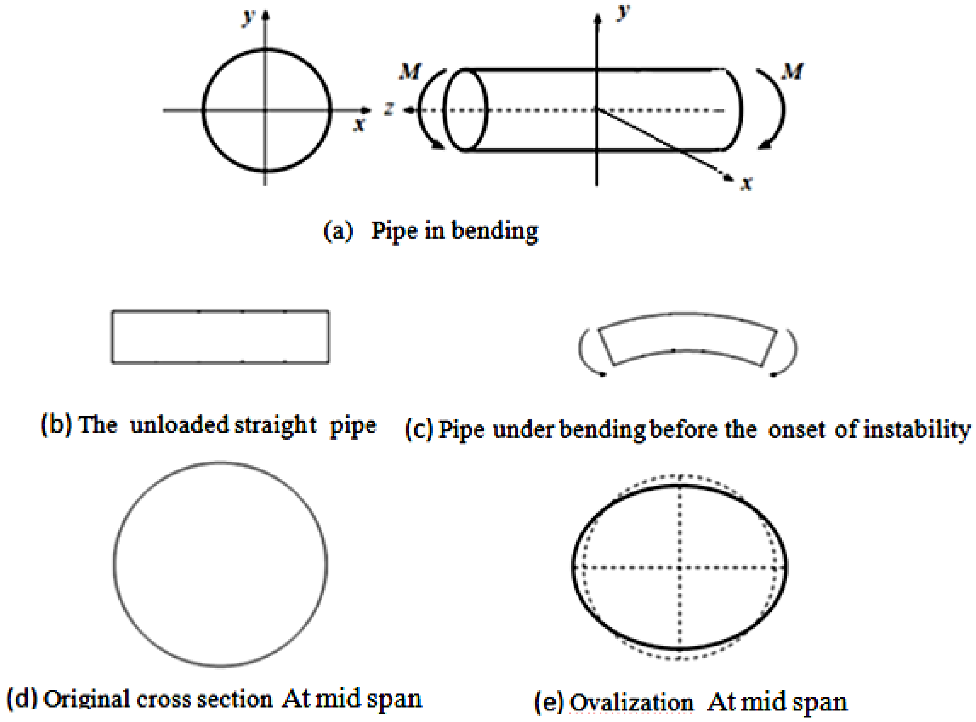

Figure 3-1. Schematic view of a pipe in bending and the oval deformation which takes place at mid span

In this Chapter, firstly the buckling phenomenon for a straight pipe under a pure bending moment is investigated by nonlinear *FEA*, considering the effect of a cross sectional oval deformation by changing the dimensions of pipes. In practice this involved changing the length-to-diameter ratio *(L/D)* varying from about 2.5 to 20 and the diameter-to-thickness ratio *(D/t)* varying from about 50 to 200. And secondly, the buckling phenomenon for curved pipes is also investigated by changing the *R/D* from 50 to 200, where *R* is the curvature radius of curved pipe.

In this thesis, for the straight pipe the reduction rate of the buckling moment due to oval deformation will be clarified under various values of *L/D* and *D/t* - not only in elastic buckling, but also in elasto-plastic buckling. Moreover, for the curved pipe, the reduction rate of the buckling moment due to oval deformation will be clarified for various values of *R/D*.

In this study, the series of calculations for buckling and collapse strength of straight and curved pipes under bending are performed by utilizing nonlinear *FE* software.

3.2 Procedures of Calculation for Estimating Nonlinear Buckling Strength of Pipe under Bending

3.2.1 Parameters for calculation

In the calculation of the straight pipe, the ratio between pipe length and diameter *(L/D)* and the ratio between diameter and thickness *(D/t)* are taken as the calculation parameters. In this paper as shown in table 3-1, *L/D* varies from 5 to 20, in which the diameter is changed from 1,000 to 4,000 mm. And *D/t* varies from 50 to 200. Where, *D* is the pipe diameter, *t* is the wall thickness, and *L* is the pipe length.

Table 3-1. The parameters for calculating the nonlinear buckling strength of straight pipe under pure bending

CASES (N mm)	D (mm)	D/t	L/D
I	1,000	50	2.5 to 20
II	2,000	100	2.5 to 20
III	4,000	200	2.5 to 20

In calculations involving the curved pipe, the diameter *(D)* is originally fixed at 4,000 mm, and the thickness *(t)* is fixed to 20 mm. *L/D* varies from 2.5 to 20 by changing the pipe length *(L)*. *R/D* varies from 50 to 200 as shown in table 3-2. Where, *R* is radius of curvature in curved pipe. The geometry for a curved pipe is shown in Figure 3-2.

Table 3-2. The parameters for calculating the nonlinear buckling strength of a curved pipe under pure bending

M (N mm)	D (mm)	t (mm)	L/D	R/D	
3.2 x 10^{11}	4,000	20	2.5 to 20	(50)	Curved pipe
				(100)	Curved pipe
				(200)	Curved pipe
				(∞) = Straight Pipe	

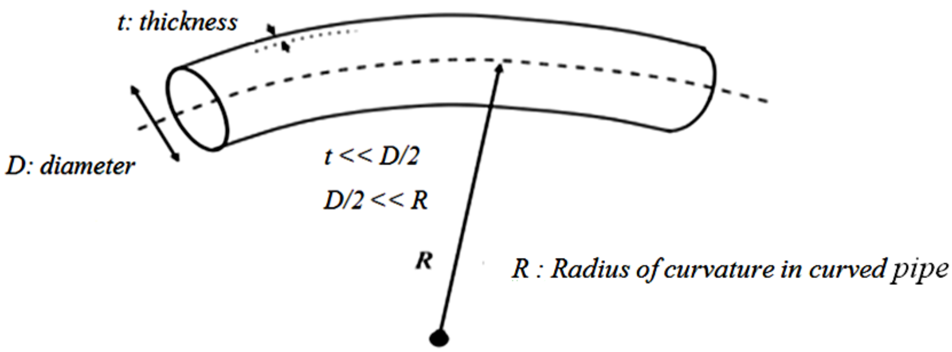

Figure 3-2. The geometry of a curved pipe

In calculation of the elasto-plastic analysis, the yield stress of material assumed to be 621 MPa which is the yield stress of material API X80. The elasto-prefect material is choosed in the numerical analysis. It means strength hardening after yielding has not been considered.

3.2.2 Model for calculation and calculation program

The buckling calculations of pipe under pure bending are performed. The full length models of straight and curved pipe are used in *FEA*. Figure 3-3 shows the finite element model for straight pipe.

General purpose *FE* software MSC Marc is used for nonlinear buckling analysis, in which the cross sectional oval deformation before buckling is taken into account. The quadrilateral 4 node element (No.75) is used. The calculating region is divided into 36 elements in a circumferential direction. The number of elements in the axial direction length is basically 120 and more elements are used to maintain the calculation accuracy in the case of a long cylinder.

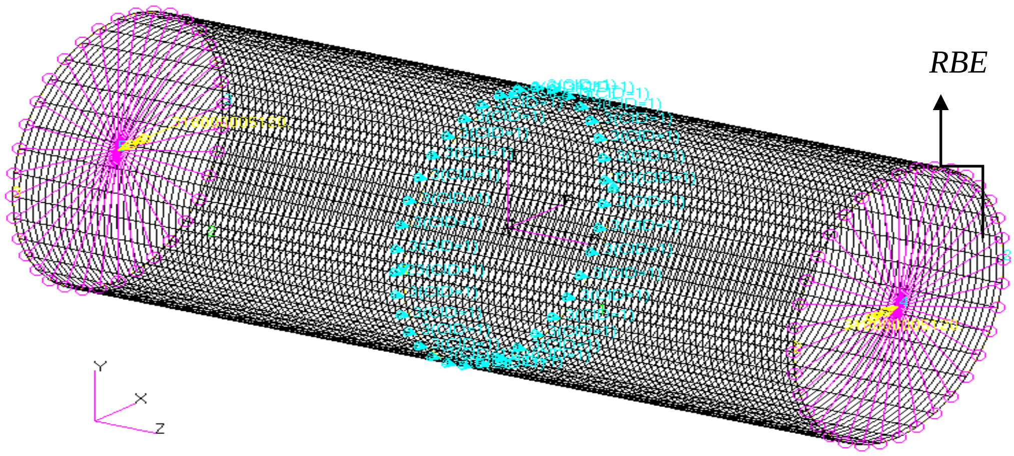

Figure 3-3. Finite element model for straight pipe in nonlinear analysis

3.2.3 Boundary conditions and loading conditions

The cylindrical coordinates are used. The boundary conditions $U_Z = 0$ are given at the mid span of the cylinder and $U_\Theta = 0$ at four points as shown in Figure 2-2.

The rigid body elements *(RBE)* are inserted at both end sections in order to connect the centre and the points on the circle. The bending moment is loaded at the centre of circle at both ends. The rigid body elements *(RBE)* prevent oval deformation of both end sections and keep the section in plane under rotational deformation through a bending moment as shown in Figure 3-3. In MSC Marc, a rigid link for either small deformation or large deformation can be implemented by using tying or *RBE.*

In the actual pipeline system, the connection between pipes using flanges can be modelled by *RBE*.

Figure 3-4 shows the caption of straight and curved pipe, respectively. The oval deformation of each section at the mid span is defined by *δ*.

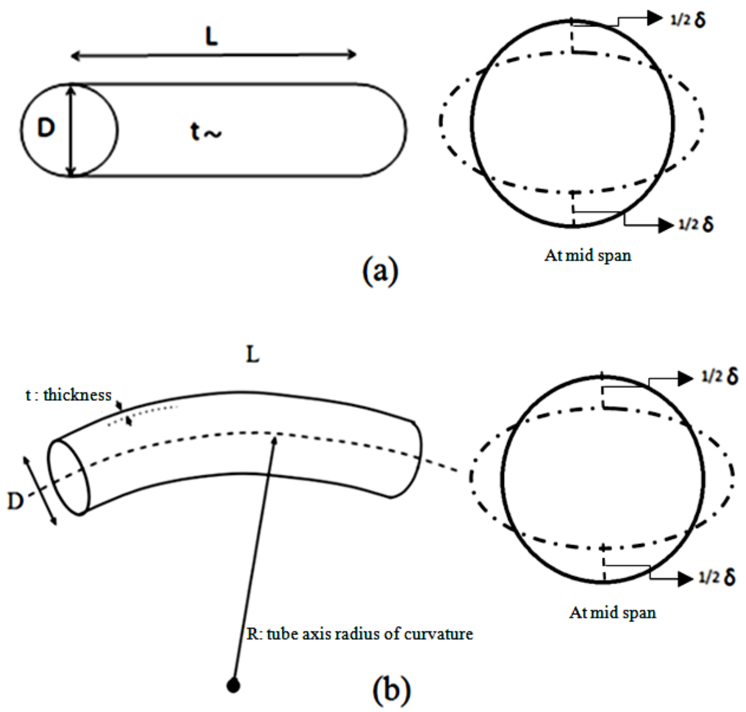

Figure 3-4. Geometry for (a) straight pipe and (b) curved pipe.

3.2.4 Method to obtain bifurcation moment in nonlinear calculation

To obtain the bifurcation buckling moment and its mode, the eigenvalue calculations are performed at the proper load increment, and the cross sectional point of the critical moment between the buckling moment and the applied moment is defined as the bifurcation buckling moment, as shown in the schematics in Figure 3-5. In this figure, the vertical axis shows the bifurcation buckling eigenvalue, and the horizontal axis shows the applied load.

The eigenvalue is calculated at each load increment considering the pre-buckling deformation. Therefore, the eigenvalue will change in response to the pre-buckling deformation. The bifurcation buckling load is judged as follows. When the value of the eigenvalue is larger than the applied load, buckling does not occur. Furthermore, when the eigenvalue is smaller than that of the applied load, the buckling has already happened. The cross section point of the eigenvalue and the applied load is treated as the bifurcation buckling load. Oval deformation will increase when the applied moment increases. Then, the bending rigidity of pipe will be decrease and the curvature radius of mid span section will increase. As a result, the eigenvalue will decrease gradually.

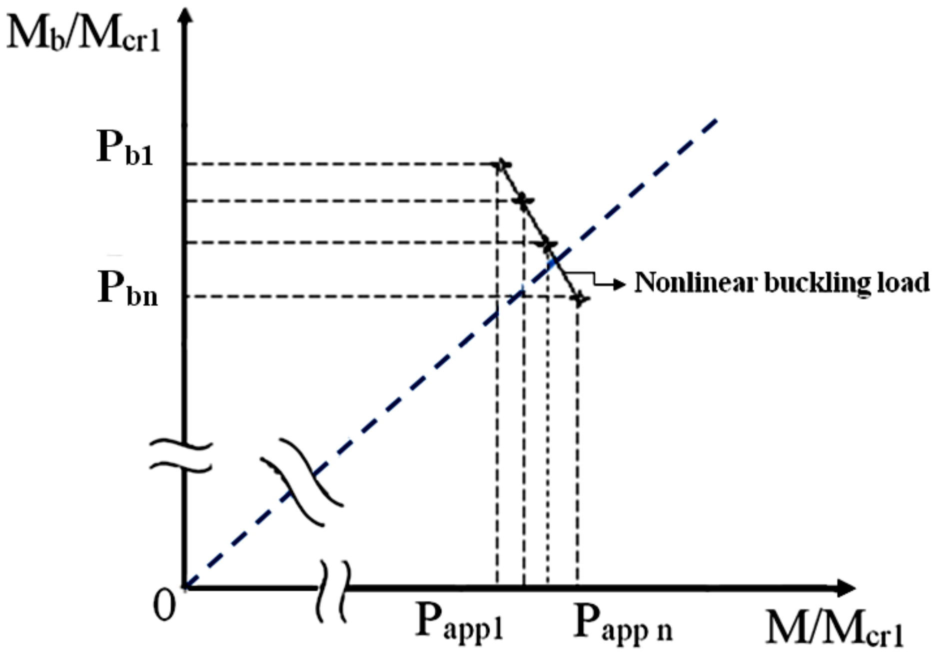

Figure 3-5. Schematic diagram for estimation of bifurcation moment

3.3 Numerical Results

The typical buckling mode, which is obtained from a nonlinear calculation, is shown in Figure 3-6. The stress at the lower side of the cylinder is compression, and that at the upper side is tension. And the oval deformation is larger in the vicinity of mid span than at the span end. Therefore, the region of buckling is restricted to the bottom area close to the centre, and is different from that in linear buckling analysis.

The mesh convergence study is done in this chapter. Table 3-3 shows the numerical results for pipe D/t = 200 and L/D = 2.5. From this table, it is found that the numerical results by MSC Marc are not so much different by changing the circumferential element number from 36 to 20 and the longitudinal one from 120 to 200. By using 36 elements in circumferential direction and 120 elements in longitudinal direction this model does not need more time for its numerical calculations. Therefore, we used 36 elements in circumferential direction and 120 elements in longitudinal direction for the following calculations.

Table 3-3. The mesh convergence study in MSC Marc

D/t	L/D	Circumferential elements	Longitudinal elements	Maximum load in MSC Marc
200	**2.5**	**36**	**120**	**1.691**
		36	**200**	**1.655**
		20	**200**	**1.755**

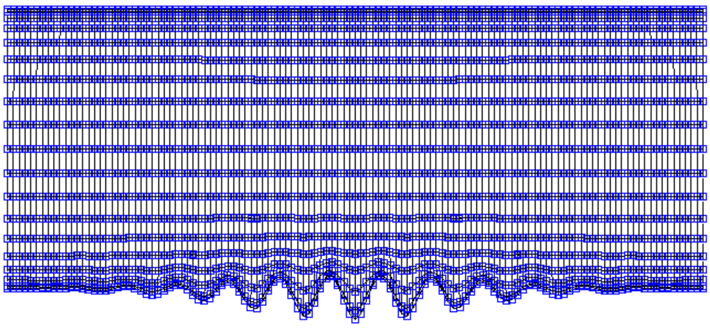

(a)

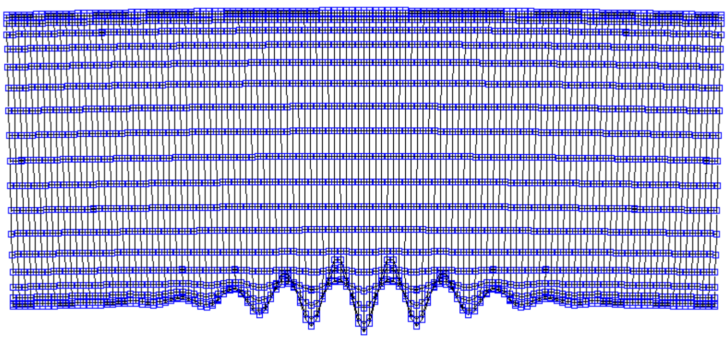

(b)

Figure 3-6. Buckling modes of pipe (*D/t* = 200, *L/D* = 2.5) under pure bending:
(a) the straight pipe and (b) the curved pipe *R/D* = 50

3.3.1 The numerical results on nonlinear buckling strength of straight pipe under pure bending

Figure 3-7 shows the relationship between the calculated buckling moment in elastic analysis and *L/D* for the pipe with *D/t* = 200. The buckling moment will be reduced by increasing the value of *L/D*. In the case of *D/t* = 200, the buckling moment in short pipes is somewhat different from the results of J. Odland, but for infinite length the difference is small or almost same.

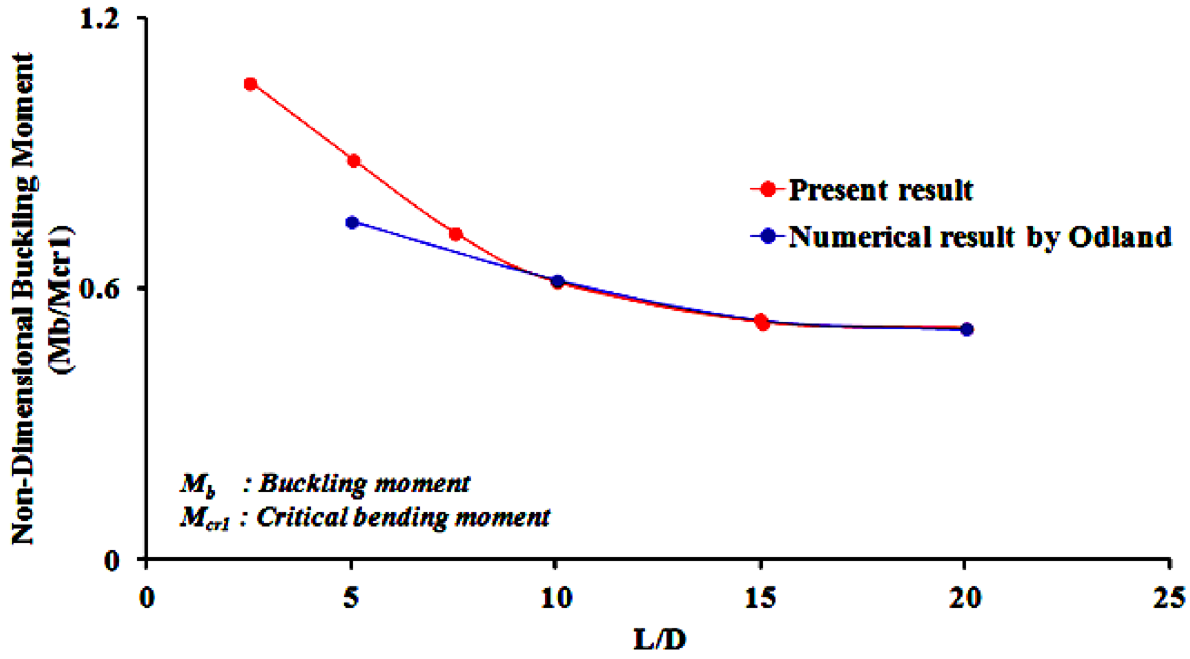

Figure 3-7. Relationship between buckling moment and *L/D* for pipe under pure bending in elastic analysis

In this study, the rigid body elements *(RBE)* are set at both ends of the pipe. The *RBE* prevents the oval deformation of both end sections, and keeps the section in plane under rotational deformation by a bending moment. Therefore, the greatest oval deformation occurred at the mid span of pipe. How the oval deformation at the mid span increases with the applied bending moments is shown in Figure 3-8. This figure shows the relationship between the applied bending moment and the oval deformation at the mid span of the pipe with *D/t* = 200 when the pipe behaves elastically. The vertical axis shows the non-dimensional moment (M/M_{cr1}). Where, M_{cr1} is the critical bending moment when the critical buckling stress of a cylinder under bending is same as the buckling stress of a cylinder under axial compression. The maximum point each curve shows the bifurcation buckling point, not the maximum load of incrementally analysis.

In a long pipe, such as L/D = 10, 15, and 20, the oval deformation increases a lot with increasing of the applied load. On the other hand, in a short pipe, such as L/D = 2.5 and 5.0, oval deformation is small due to the restriction of the sectional deformation at both ends. It means that when no there is no constraint at the ends of the pipe, the oval deformation at the mid span will be uniform along the length of pipe.

The maximum moment of each curve shows the bifurcation buckling moment explained in Figure 3-5. Due to the oval deformation before the buckling, the maximum moments of the long pipes reduced more in comparison with the short pipes.

Figure 3-9 shows the relationship between the applied bending moment and the oval deformation at the mid span considering the yielding effect of the material when the yield strength of material is 621 MPa. In this figure, the elastic numerical results are also plotted with dotted curves. The maximum moments of elasto-plastic calculation is much smaller than that of elastic calculation. Although the oval deformations of the long pipes are greater than those of short pipes, the maximum bending moments of the former are not much lower than those of short pipes because the maximum bending moments are limited by yielding.

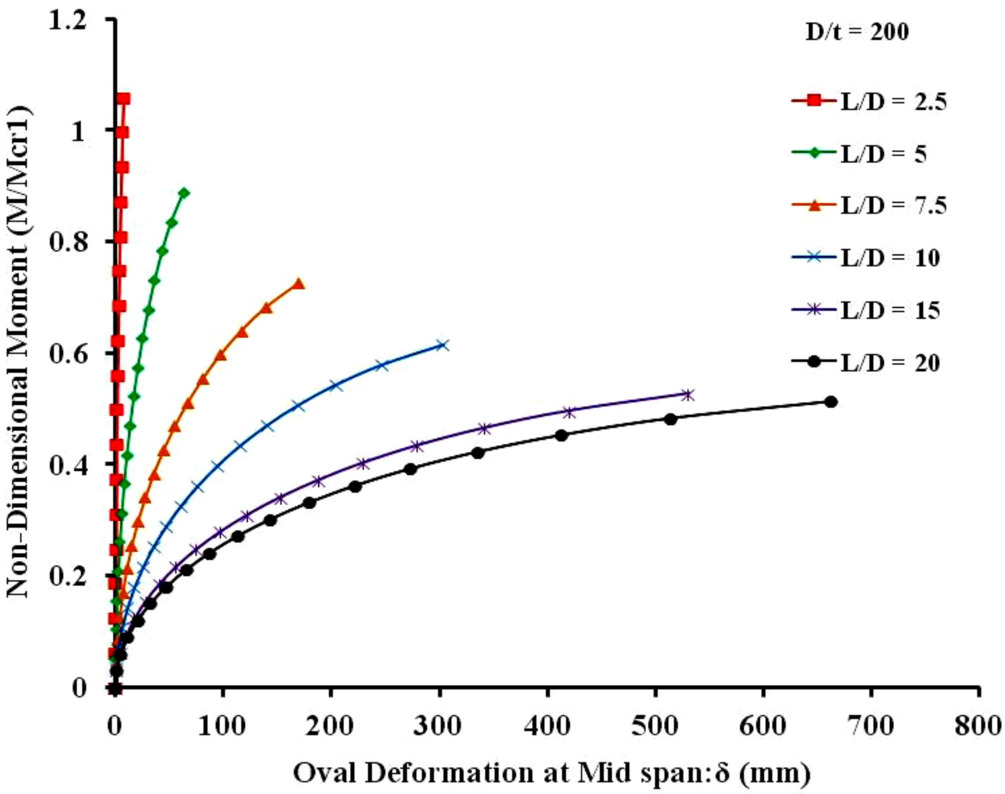

Figure 3-8. Ovalization at the mid span for straight pipe (*D/t* = 200) in elastic analysis

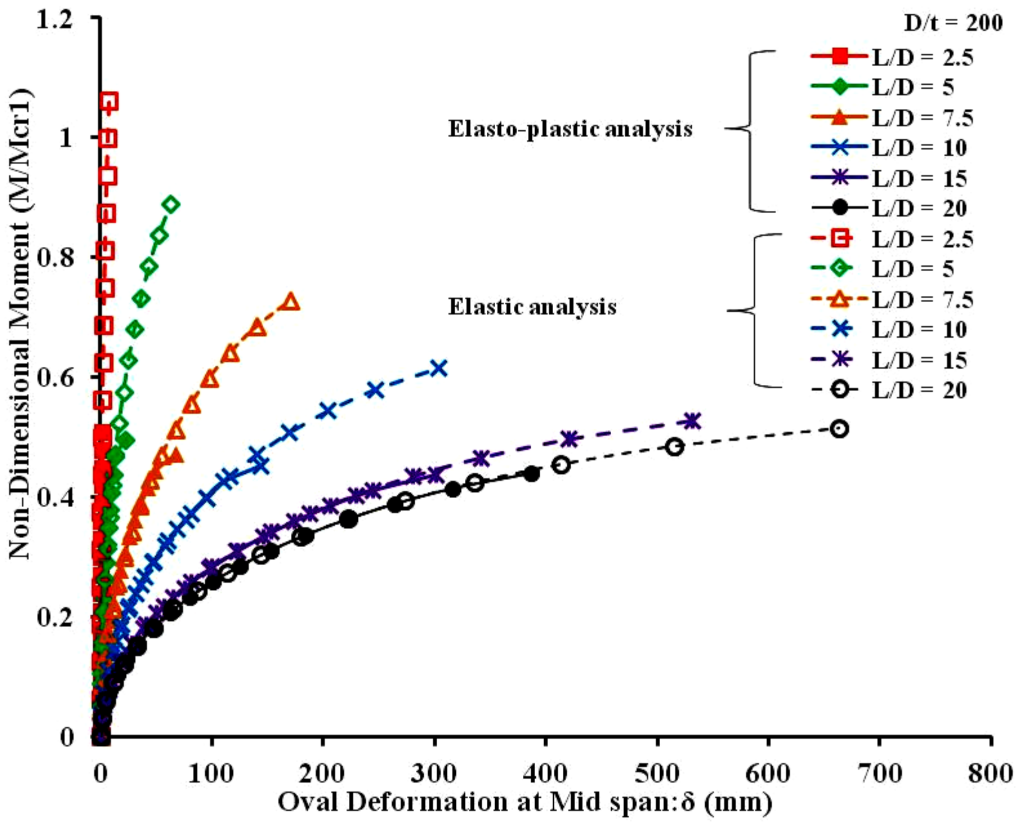

Figure 3-9. Ovalization at the mid span for straight pipe (*D/t* = 200)

The distributions of oval deformations in elastic range for the pipe with *L/D* = 20 are shown in Figure 3-10. Figure 3-10 (a), (b) and (c) show the results for the pipe with *D/t* = 50, 100 and 200, respectively. The oval deformation becomes constant when the location approaches mid span of pipe. For the cylinder with *D/t* = 50, the effect of end constraint on oval deformation tends to vanish at 1/4 of pipe length. This means that, if *L/D* is larger than 5, the oval deformation is almost same as the infinite cylinder. On the other hand, for the cylinder with D/t = 200, the oval deformation at 1/4 of pipe length is smaller than that at the mid-span. For a short pipe, the effect of constraint at both ends of pipe is greater than with a longer pipe. From these results, it is found that the effect of restricting sectional deformation at both ends on the oval deformation at the mid span is greater in the pipe with a larger value of *D/t* than in the pipe with a smaller value of *D/t*.

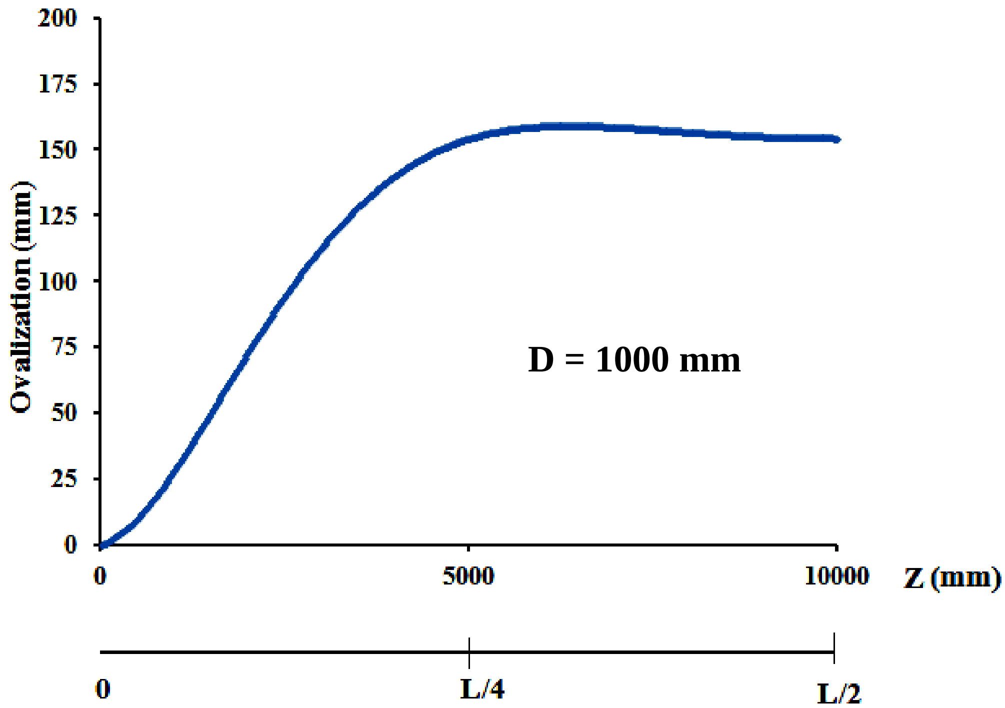

(a) *D/t* = 50

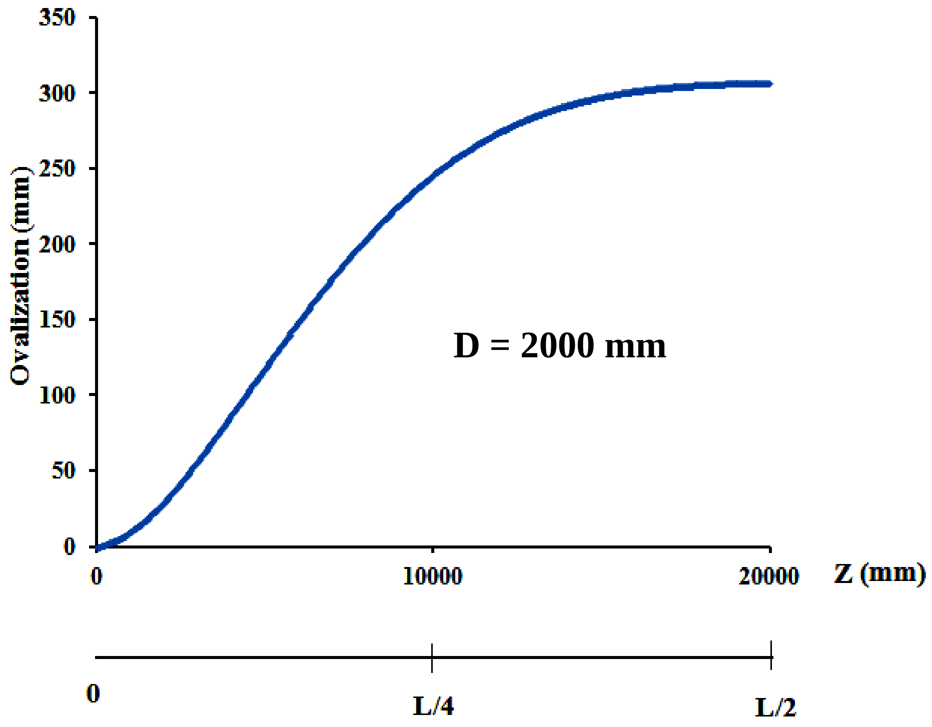

(b) D/t = 100

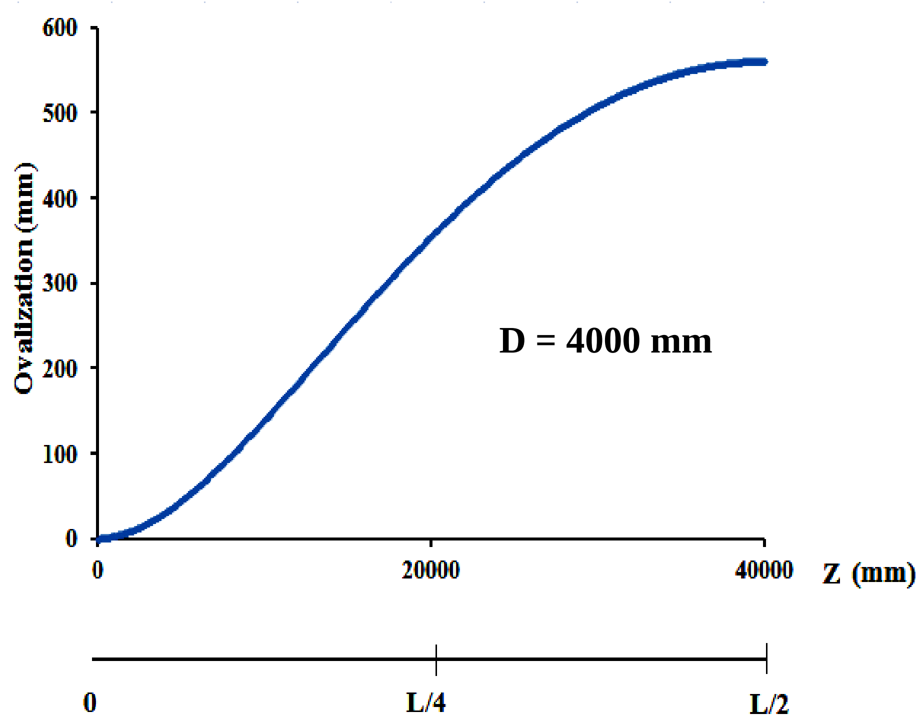

(c) D/t = 200

Figure 3-10. Relationships between ovalization and position from pipe end

(for cylinder with L/D = 20, at just before buckling)

The relationship between the buckling moment and *L/D* is shown in Figure 3-11. In this figure, the elastic numerical results are plotted with solid curves and the elasto-plastic numerical results are plotted with dotted curves. The buckling moments are summarized in Table 3-4. In elastic analysis, the buckling moment will be decreased with an increasing *L/D* value and become constant when the pipe has an infinite length. From the numerical results, the maximum moment for a long pipe considering oval deformation is shown as follows.

$$M_{\max} = 0.52 M_{cr1} = 0.314 \pi E r t^2 \tag{3. 2}$$

The maximum moment in Eq. (3. 2) is only 5 % lower than Eq. (1. 27) and 20 % lower than Eq. (1. 29). From the calculation results, Eq. (1. 27) and Eq. (1. 29) have the possibility to give a prediction of the buckling moment that is on the unsafe side.

In elastic analysis, the buckling strength of shorter pipes is greater than longer pipes, because the effect of the boundary condition on the oval deformation at the mid span of the pipe is larger. In elasto-plastic analysis, the buckling moment is almost constant regardless of pipe length, because the maximum bending moment is limited by yielding. In the cases of *D/t* =200, in which the pipes buckle more elastically than *D/t* = 50 and 100, the buckling strength of shorter pipes are a little bit higher than longer pipes, even in the elasto-plastic analysis.

For thick pipes, such as *D/t* = 50, the difference of the buckling moment between elastic and elasto-plastic analysis is very large. But for a thin pipe, such as *D/t* = 200, the difference is not so large. This means that the pipes with a large *D/t* value buckle elastically and the pipes with a small *D/t* value buckle in the elasto-plastic region.

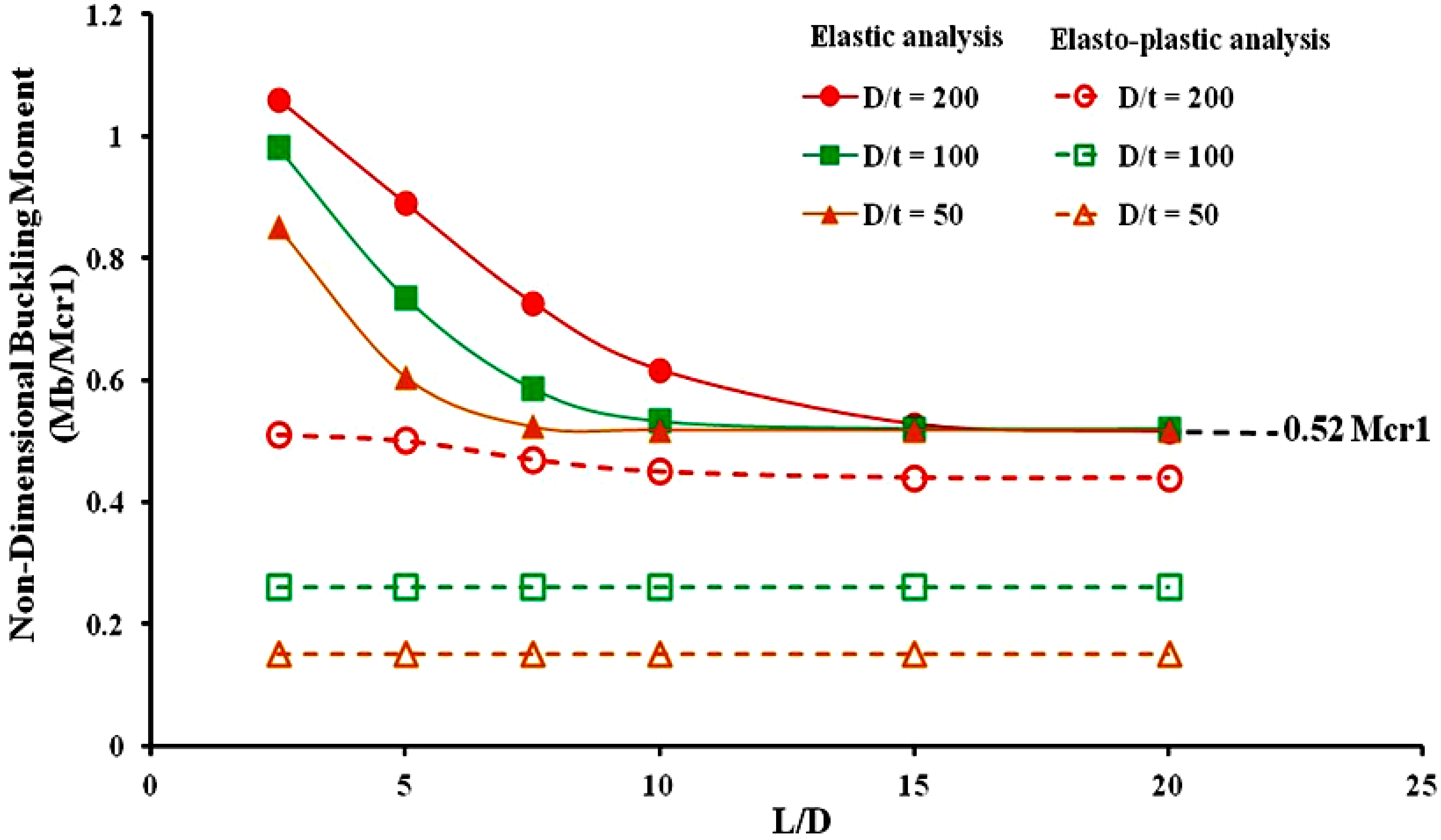

Figure 3-11.Relationship between buckling moment and *L/D* for straight pipe, $\sigma_Y = 621$ MPa

Table 3-4. The nonlinear buckling moment in elastic and elasto-plastic analysis

	L/D	M_b / M_{cr1} Elastic Analysis	M_b / M_{cr1} Elasto-Plastic Analysis
D/t = 50	2.5	0.85	0.15
	5	0.6	0.15
	7.5	0.52	0.15
	10	0.52	0.15
	15	0.52	0.15
	20	0.52	0.15
D/t = 100		0.98	0.26
	5	0.74	0.26
	7.5	0.59	0.26
	10	0.53	0.26
	15	0.52	0.26
	20	0.52	0.26
D/t = 200	2.5	1.06	0.51
	5	0.89	0.50
	7.5	0.73	0.47
	10	0.62	0.45
	15	0.53	0.44
	20	0.52	0.44

The relationship between the buckling moment and *D/t* is shown in Figure 3-12. The elastic numerical results are plotted with solid curves, and the elasto-plastic numerical results are plotted with dotted curves, similarly to Figure 3-11.

For the pipe with a small *D/t* or with a large *D/t* and small *L/D*, the difference of the buckling moment between elastic and elasto-plastic analysis is large. On the other hand, for the pipe with large *D/t* and large *L/D*, the difference is small. The elastic buckling stress of the former pipe is larger than the latter, and then the former pipe buckles more plastically than the latter. Therefore, the difference in buckling strength of the former pipe in elastic and elasto-plastic analysis is large.

When the pipe has small *D/t* value, the difference of the buckling moment between elastic and elasto-plastic analysis is very large. But for pipes with a large *D/t* value, the difference is not so large as shown in Figure 3-12. This means that the pipes with a large value of *D/t* buckle elastically and the pipes with a small value of *D/t* buckle in the elasto-plastic region. The short pipe buckles more plastically than the long pipe.

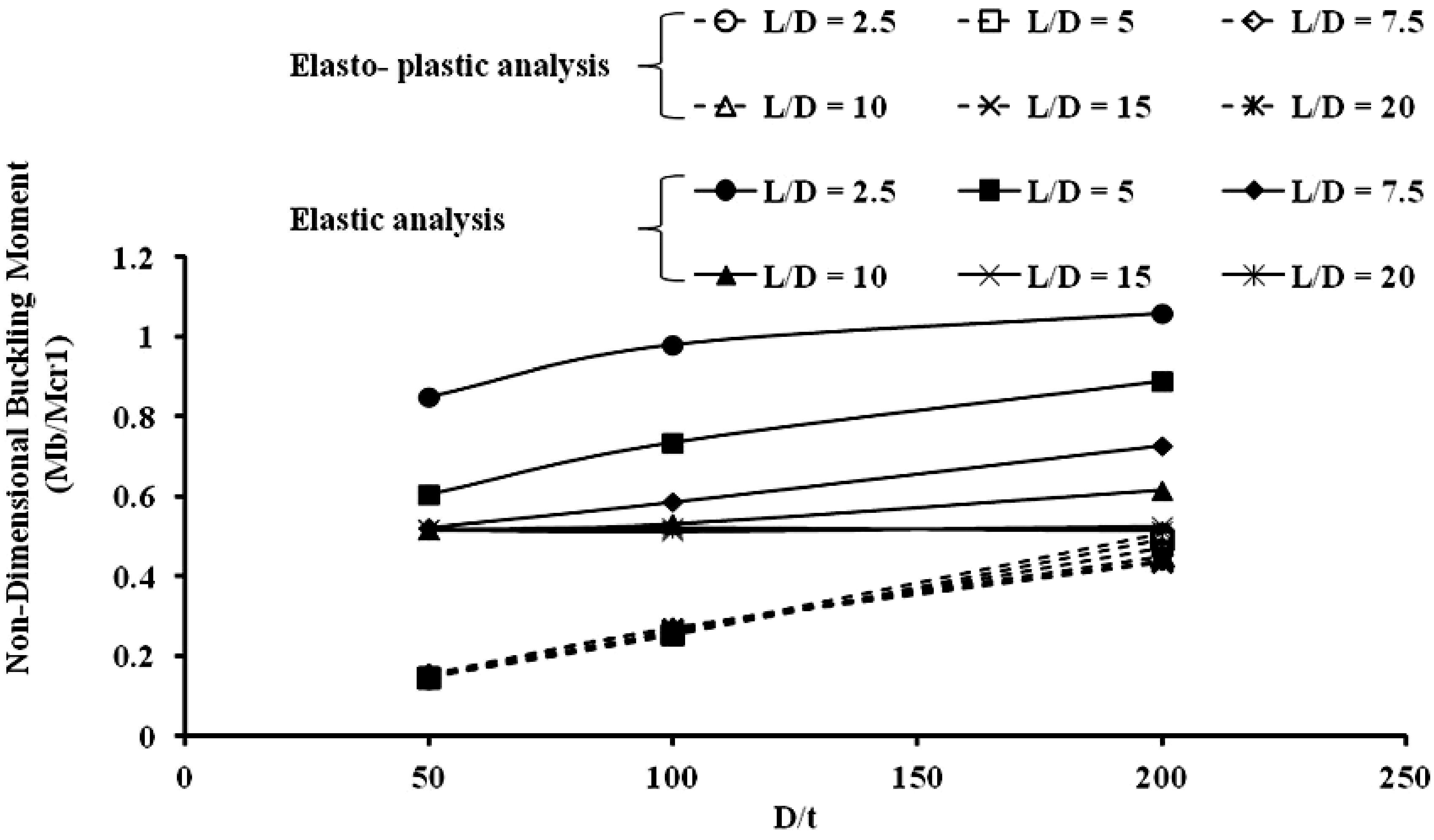

Figure 3-12. Relationship between buckling moment and D/t for straight pipe, $\sigma_Y = 621$ MPa.

To investigate the yielding effect on the buckling strength of pipe in bending, the non-dimensional parameter *(β)* shown below is proposed.

$$\beta = (D/t)(\sigma_Y / E) \propto \left(M_{cr1} / M_Y\right) \tag{3. 3}$$

This parameter is proportionate to the ratio of the linear buckling moment and the initial yielding moment. The elasto-plastic buckling strength is examined by changing the yield stress and the diameter of the pipe.

Figure 3-13 shows the relationship between the buckling moment and *L/D*. The vertical axis is the maximum moment, which is shown non-dimensionally by dividing it with the initial yielding moment (M_Y).

The solid curves are the numerical results for σ_Y = 621 MPa. They show the numerical results for $(D/t)\ (\sigma_Y/E)$ equal to 0.15, 0.3, and 0.6, respectively. In this calculation, the diameter of pipe is taken as the calculating parameter. The dotted curve with the circle marker shows the results for σ_Y = 315MPa and $(D/t)\ (\sigma_Y/E)$ equals to 0.3. Moreover, the dotted curve with a triangle marker represents the results for σ_Y = 1260 MPa and $(D/t)\ (\sigma_Y/E)$ equals to 0.6. The solid and dotted curves with both circle and triangle marker are the pipe with the same value of $(D/t)\ (\sigma_Y/E)$ and with the different yield strength. When the value of $\beta = (D/t)\ (\sigma_Y/E)$ is same, the non-dimensional buckling moment is almost the same.

Therefore, it is possible for β to be the parameter which represents the yielding effect on the buckling strength of pipe under bending. When β is large, the pipes buckle elastically. And when β is small, the pipes buckle in the elasto-plastic region.

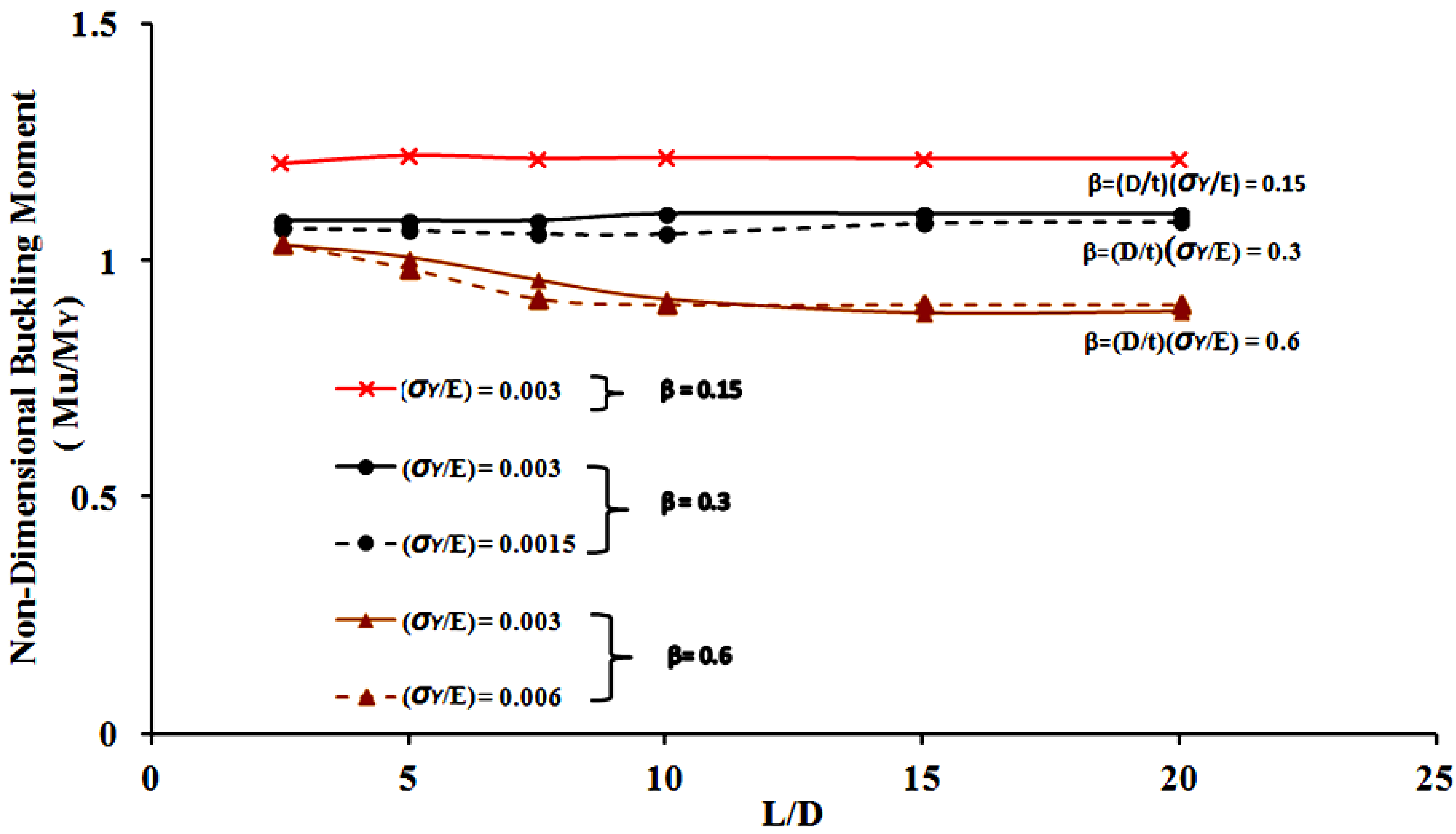

Figure 3-13. Relationship between buckling moment and *L/D* for straight pipe in elasto-plastic analysis

3.3.2 The numerical results on nonlinear buckling strength of curved pipe under pure bending

Figure 3-15 shows the distribution of oval deformation along the pipe length for a curved pipe with *D/t* = 200, in which *R/D* varies from 50 to 200. As the pipe length is 80,000 mm in this calculation, the zero point in the horizontal axis is mid span of pipe and the point of 40,000 mm means the location of pipe end. The maximum oval deformation occurs at the mid span and no oval deformation occurs at both ends of pipe because of boundary condition. The oval deformation decreases with increasing *R/D*. The oval deformation will be uniform all over the pipe without a boundary condition.

For a curved pipe, the stresses which are parallel to the pipe axis have the component of vertical direction in both compression side and tension side as shown in Figure 3-15. These vertical components will result in the oval deformation of the section. The smaller R/D is, the larger the magnitude of the vertical component of axial stress. Therefore, the magnitude of oval deformation at the mid span is inversely proportionate to the value of *R/D*.

The oval deformation of a curved pipe in bending is much more than that of a straight pipe if the same cross section of pipe is used. Therefore, the buckling strength will become smaller when the smaller *R/D* of pipes is used.

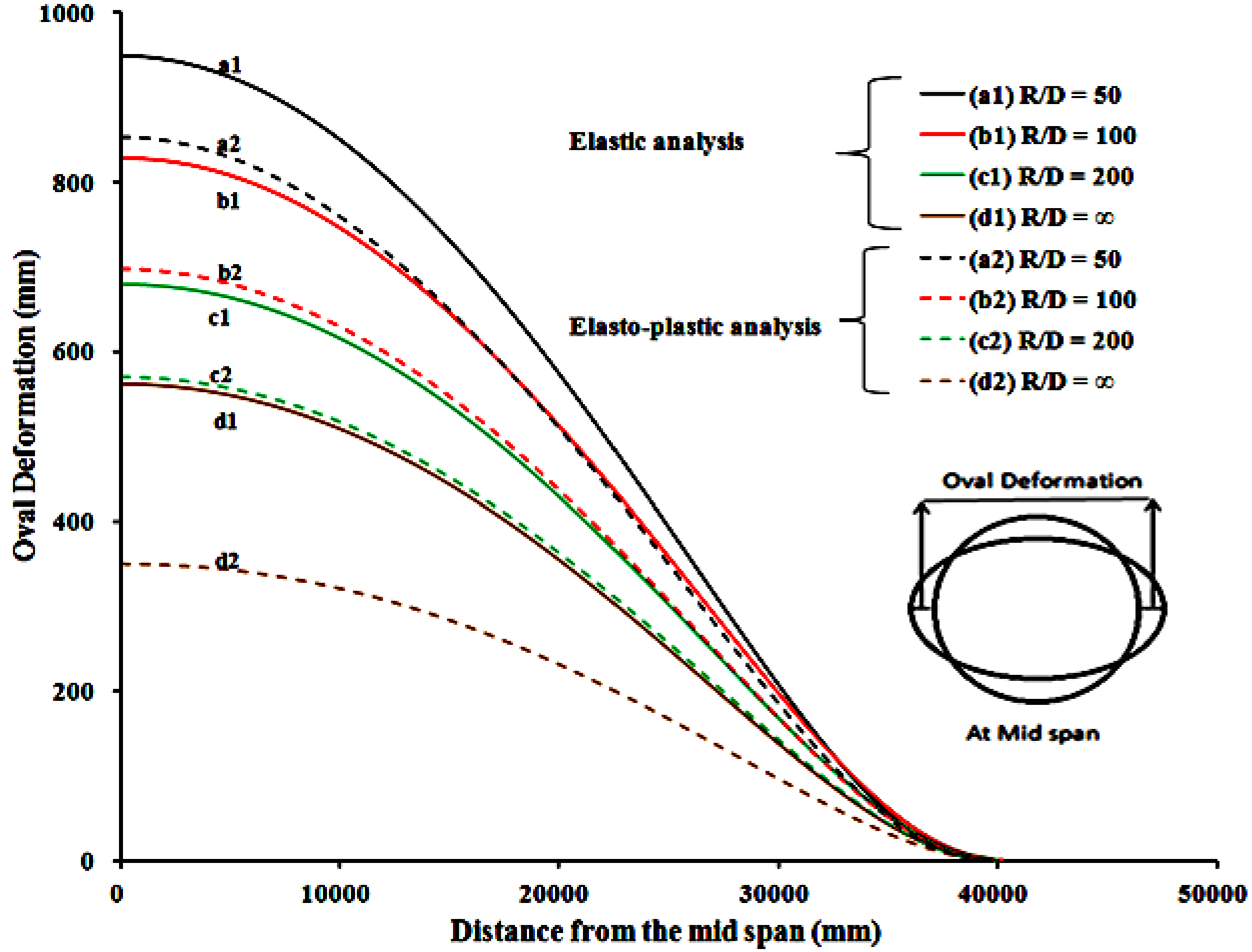

Figure 3-14. Distribution of oval deformation along the pipe length for curved pipe ($L/D = 20$, $D/t = 200$), $\sigma_Y = 621$ MPa.

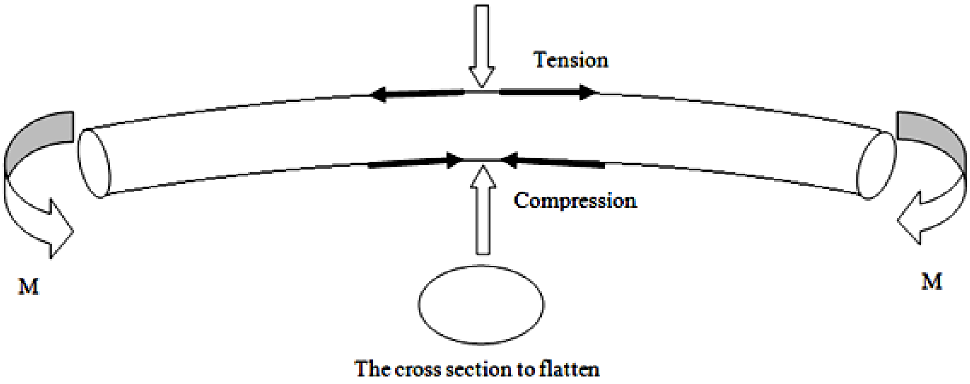

Figure 3-15. The mechanism of oval deformation due to axial stresses in curved pipe under bending

Figure 3-16 shows the relationship between the applied bending moment and the oval deformation at the mid span when the pipe behaves elastically. When decreasing the value of *R/D*, the oval deformation at the mid span increases. The maximum moment of each curve explains the bifurcation buckling moment.

Due to the oval deformation at the mid span, the buckling moment of a curved pipe decreases with decreasing the value of *R/D*.

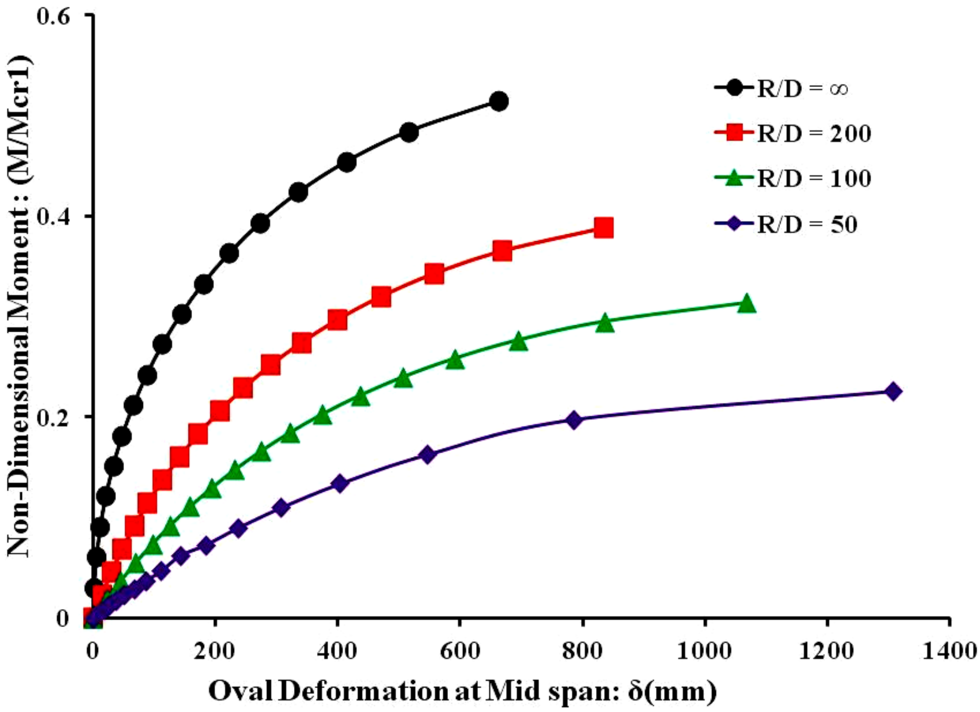

Figure 3-16. Ovalization at the mid span for curved pipe (*L/D* = 20, *D/t* = 200) in elastic analysis.

Figure 3-17 shows the relationship between the applied bending moment and the oval deformation at the mid span, considering the yielding effect of material when the yield strength of material is 621 MPa. In this figure, the elastic numerical results are also plotted with dotted curves. The vertical axis shows the non-dimensional moment *(M/Mcr1)*. The maximum moments considering yielding effect are smaller than that of elastic calculation especially for the pipe with large value of *R/D*.

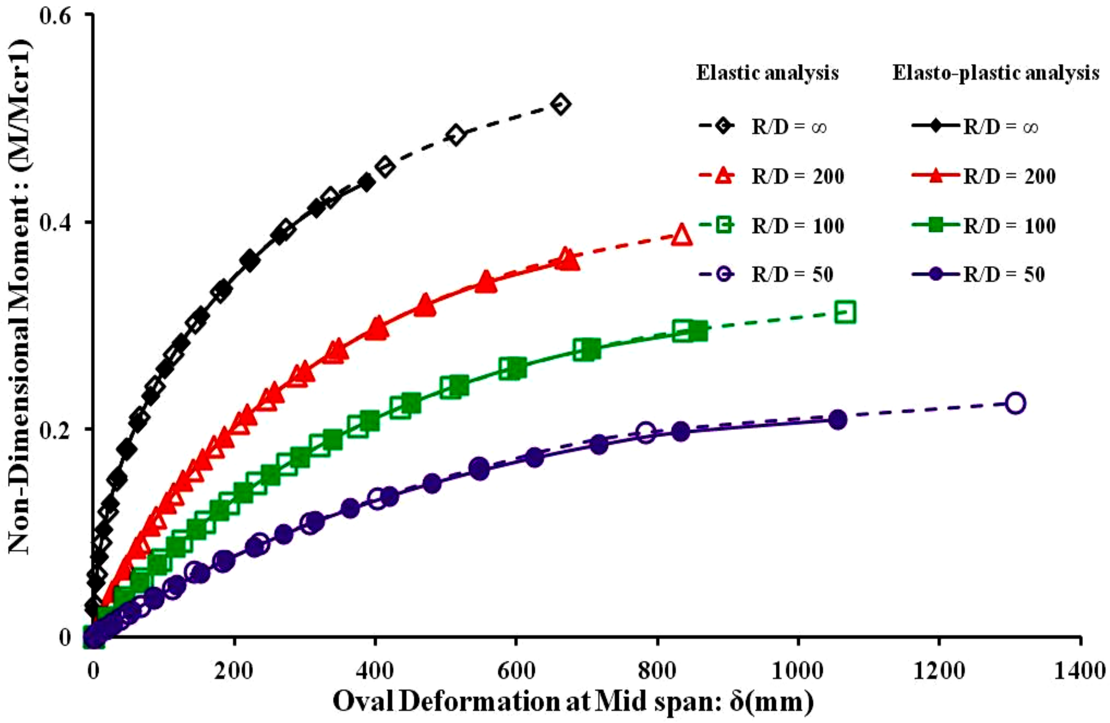

Figure 3-17. Ovalization at the mid span for curved pipe (*L/D* = 20, *D/t* = 200, σ_Y = 621 MPa).

The relationship between the buckling moment and *L/D* is shown in Figure 3-18. In this figure, the elastic numerical results are plotted with solid curves, and the elasto-plastic numerical results are plotted with dotted curves. In elastic analysis, the buckling moment will be decreased with increasing value *L/D* and become constant when the pipe has infinite length. When *L/D* is small, the buckling moment of pipes with different values of *R/D* is similar. It is supposed that the effect of the curvature of a curved pipe on buckling strength is reduced by the effect of constraint at the supported end. As well as in elastic analysis, the buckling moments of small *L/D* are almost the same regardless of the value of *R/D* in elasto-plastic analysis.

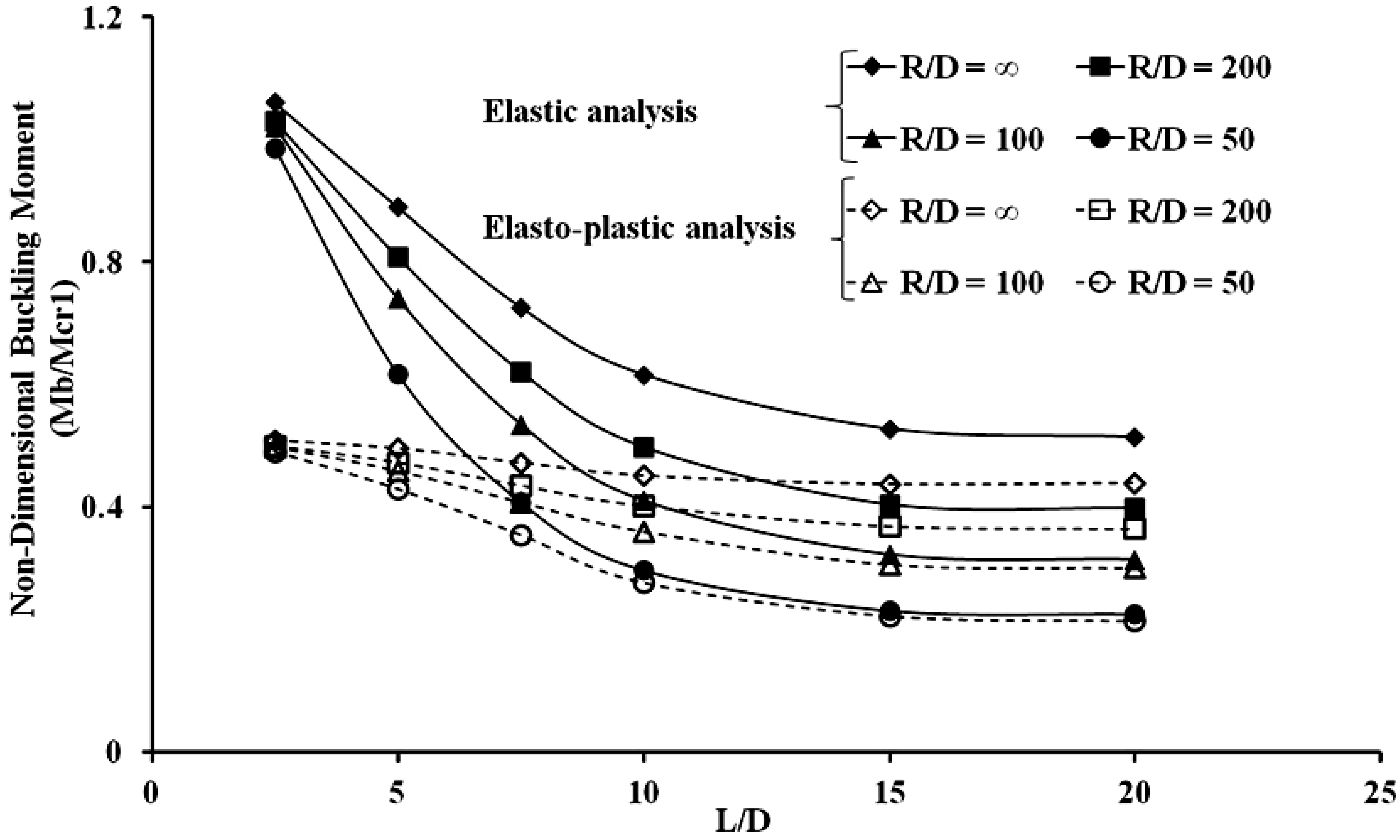

Figure 3-18. Relationship between the buckling moment and L/D for curved pipe ($D/t = 200$, $\sigma_Y = 621$ MPa)

Figure 3-19 shows the difference in the buckling moment between the elastic analysis and the elasto-plastic analysis. The vertical axis represents the non-dimensional buckling moment and the horizontal axis is *R/D*. For a small value of *R/D* and large value *L/D*, the differences between them are very small. It is because the buckling stress is low and the buckling takes place elastically in these cases. On the other hand, the difference is very large for a small value of *L/D*. For pipe with small value of *R/D*, the buckling takes place more elastically than with a large value of *R/D* because of the fact that flexibility of curved pipe in bending will increase with decreasing *R/D*.

As well as the straight pipe, the non-dimensional parameter (β) shown below is considered to investigate the yielding effect on the buckling strength of a curved pipe in bending.

$$\beta = (D/t)(\sigma_Y / E) \propto \left(M_{cr1} / M_Y\right) \qquad (3.\ 3)$$

Figure 3-20 shows the relationship between the buckling moment and *L/D*. The vertical axis is the maximum moment, which is shown non-dimensionally by dividing it with the initial yielding moment (M_Y).

The solid curves are the numerical results for curved pipe of *D/t* = 200 and *R/D* = 200. Solid curves are the results for $(D/t)\ (\sigma_Y/E)$ equals to 0.15, 0.3, and 0.6, respectively. In this calculation, the yield stress of the material is taken as the calculating parameter, that is, σ_Y equals to 157 MPa , 315 MPa, 621 MPa, respectively.

The dotted curve with the cross marker shows the results for *D/t* = 100, *R/D* = 200 and $(D/t)\ (\sigma_Y/E)$ equals to 0.15. Moreover, the dotted curve with a triangle marker defines the results for *D/t* = 100, *R/D* = 200 and $(D/t)\ (\sigma_Y/E)$ equals to 0.6. The solid and dotted curves with both cross and triangle marker are the pipe with same value of $(D/t)\ (\sigma_Y/E)$ and with different yield strength. When the value of $\beta = (D/t)\ (\sigma_Y/E)$ is the same, the non-dimensional buckling moment is almost the same. Therefore, the parameter β is possibly the parameter which represents the yielding effect on the buckling strength of curved pipe under bending. As with the straight pipe, when β is large, the curved pipes buckle elastically. And when β is small, the curved pipes buckle plastically.

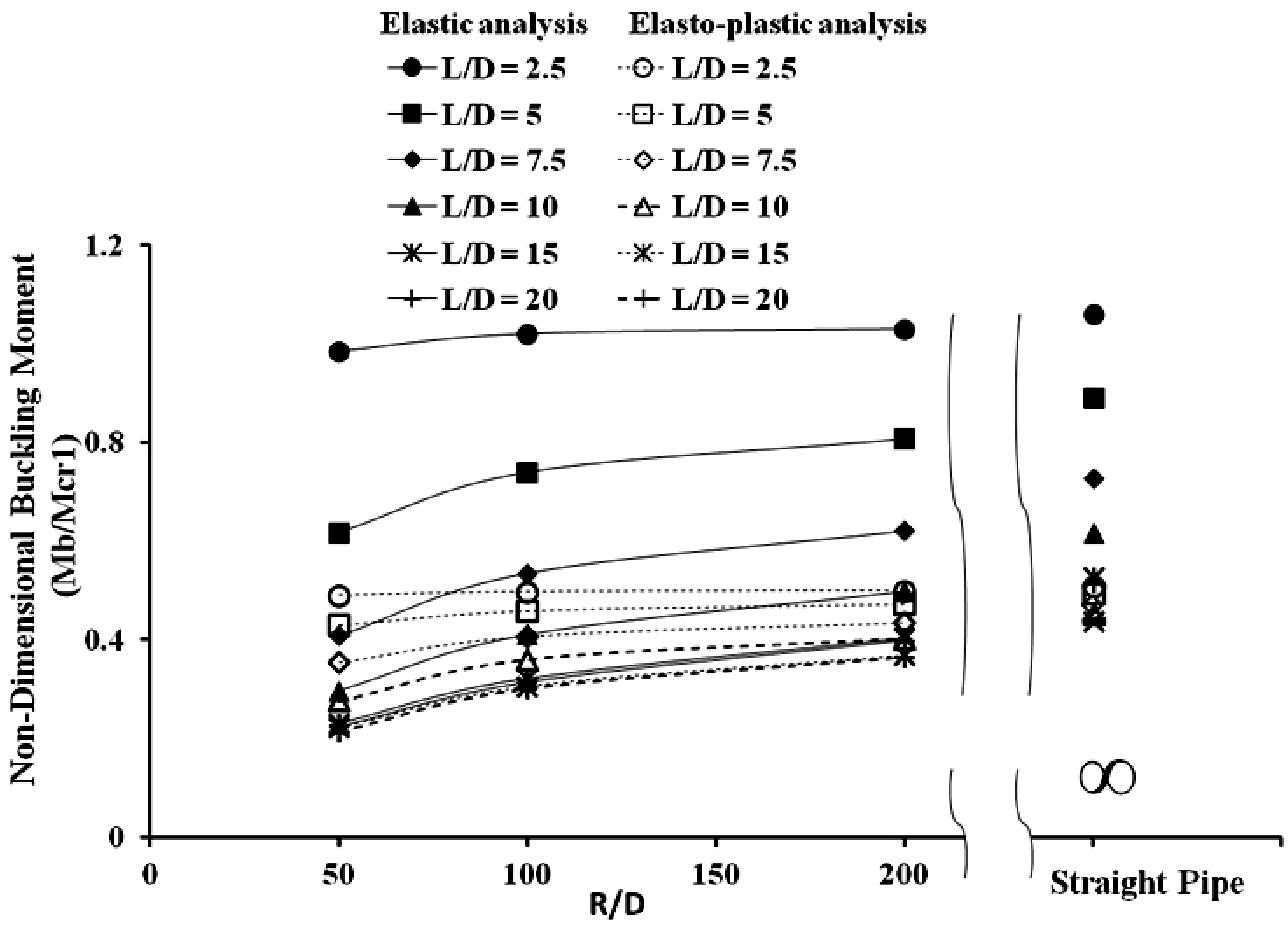

Figure 3-19. Relationship between buckling moment and *R/D* for curved pipe ($D/t = 200$, $\sigma_Y = 621$ MPa)

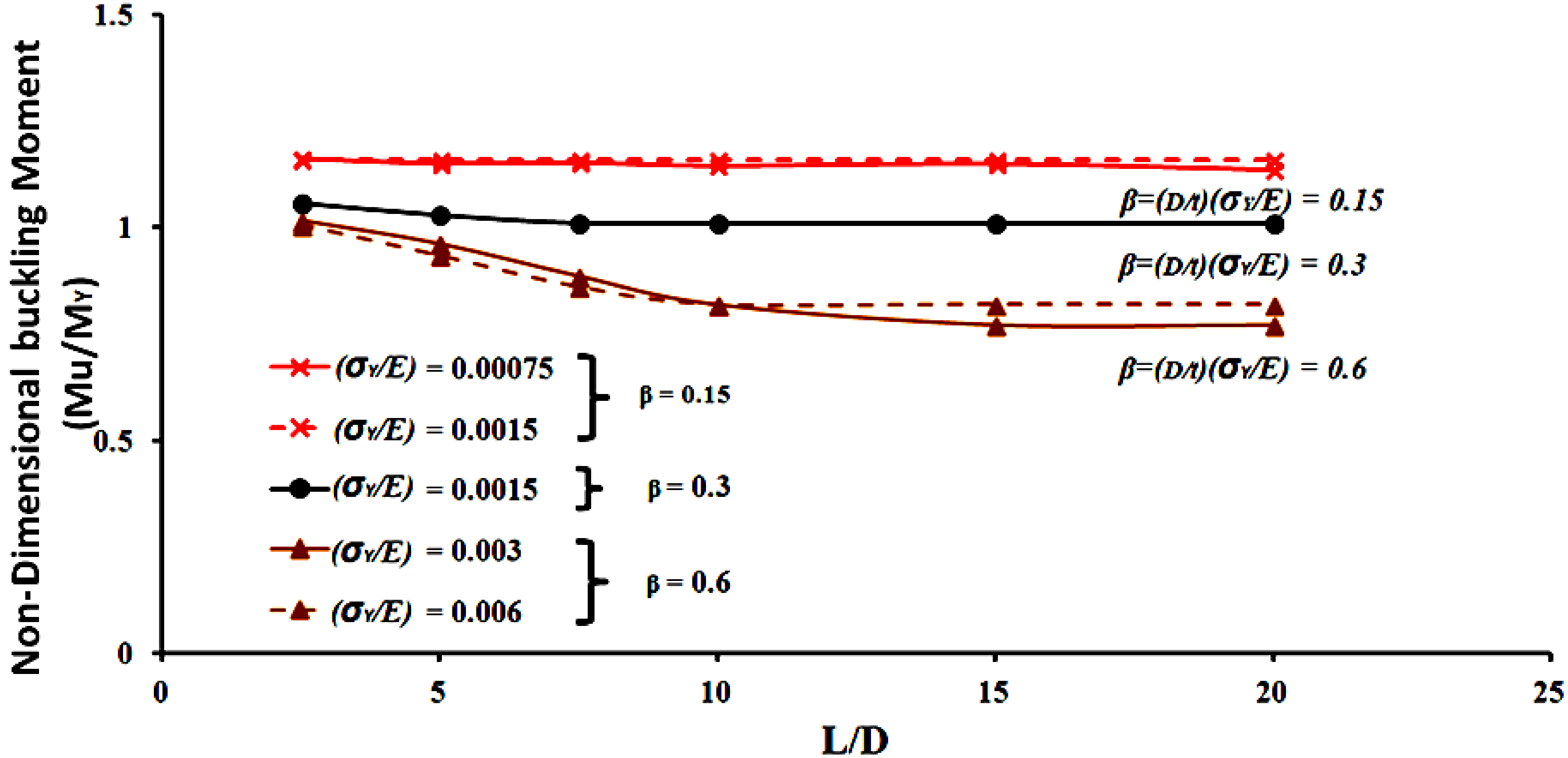

Figure 3-20. Relationship between buckling moment and *L/D* for curved pipe in elasto-plastic analysis (*R/D* = 200)

3.4 Conclusions

In this study, the series of calculations of buckling and collapse strength of straight and curved pipe under bending were performed by utilizing nonlinear *FE* software. In nonlinear calculation, the eigenvalue is calculated at each load increment considering the pre-buckling deformation. The nonlinear buckling load is judged as follows. When the value of eigenvalue is larger than the applied load, the buckling does not happen. Furthermore, when the value of eigenvalue is smaller than the applied load, the buckling has already happened. The cross section point of the eigenvalue and applied load is treated as the bifurcation buckling load.

Utilizing the above mentioned procedure, the nonlinear buckling strength for straight pipe and curved pipe were obtained. The following findings have been clarified by the numerical calculations.

The region of buckling is limited at the compressive side in the vicinity of mid span.

For the straight pipe, the reduction rate of the buckling moment due to oval deformation of pipe was clarified for various values of *L/D* and *D/t* in elastic and elasto-plastic buckling.

In a short pipe, the oval deformation before buckling is small, due to the restriction of sectional deformation at both ends. Therefore, the reduction of buckling strength due to oval deformation is smaller in shorter pipes than longer pipes.

From the results of elastic analysis considering the oval deformation, the maximum moment for long pipes, can be represented as follows:

$$M_{\max} = 0.52 M_{cr1} = 0.314 \pi E r t^2$$

In elasto-plastic analysis, the buckling moment is lower than elastic analysis. The buckling moment is almost constant regardless of the pipe length, if the pipes have the same value of *D/t* smaller than 200. This is because the maximum bending moment is limited by yielding. The pipes with a small *D/t* buckle more plastically, and the pipes with a small *L/D* buckle more plastically because of the restriction of the sectional deformation at both ends.

The non-dimensional parameter β is proposed. The parameter of $\beta = (D/t)\ (\sigma_Y/E)$ is possibly the parameter which represents the yielding effect on buckling strength of pipe under bending. Using Figures 3-13 and 3-20, the buckling moment can be predicted without *FEA*.

The buckling moment of the curved pipe is smaller than in the straight pipe, because the oval deformation is larger. The oval deformation increases when *R/D* decreases. This is because that the axial stresses in bending have a larger component of vertical direction in the pipe with smaller *R/D*, than the pipe with larger *R/D.* Flexibility of a curved pipe in bending increases with decreasing *R/D*, while the oval deformation is remarkable for large *L/D* as with the straight pipe.

Chapter IV

The Effect of Initial Imperfection on Buckling Strength for Straight and Curved Pipe under Pure Bending

4.1 Introduction

It is important to predict the buckling strength of straight and curved pipe on designing the offshore pipelines. The various kinds of loads, such as axial compression, external pressure and bending are applied to the offshore pipelines.

The buckling phenomenon for straight and curved pipe under pure bending was explained in Chapter III. For straight pipes under pure bending moment, the nonlinear *FEA* considering the effect of the cross sectional oval deformation was performed by changing the geometrical parameters of pipes. The parameters in the calculations were the ratio of length to diameter (*L/D*) varying from 2.5 to 20 and the ratio of diameter to thickness (*D/t*) varying from 50 to 200. From the numerical results obtained in Chapter III, the maximum moment for long pipe considering oval deformation is shown as follow:

$$M_{\max} = 0.52 M_{cr1} = 0.314 \pi E r t^2 \tag{4. 1}$$

Eq. (4. 1) is the numerical result for perfect pipe. The buckling strength of a pipe is much reduced as a result of initial imperfections. But, the comprehensive study of the effect of initial imperfection on buckling strength of pipe under bending has not been undertaken.

In this Chapter, the effect of initial imperfection on the buckling strength of a straight pipe under bending will be investigated by nonlinear *FEA*, considering the effect of a cross sectional oval deformation by changing the variables of pipes. These variables will be *L/D* varying from about 2.5 to 20, *D/t* varying from about 50 to 200 and also with imperfection (δ_o/t) varying 0.05 to 0.5. Moreover, the buckling strength of curved pipes (*D/t* = 200) will be investigated by changing *R/D* from 50 to 200 and with imperfection (δ_o/t) varying 0.05 to 0.5. As well as the elastic buckling, the elasto-plastic buckling will investigated. The effect of buckling mode and oval mode of imperfection are also investigated in this chapter.

In this study, the series calculations of buckling and collapse strength of imperfect straight and curved pipe under bending are performed by utilizing nonlinear *FE* software.

4.2 Procedures of Calculation for Estimating Nonlinear Buckling Strength of Imperfect Pipe under Bending

4.2.1 Parameters for calculation

In calculation of straight pipe, the ratio of length to diameter *(L/D)* and the ratio of diameter to thickness *(D/t)* are taken as the calculation parameters. *L/D* varies from 2.5 to 20, in which the diameter is changing from 1000 to 4000 mm. And *D/t* varies from 50 to 200. Where, *D* is the pipe diameter, *t* is the wall thickness, and *L* is the pipe length as shown in table 3-1.

In calculation of a curved pipe, the pipe diameter is originally fixed to 4000 mm, and the thickness is fixed to 20 mm. *L/D* varies from 2.5 to 20 by changing the pipe length. *(R/D)* varies from 50 to 200 as shown in table 3-2. Where, *R* is radius of curvature of a curved pipe as shown in Figure 3-2.

As well as for perfect pipe under pure bending, in calculation of the elasto-plastic analysis for imperfect pipe under pure bending, the yield stress of material assumed to be 621 MPa which is the yield stress of material API X80. The elasto-prefect material is choosed in the numerical analysis. It means strength hardening after yielding has not been considered.

4.2.2 Model for calculation and calculation program

The full length models of straight and curved pipes with initial imperfection are used in *FEA* as shown in Figure 4-1. The nonlinear buckling calculations of pipe under pure bending are performed. In this model, the initial imperfection of buckling mode, which can be obtained by linear buckling calculation for perfect pipe as shown in Figure 2-4, is introduced.

General purpose *FE* software - MSC Marc is used for the nonlinear buckling analysis in which the oval deformation of cross section before buckling is taken account. The quadrilateral 4 node element (No.75) is used. The calculating region is divided into 36 elements in circumferential direction. The element number in length is basically 120 and more elements are used to maintain the calculation accuracy in the case of long cylinder. The mesh convergence study was carried out in chapter III.

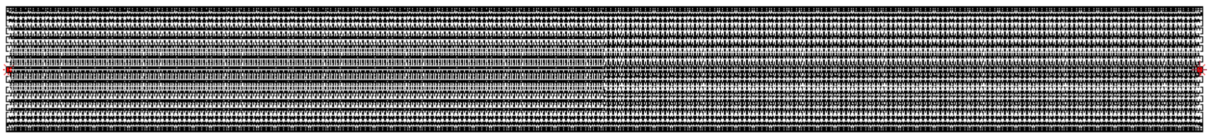

(a)

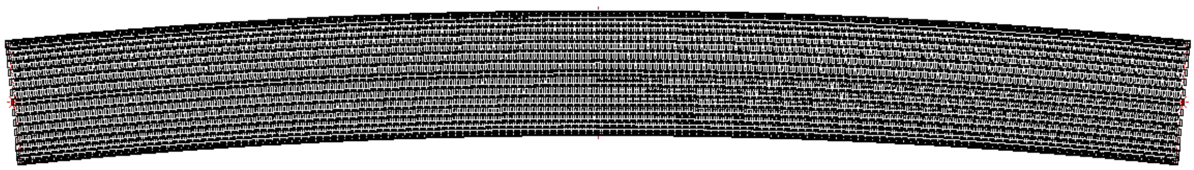

(b)

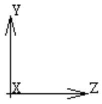

Figure 4-1. Finite element modelling for full imperfect pipe
(a) the straight pipe, (b) the curved pipe

4.2.3 Boundary conditions and loading conditions

The cylindrical coordinates are used. The boundary conditions $U_Z = 0$ are given at the mid span of the cylinder and $U_\Theta = 0$ at four points as shown in Figure 4-2.

The rigid body elements *(RBE)* are inserted at both end sections in order to connect the centre of circle and the points on circle as shown in Figure 4-2. The bending moment is loaded at the centre of circle at both ends. The rigid body elements (*RBE*) prevent the oval deformation of both end section, and keep the section in plane under rotational deformation by bending moment. In MSC Marc, a rigid link for either small deformation or large deformation can be implemented by using tying or using *RBE*

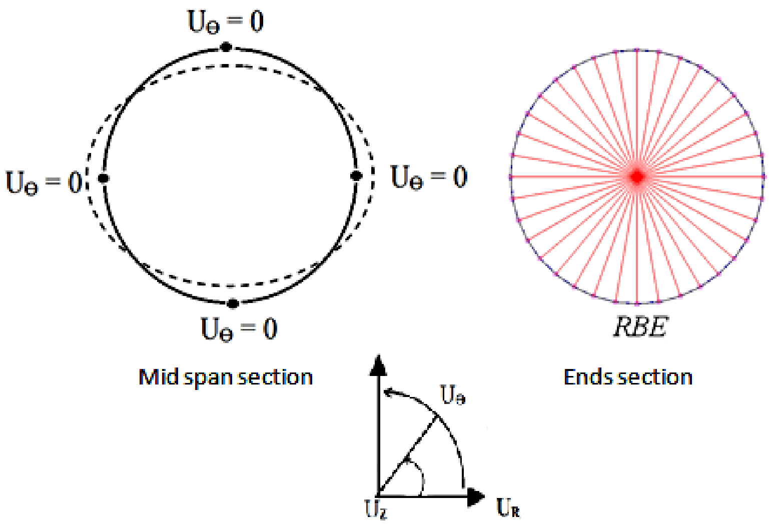

Figure 4-2. Mid span section & *RBE* at both end section

4.2.4 Method to obtain bifurcation moment in nonlinear calculation

To obtain the bifurcation buckling moment and its mode, the eigenvalues are calculated at each load increment, considering the pre-buckling deformation. The buckling load is judged as follows. When the eigenvalue is larger than the applied load, buckling does not happen. And when the eigenvalue is smaller than the applied load, the buckling has already happened. The cross section point at which the applied moment coincides with the eigenvalue as shown in Figure 3-5, is treated as the buckling load.

4.3 The Numerical Results on Nonlinear Buckling Strength of Imperfect Straight Pipe under Pure Bending

Figure 4-3 shows the relationship between the applied bending moment and the oval deformation at the mid span when the pipe behaves elastically. In this figure, the results for the pipe with *D/t* =200 are shown.

The vertical axis shows the non-dimensional moment *(M/Mcr1)*. The red curves are numerical results for the pipes without imperfection and the black curves are numerical results for the pipes with imperfection of buckling mode, δ_o /t = 0.05. Where, δ_o is the maximum amplitude of imperfection. The buckling strength for the imperfect pipe is lower than the original pipe; especially for short pipe (where *L/D* is small).

In longer pipes, such as *L/D* = 10, 15 and 20, the oval deformation increases much with increasing the applied load. On the other hand, in shorter pipes, such as *L/D* =2.5 and 5.0, the oval deformation is small by the restriction of sectional deformation at both ends. The maximum moment of each curve shows the bifurcation buckling moment as explained above.

Figure 4-4 shows the deformation just before buckling at the mid span for the original pipe of *D/t* = 200. Where, figure (a) and (b) are for the pipe of *L/D* = 2.5 and *L/D* = 20, respectively. The oval deformation at the pre-buckling stage is more remarkable in a long pipe (*L/D* = 20) than in a short pipe (*L/D* = 2.5). Due to the oval deformation before buckling at the mid span, the maximum moments of long pipes reduced more compared to the short pipes.

Figure 4-5 shows the deformation just before buckling at the mid span for the pipe of *D/t* = 200 with the imperfection of buckling mode δ_o /t = 0.05. Where figure (a) and (b) are for the pipe of *L/D* = 2.5 and *L/D* = 20, respectively. In a long pipe, the oval deformation is dominant. On the other hand, the deformation of buckling mode grows in a short pipe.

Therefore, the reduction of buckling strength due to imperfection is larger in shorter pipes than in longer pipes.

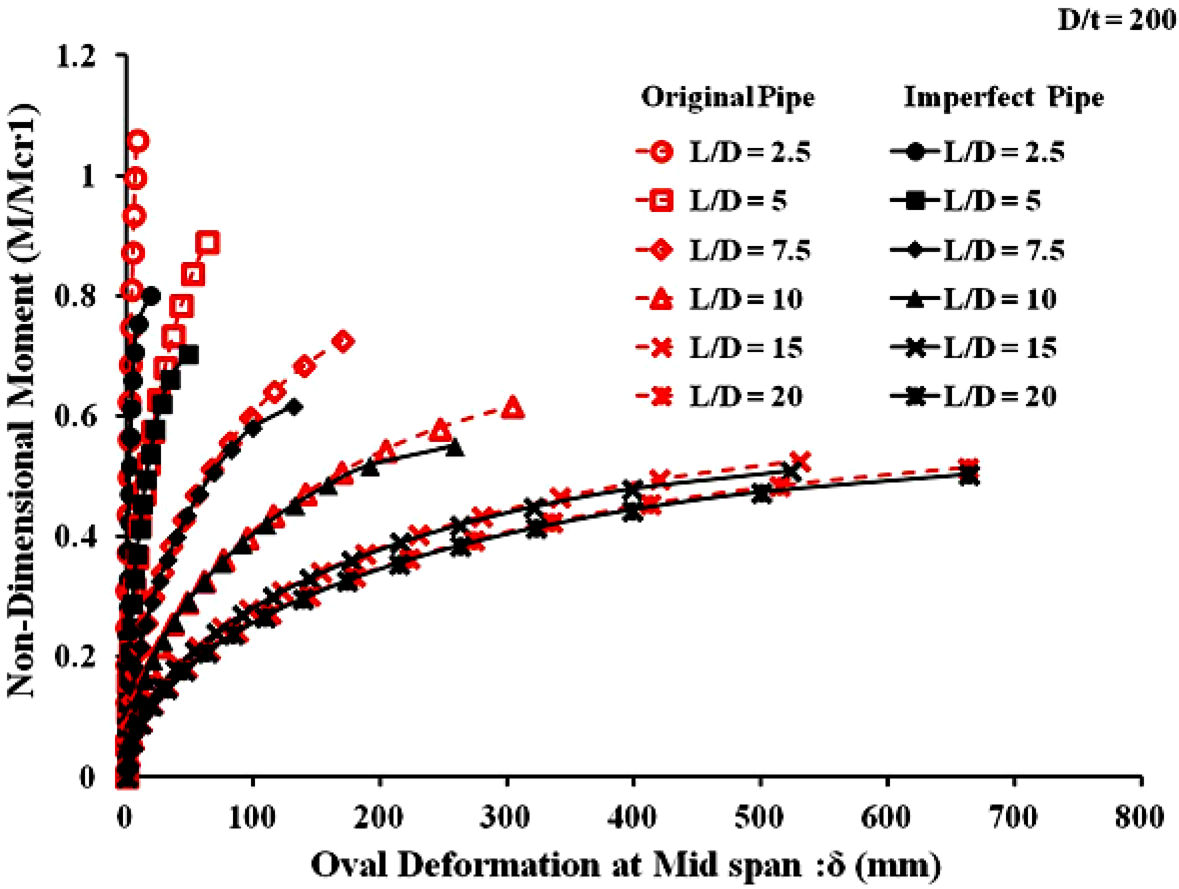

Figure 4-3. Relationships between the applied moment and oval deformation at the mid span for the perfect pipe and the imperfect pipe in elastic analysis (imperfection of buckling mode, $\delta o/t$ = 0.05, D/t = 200)

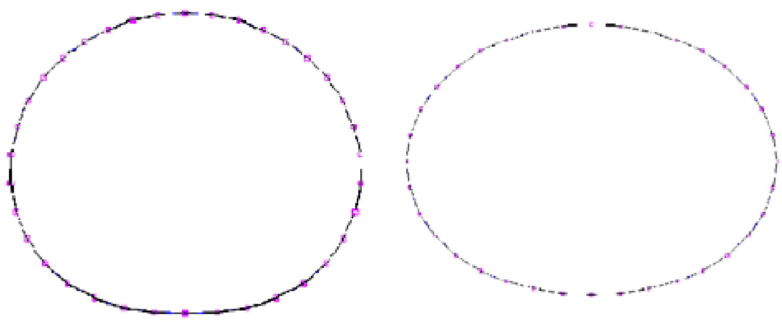

(a) (b)

Figure 4-4. Deformation just before buckling at the mid span for original straight pipe, (a) L/D = 2.5, (b) L/D = 20 (in elastic analysis, D/t = 200)

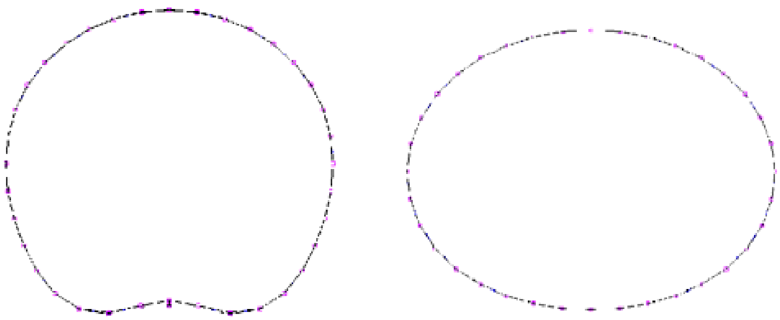

(a) (b)

Figure 4-5. Deformation just before buckling at the mid span for straight pipe with imperfection of buckling mode, δ_o/t = 0.05 (a) L/D = 2.5, (b) L/D = 20 (in elastic analysis, D/t = 200)

Figure 4-6 shows the relationship between the buckling moment and *L/D*. The red curves are the numerical results for pipe without imperfection and the black curves are the numerical results for pipe with imperfection of buckling mode δ_o/t = 0.05. The dotted curves are the elastic numerical results and the solid curves are the elasto-plastic numerical results. In elasto-plastic analysis, the yield stress of material is set to 621MPa.

In elastic analysis, the buckling moment decreases with increasing length of pipe and becomes constant in the longer pipes. As mentioned above, the buckling moment reduces more in shorter pipes than longer pipes due to imperfection. In the longer pipes, the buckling moment is only 3% lower than the original pipe due to the imperfection of $\delta o/t$ = 0.05, where the maximum moment for the original straight pipe is as shown by Eq. (4. 1).

In elasto-plastic analysis, the effect of imperfection for the straight pipes is smaller than in elastic analysis. Moreover, the buckling moments of all length of pipes with same *D/t* are almost same, because the maximum buckling moments are limited by yielding.

Figure 4-7 shows the relationship between the maximum buckling moment *(Mb/Mo)* and the imperfection (δ_o/t) for the straight pipes when the pipes behave elastically. It is shown that the buckling moment decreases with increased imperfection.

The effect of imperfection for shorter pipes such as *L/D* = 2.5 and 5.0 is great. On the other hand the imperfection has a smaller effect on the buckling moment for longer pipes. This is because the effect of oval deformation on buckling strength becomes more significant than the effect of imperfection in the case of longer pipes.

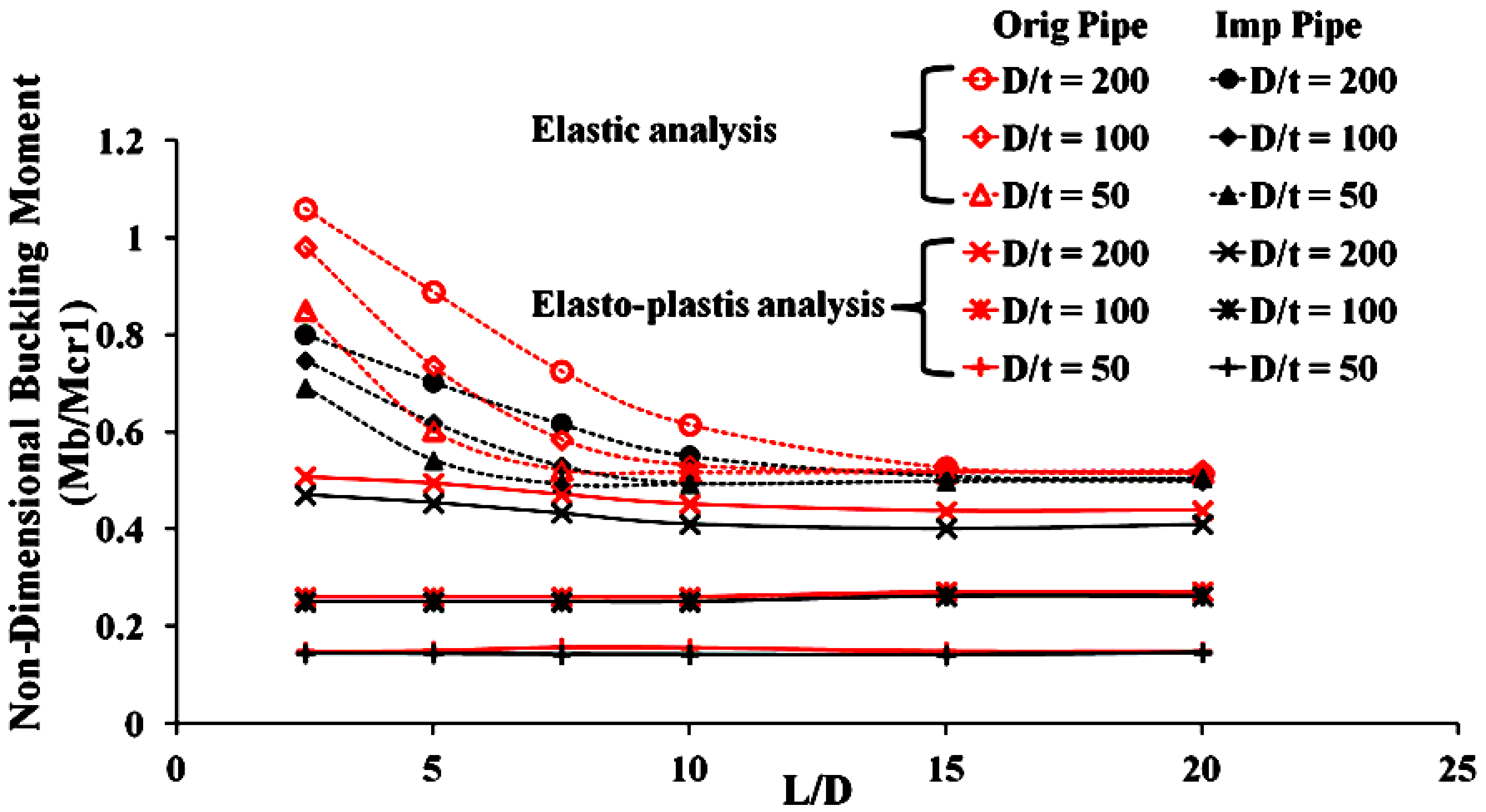

Figure 4-6. Relationships between the buckling moment and *L/D* for original straight pipe and pipe with imperfection of buckling mode $\delta_o/t = 0.05$, $\sigma_Y = 621$ MPa.

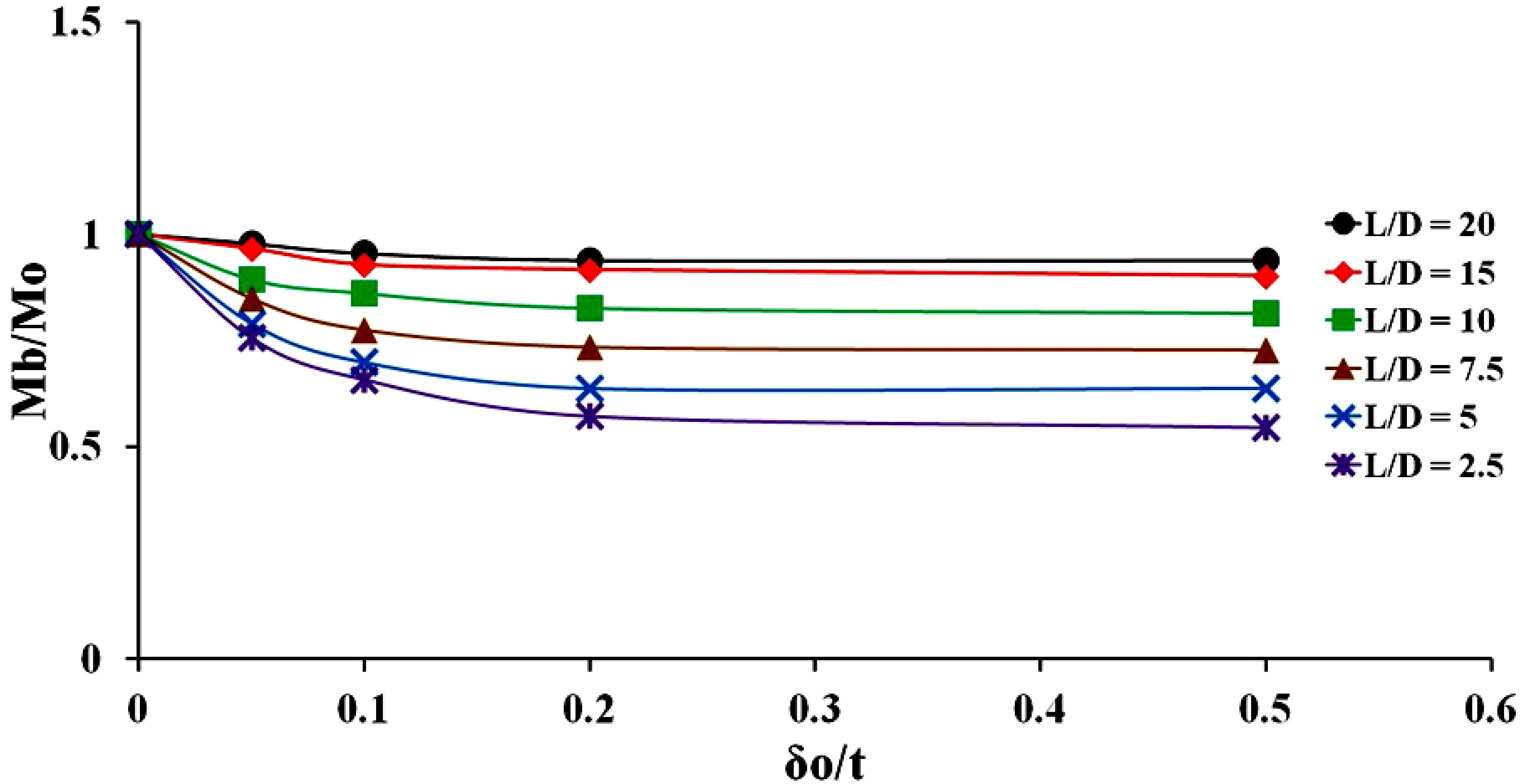

Figure 4-7. Relationship between the maximum buckling moment and the imperfection of buckling mode for straight pipe (in elastic analysis, $D/t = 200$)

From Figure 4-7, it can be seen that the effect of imperfection on the buckling moment is great in shorter pipes. Following this the extent to which the effect of imperfection on buckling moments is affected by *D/t* for short pipes, such as *L/D* =2.5 is examined.

Figure 4-8 shows the relationship between the maximum buckling moment *(Mb/Mo)* and the magnitude of imperfection (δ_o/t), for the straight pipes with different values of *D/t* when pipes behave elastically. This figure shows the effect of imperfection for straight pipes with big values of *D/t* is larger than those with small values of *D/t.*

Figure 4-9 shows the relationship between the applied bending moment and the oval deformation at the mid span when the pipe behaves elastically. The numerical results for perfect straight pipe with a value of *L/D* = 2.5 and a value of *D/t* varying from 50 ~ 200 were presented in this figure. When decreasing the value of *D/t*, the oval deformation at the mid span increases.

From Figures 4-8 and 4-9, it can be said that the effect of imperfection is great when the oval deformation before buckling is small. When seeing Figures 4-3 and 4-7 the same is found - that the effect of imperfection is large when the oval deformation before buckling is small.

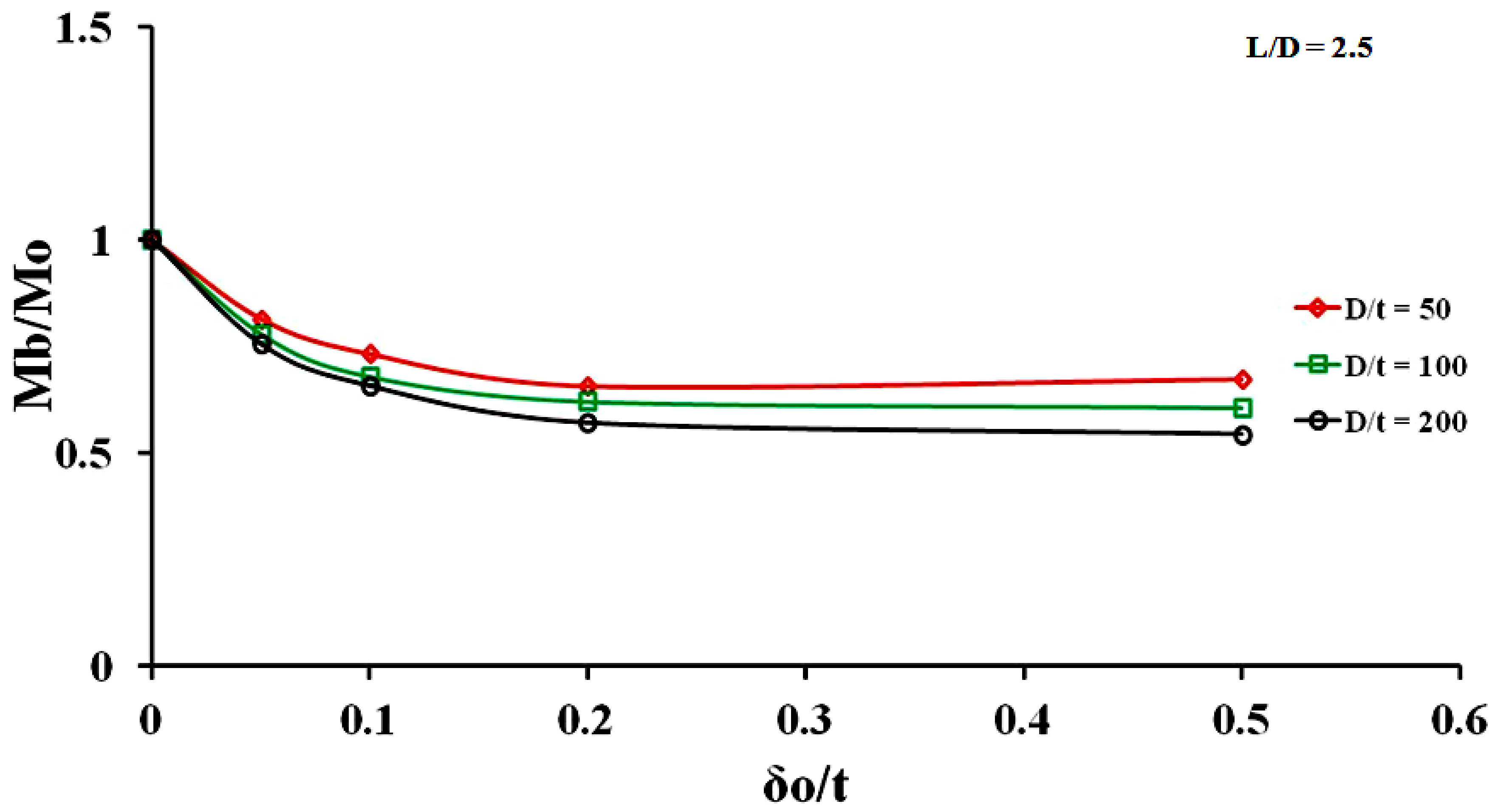

Figure 4-8. Relationship between the maximum buckling moment and the imperfection of buckling mode for straight pipe (in elastic analysis, $L/D = 2.5$)

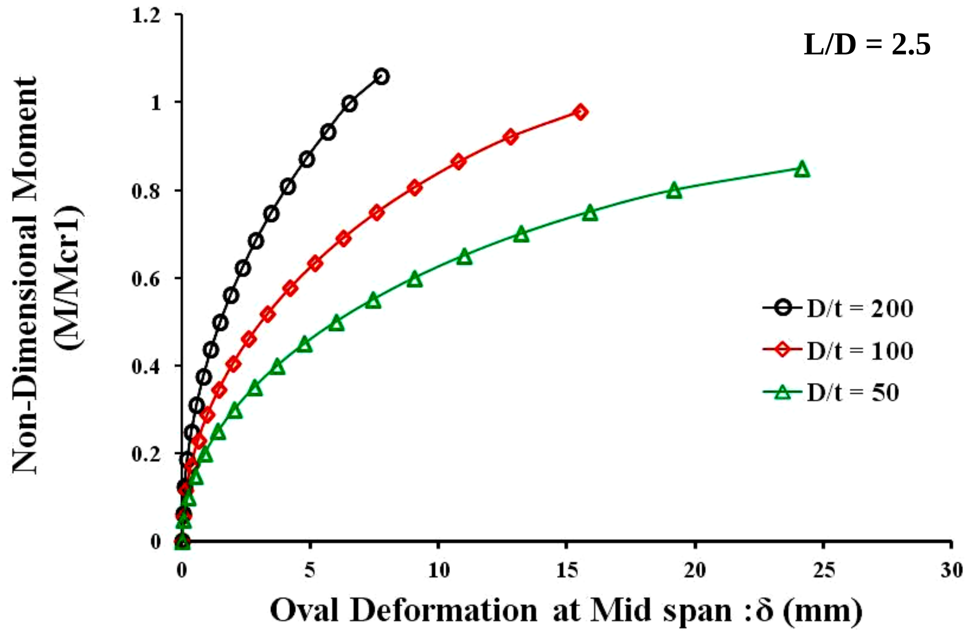

Figure 4-9. Ovalization at the mid span for straight pipe (*L/D* = 2.5 and *D/t* = 50 ~ 200) in elastic analysis

In order to investigate the yielding effect on the buckling strength of pipe in bending, the non-dimensional parameter *(β)* shown below is considered.

$$\beta = (D/t)(\sigma_Y / E) \propto \left(M_{cr1} / M_Y\right) \tag{4. 2}$$

This parameter is proportion to the ratio of the linear buckling moment and the initial yielding moment. The elasto-plastic buckling strength is examined by changing the yield stress and the diameter.

Figures 4-10 and 4-11 shows the relationship between the buckling moment and the imperfection (δ_o/t) for the pipes of *L/D* =2.5 and 20, respectively. The maximum moment is expressed non-dimensionally by dividing with the initial yielding moment (M_Y).

The solid curves with triangle, diamond and rectangular marker are the numerical results for the pipes of *D/t* = 200, whose yield strength are σ_Y = 157.5MPa, 315MPa, and 621MPa, where β equals to 0.15, 0.3 and 0.6, respectively. The dotted curves with triangle, diamond and rectangular marker are the numerical results for the pipes of D/t = 50, whose yield stress is σ_Y = 621MPa, 1260MPa, and 2520MPa, where β equals to 0.15, 0.3 and 0.6, respectively.

When β is large, the pipe buckles elastically. And when β is small, the pipe buckles plastically. The non-dimensional buckling moment with imperfection decreases with increasing the value of β. And, the non-dimensional buckling moments is almost the same for the same value of β. Therefore, the parameter of β is possible to be the parameter which represents the yielding effect on buckling strength of pipe with imperfection under bending. The effect of imperfection on buckling in plastic range is smaller than in elastic range.

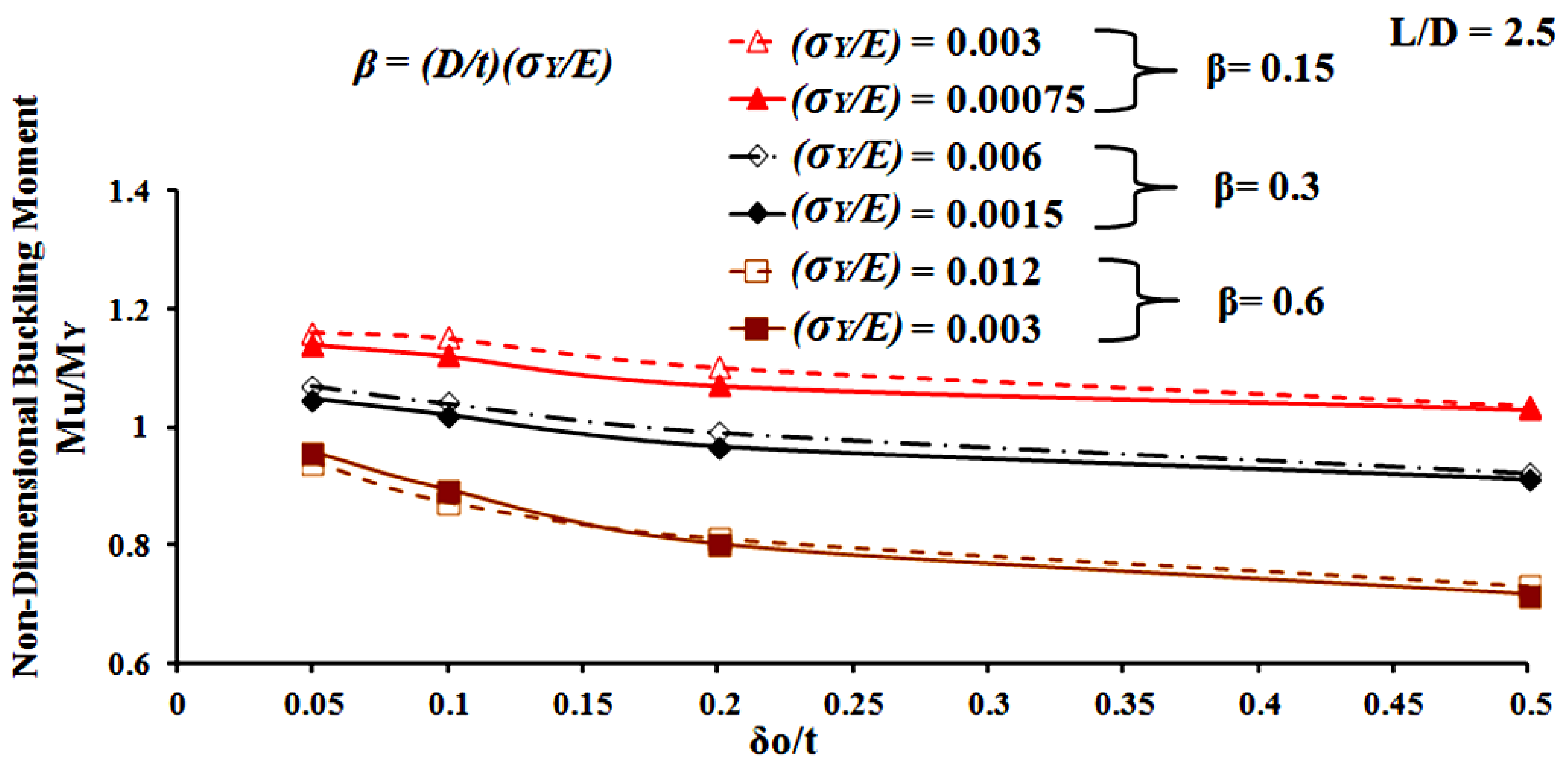

Figure.4-10. Relationship between the maximum buckling moment and the imperfection of buckling mode for straight pipes ($L/D = 2.5$) in elasto-plastic analysis

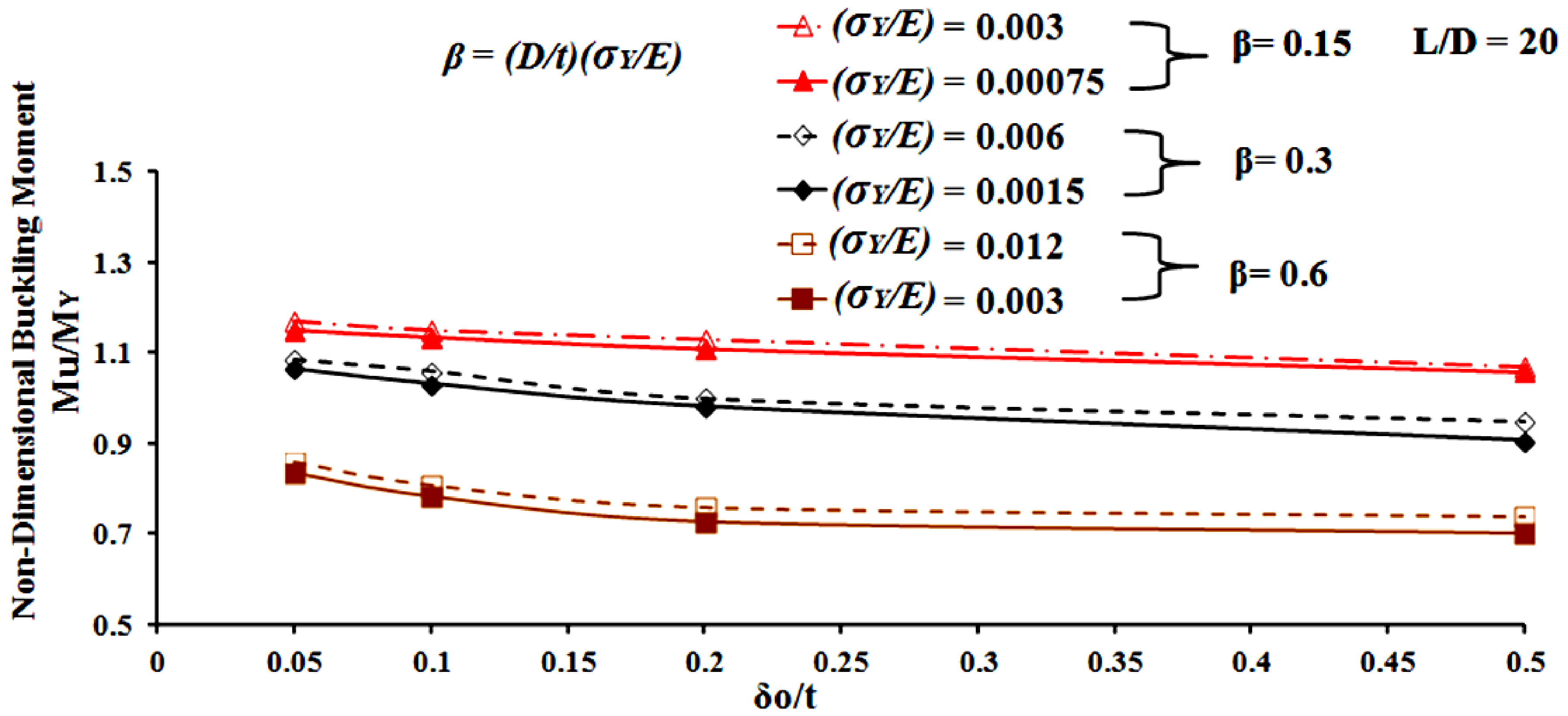

Figure 4-11. Relationship between the maximum buckling moment and the imperfection of buckling mode for straight pipes ($L/D = 20$) in elasto-plastic analysis.

Figure 4-12 shows the effect of imperfection on the buckling moment comparing the imperfection of the buckling mode and the oval mode. In this figure, the elastic numerical results are plotted with dotted curves, and the elasto-plastic numerical results are plotted with solid curves. The curve with a rectangular marker is the original pipe, the curve with diamond marker is the pipe with the imperfection of the oval mode δ_o/t = 0.2 and the curve with a triangle marker is the pipe with the imperfection of the buckling mode δ_o/t = 0.2.

The effects of the imperfections of buckling modes are larger than the effects of imperfections of the oval mode. The imperfection of the buckling mode reduces the buckling strength more than the imperfection of the oval mode, especially for the pipe with a small *L/D*.

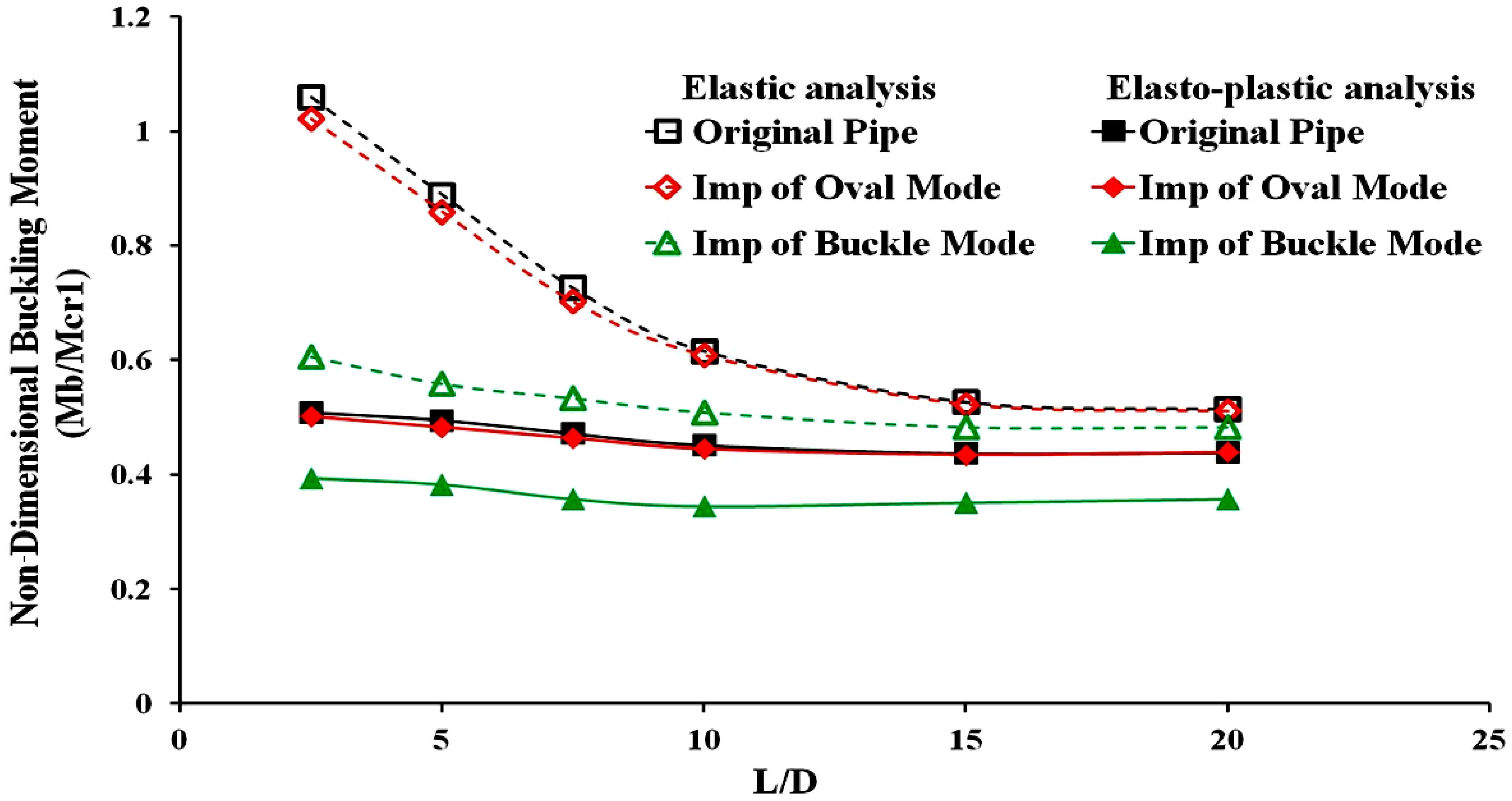

Figure 4-12. Relationships between buckling moment and *L/D* by changing the mode of imperfection for straight pipe

($D/t = 200$, $\delta_o/t = 0.2$, $\sigma_Y = 621$ MPa)

4.4 The Numerical Results on Nonlinear Buckling Strength of Imperfect Curved Pipe under Pure Bending

Figure 4-13 shows the relationship between the applied bending moment and the oval deformation at the mid span for the curved pipe when the pipe behaves elastically. The vertical axis shows the non-dimensional moment *(M/Mcr1)*. The red curves are the numerical results for the pipes without imperfection and the black curves are the numerical results for the pipes with the imperfection of buckling mode, δ_o /t = 0.05.

In longer pipes, such as *L/D* = 10, 15, and 20, the oval deformation increases significantly with the increasing of the applied load. On the other hand, in shorter pipes, such as *L/D* =2.5 and 5.0, the oval deformation is smaller as a result of the restriction of sectional deformation at both ends. The maximum moment of each curve show the bifurcation buckling moment explained above. As well as in straight pipes, the reduction of buckling moment due to imperfection is also larger in shorter pipes than longer pipes in the case of curved pipes.

Figure 4-14 shows the deformation just before buckling at the mid span for the original pipe of *D/t* = 200 and *R/D* = 200. Where, figure (a) and (b) are for the pipe of *L/D* = 2.5 and *L/D* = 20, respectively. As with the straight pipes, the oval deformation in a long pipe (*L/D* = 20) is more remarkable than in a short pipe (*L/D* = 2.5). Due to the oval deformation before buckling at the mid span, the maximum moments of the long pipes reduced more compared to the short pipes.

Figure 4-15 shows the deformation just before buckling at the mid span for the pipe of *D/t* = 200 and *R/D* = 200 with imperfection of buckling mode δ_o/t = 0.05. Where, figure (a) and (b) are for the pipe of *L/D* = 2.5 and *L/D* = 20, respectively. As with the straight pipes, the oval deformation is dominant in a long pipe. On the other hand, the deformation of buckling mode increases in short pipes. Therefore, the reduction of buckling strength due to imperfection is greater in shorter pipes than in longer pipes.

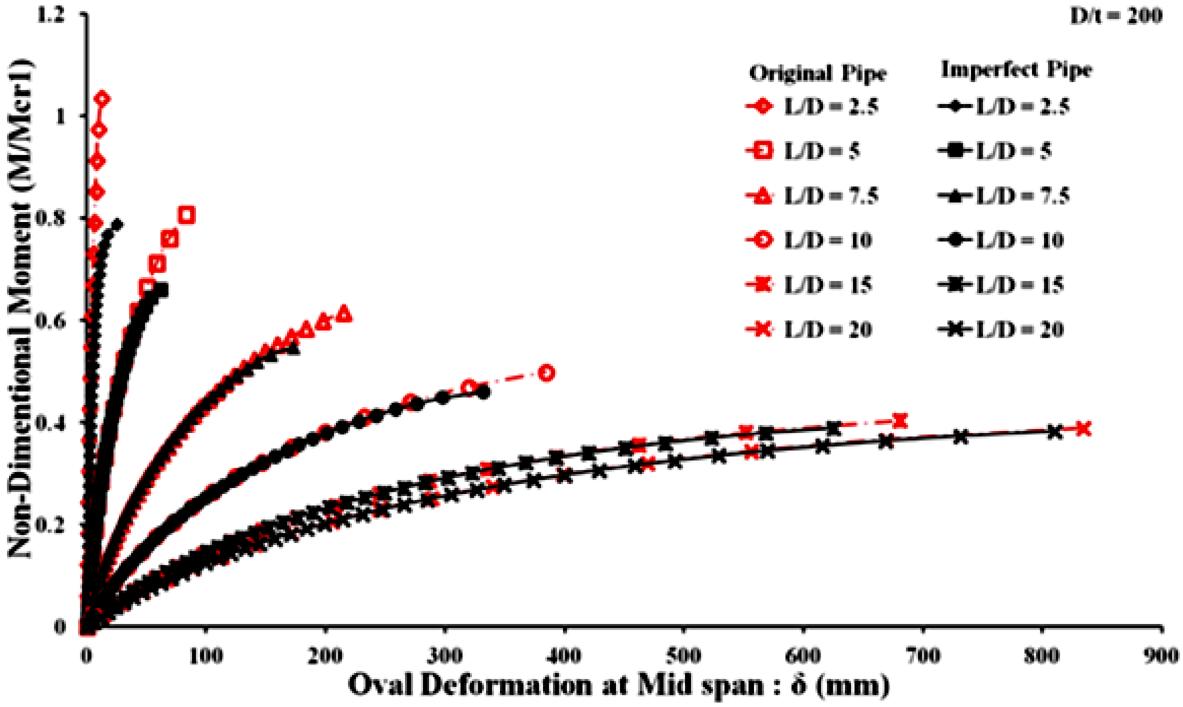

Figure 4-13. Relationships between the applied moment and oval deformation at the mid span for the perfect pipe and the imperfect pipe in elastic analysis (imperfection of buckling mode $\delta_o/t = 0.05$, $D/t = 200$, $R/D = 200$)

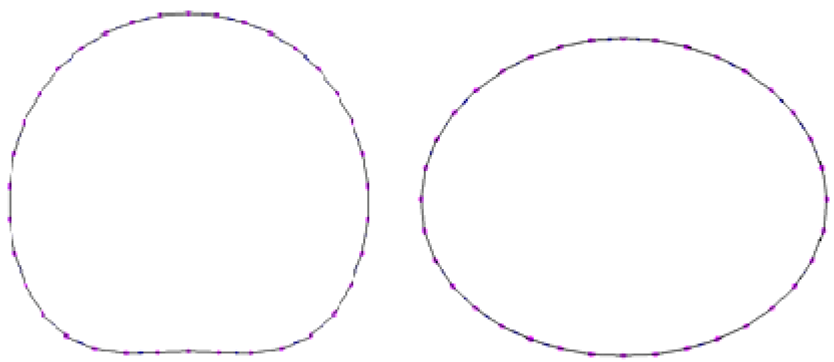

(a) (b)

Figure 4-14. Oval deformation at the mid span for original pipe, (a) $L/D = 2.5$, (b) $L/D = 20$ (in elastic analysis, curved pipe, $D/t = 200$, $R/D = 200$)

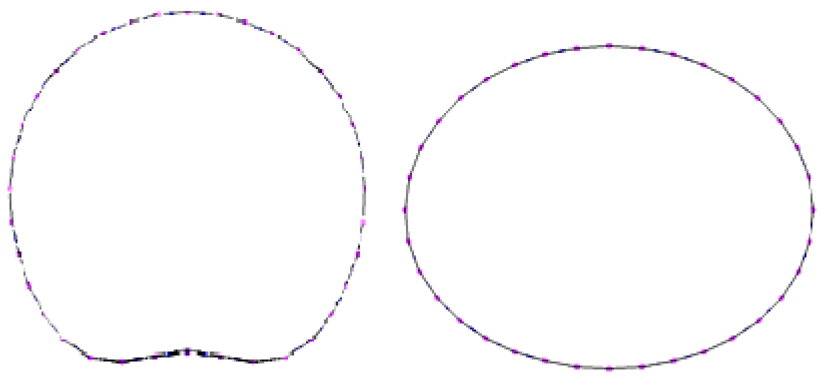

(a) (b)

Figure 4-15. Oval deformation at the mid span for pipe with imperfection of buckling mode δ_o/t = 0.05
(a) L/D = 2.5, (b) L/D = 20 (in elastic analysis, curved pipe D/t = 200, R/D = 200)

Figure 4-16 shows the relationship between the buckling moment and L/D for the straight pipe and the curved pipes of D/t = 200. The curve with circle marker is numerical result for a straight pipe. The curves with diamond marker, rectangular marker, and triangle marker are the numerical results for the curved pipes of R/D = 200, 100 and 50, respectively. The red curves are the numerical results for original pipes and the black curves are the numerical results for the imperfect pipes with δ_o/t = 0.05 when the pipes behave elastically. The buckling moment of curved pipes reduces more when the curvature of pipe increases in both original and imperfect pipes, especially for longer pipes.

The buckling moments for the imperfect pipes are smaller than the original pipes. However, the reduction rate of buckling moment due to imperfection decreases with increasing L/D. Similarly to the straight pipe, it is because the effect of oval deformation on buckling strength becomes larger than the effect of imperfection in the case of longer pipes. For a short pipe such as L/D = 2.5 the effects of imperfection are larger than a long pipe because the oval deformation is small.

Figure 4-17 shows the relationship between the buckling moment and L/D for a straight pipe and curved pipes with imperfection, δ_o/t = 0.05. In this figure, the elastic numerical results are plotted with dotted curves and the elasto-plastic numerical results are plotted with solid curves. In elasto-plastic analysis, the yield strength of material is set to 621MPa

In elastic analyses, the buckling moment decreases with increasing *L/D* values and becomes constant in longer pipes. The non-dimensional buckling moments of pipes with small *L/D* values are almost the same for each value of *R/D.* It is supposed that the effect of curvature of curved pipe on buckling strength is reduced by the constraint effect at the support end. Similarly, the buckling moments of small *L/D* in elasto-plastic analysis are almost the same regardless of *R/D* value.

The buckling moments in elasto-plastic analysis are smaller than in elastic analysis, and the effects of imperfection on buckling moment in elasto-plastic analysis are smaller than in elastic analysis.

For a short curved pipe such as *L/D* = 2.5 the differences in the buckling moment in elastic analysis and elasto-plastic analysis are so large because the short pipe buckles more plastically than the long pipe.

Figure 4-18 shows the relationship between the maximum buckling moment *(Mb/Mo)* and the magnitude of imperfection (δ_o/t), for the curved pipes with different values of *L/D* when pipes behave elastically. The buckling moment decreases with increasing imperfection. The effect of imperfection on the buckling moment for a short pipe such as *L/D* = 2.5 is large, on the other hand the effect is small for a long pipe. The buckling moment becomes constant when a large imperfection exists. Comparing the results of straight pipe as shown in Figure 4-7, no remarkable discrepancy in either tendency or magnitude of the effect of imperfection on buckling strength is found.

Figure 4-19 shows the relationship between the maximum buckling moment *(Mb/Mo)* and the magnitude of imperfection (δ_o/t), for the curved pipes with different values of *R/D* when pipes behave elastically. The figure shows that the effect of imperfection for curved pipe with large values of *R/D* is little bit large. As shown in Figure 3-16, the oval deformation before buckling is larger in curved pipe than straight pipe.

As well as for straight pipe, in changing *D/t* (see Figures 4.8 and 4.9) and *L/D* (see Figures 4.3 and 4.7), the effect of imperfection for the curved pipe become large when the oval deformation is small.

The non-dimensional parameter $(\beta = (D/t)\ (\sigma_Y/E))$ shown by Eq. (4.2) is also considered for the curved pipe in order to investigate the yielding effect on the buckling strength in bending. Figures 4-20 and 4-21 show the relationship between the buckling moment and imperfection (δ_o/t). The vertical axis shows the non-dimensional maximum moment divided by the initial yielding moment (M_Y).

The solid curves with diamond, rectangular and triangle marker are the numerical results for the curved pipe of *D/t* = 200, *R/D* = 200, whose yield stress is σ_Y = 157.5MPa, 315MPa, and 621MPa, where β is equals to 0.15, 0.3 and 0.6 respectively. The non-dimensional buckling moment decreases with increasing the value of β.

The dotted curves with diamond, rectangular and triangle markers are the numerical results for the curved pipes of *D/t* = 100, *R/D* = 200, whose yield stress is σ_Y = 315 MPa, 621MPa and 1260MPa, where β equals to 0.15, 0.3 and 0.6, respectively. The effect of imperfection on the buckling strength in curved pipe is similar to that in straight pipes.

As well as with the imperfect straight pipe, the parameter of β is able to be the parameter which represents the yielding effect on the buckling strength of imperfect curved pipe under bending.

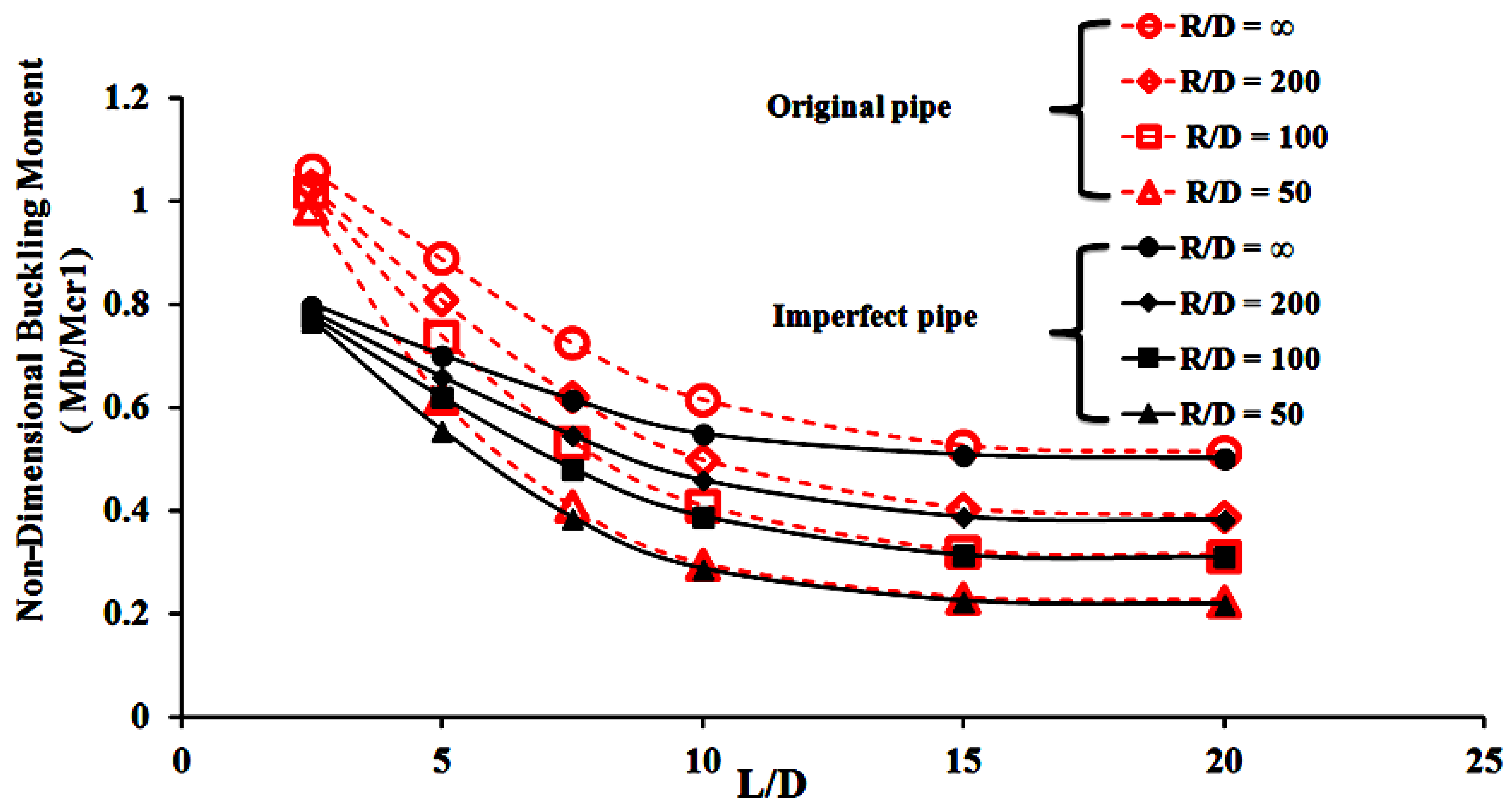

Figure 4-16. Relationship between buckling moment and L/D for original curved pipe and pipe with imperfection of buckling mode $\delta_o/t = 0.05$ (in elastic analysis, $D/t = 200$)

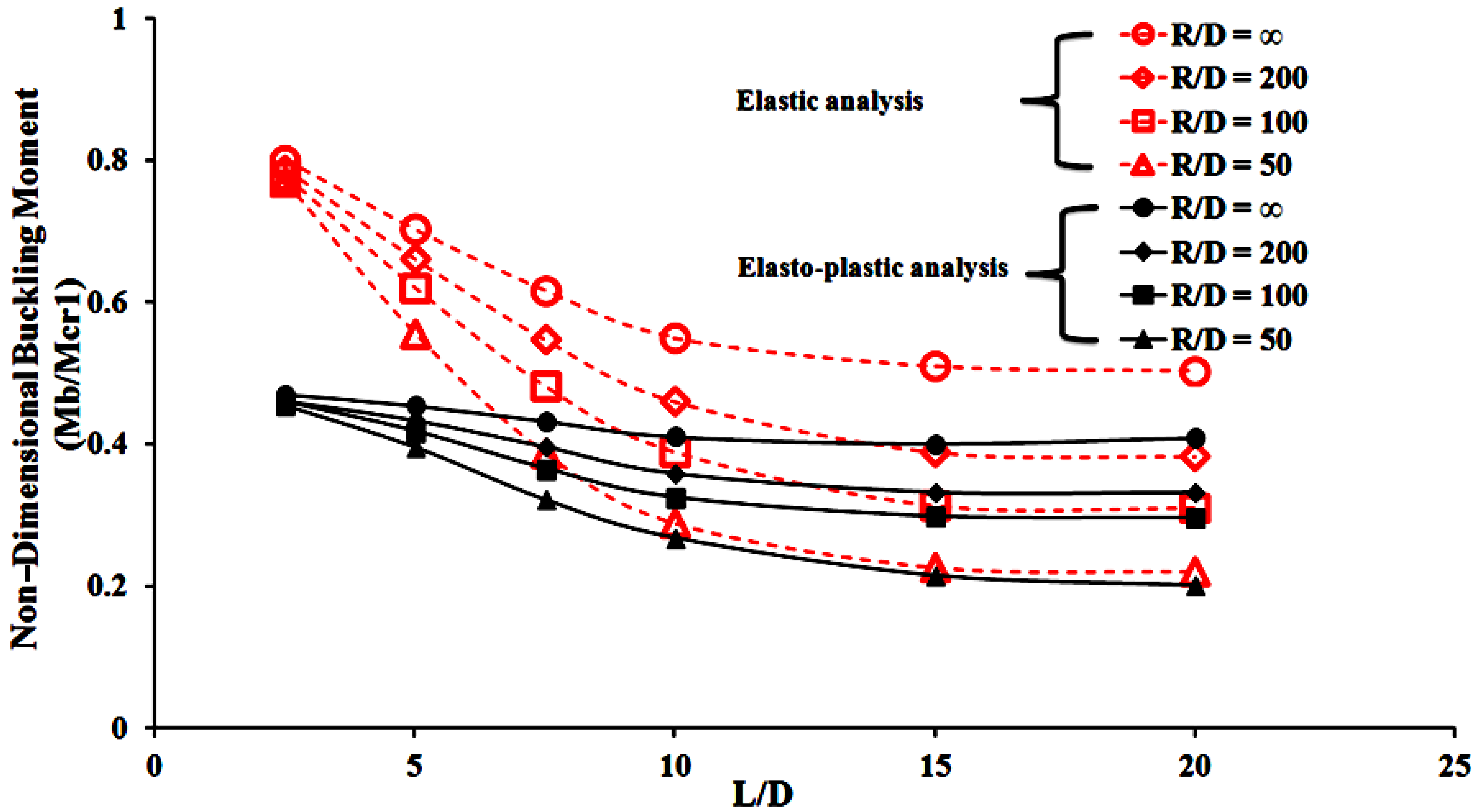

Figure 4-17. Relationship between buckling moment and L/D for curved pipe with imperfection of buckling mode $\delta_o/t = 0.05$

(σ_Y = 621MPa, D/t = 200)

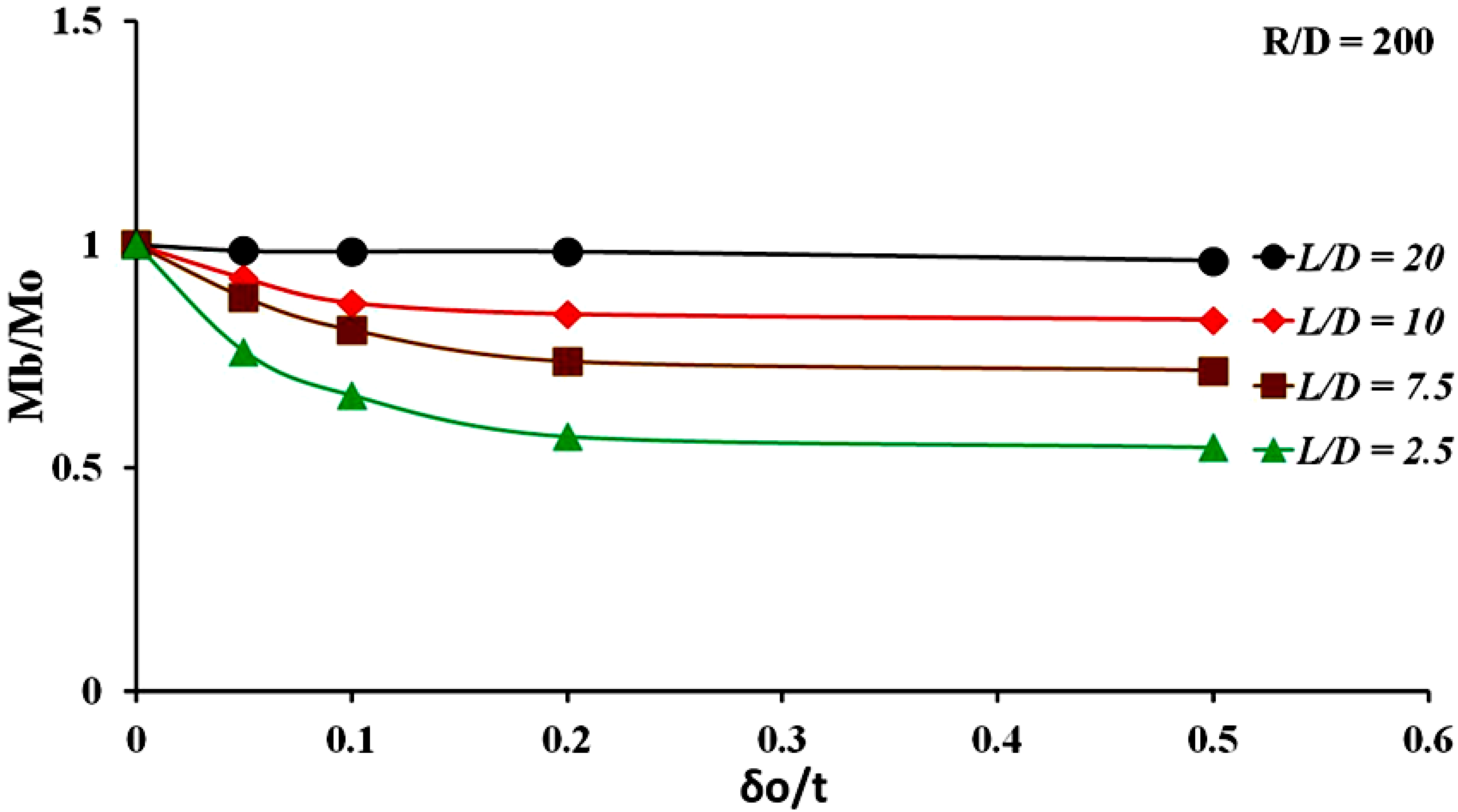

Figure 4-18. Relationship between maximum buckling moment and imperfection of buckling mode for curved pipe

(in elastic analysis, $D/t = 200$, $R/D = 200$)

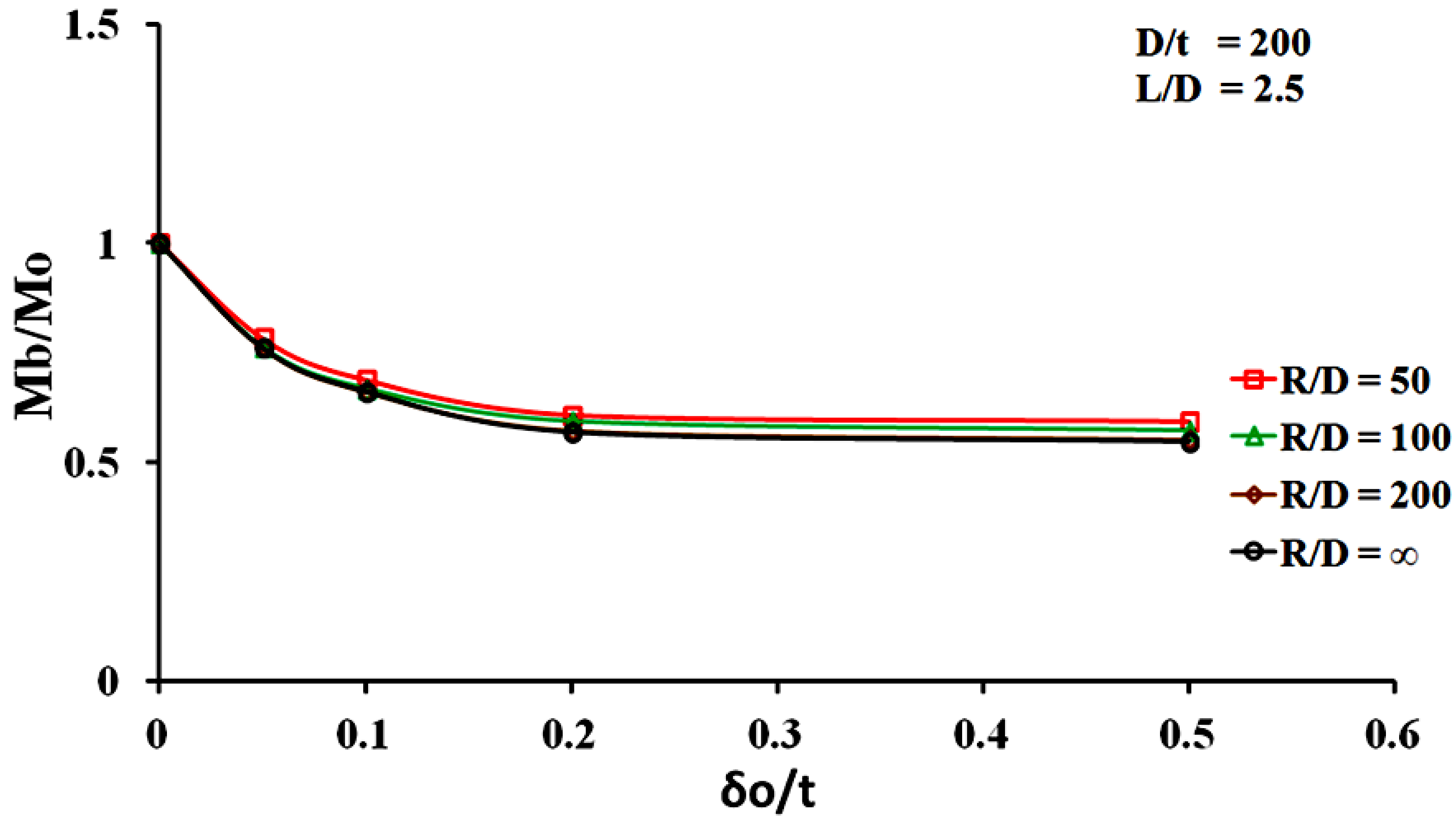

Figure 4-19. Relationship between maximum buckling moment and imperfection of buckling mode for curved pipe
(in elastic analysis, $D/t = 200$ and $L/D = 2.5$)

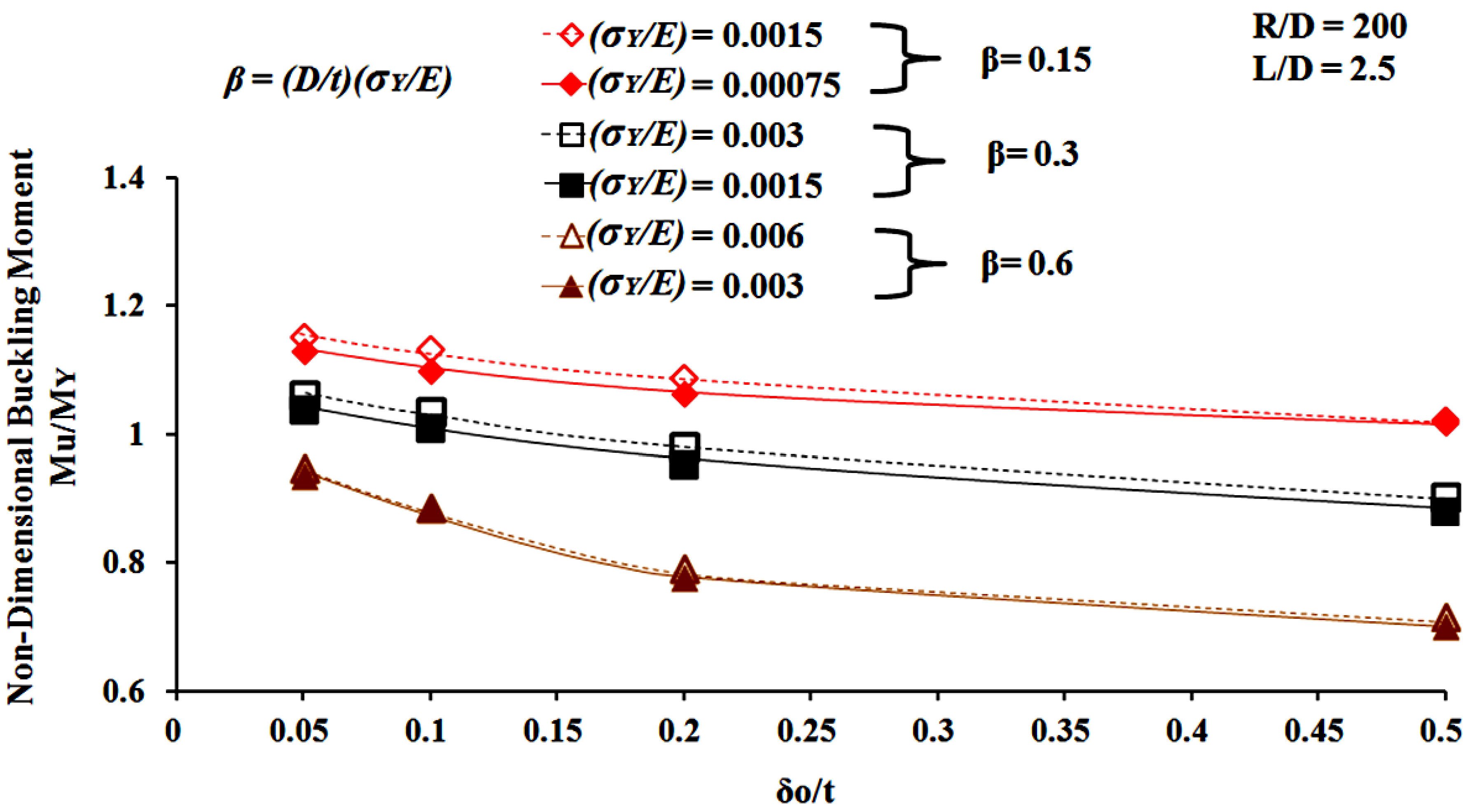

Figure.4-20. Relationship between maximum buckling moment and imperfection for curved pipe (R/D = 200, L/D = 2.5) in elasto-plastic analysis

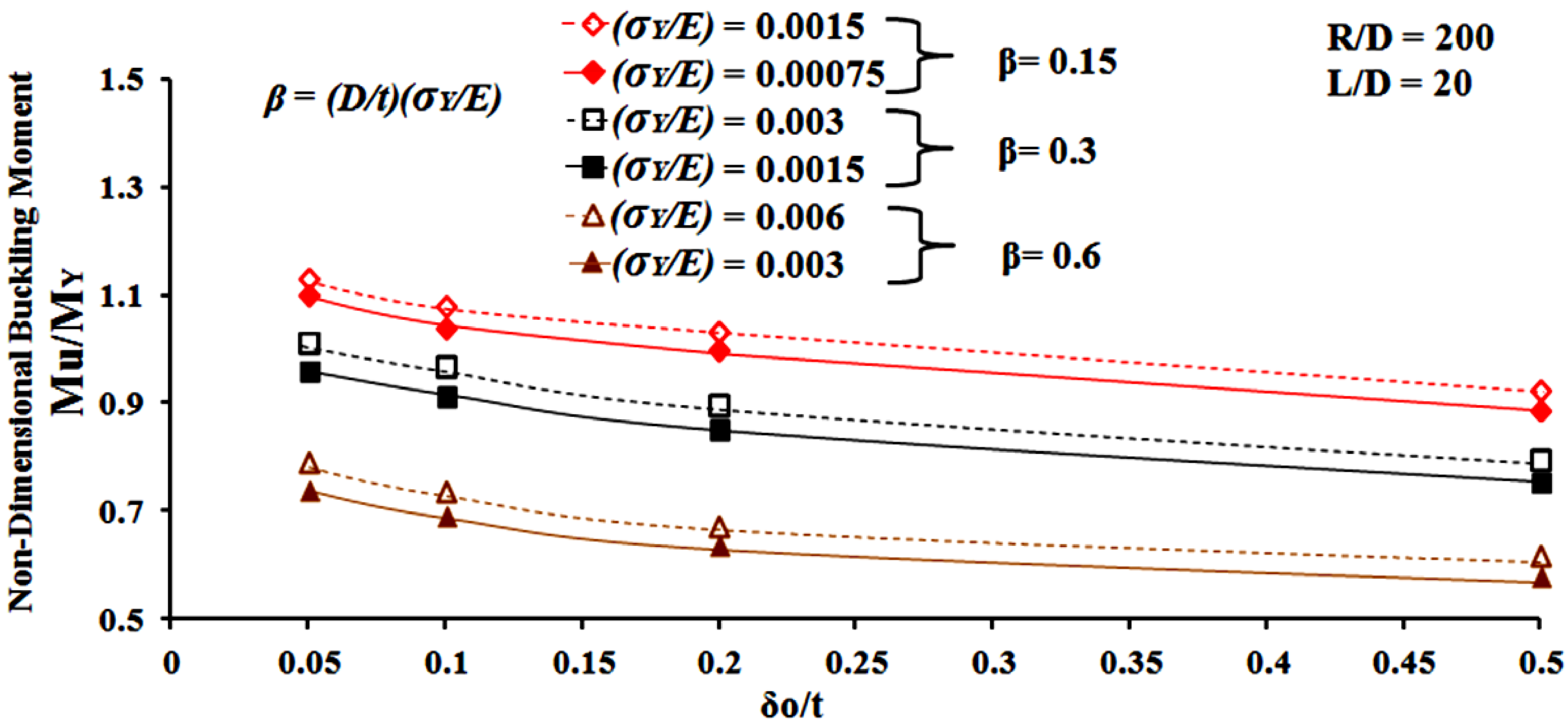

Figure 4-21. Relationship between maximum buckling moment and imperfection for curved pipe (R/*D* = 200, *L/D* = 20) in elasto-plastic analysis

4.5 Conclusions

It is well known that the buckling moment of pipe decreases with increasing imperfection. In this study, the series calculations of buckling and collapse strength of straight and curved pipes with initial imperfection under bending are performed by utilizing nonlinear *FE* software.

The followings are clarified by the numerical calculation.

In elastic analysis for straight pipe, the buckling strength reduced more in longer pipes than in shorter pipes due to pre-buckling oval deformation. However, the reduction of buckling strength due to imperfection is greater in shorter pipes than in longer pipes. This is because the effect of oval deformation on the buckling strength becomes more significant than the effect of imperfection in the case of longer pipe.

The reduction of buckling strength due to imperfection is a little bit greater in the case of larger D/t than in that of smaller D/t. This is because the oval deformation before buckling in the case of smaller D/t is larger than that in cases of larger D/t.

As with the perfect pipe, the buckling moment of the imperfect pipe in elasto-plastic analysis is lower than in elastic analysis. The buckling moment is almost constant regardless of the pipe length for pipes with same value of D/t, because the maximum bending moment is limited by yielding.

The effect of the imperfection of buckling modes on the buckling moment is larger than that of the oval mode. Therefore, buckling strength reduces more due to the imperfection of buckling mode than by that of oval mode.

As well as the perfect pipe, it is possible to see the parameter of $\beta = (D/t)\ (\sigma_Y/E)$ as the parameter which represents the yielding effect on buckling strength of a pipe under bending for the case of the imperfect pipe. When β is large, the pipe buckles elastically. And when β is small, the pipe buckles plastically.

For the curved pipe, the effect of the imperfection on buckling moment is a little bit smaller than for the straight pipe. This is because the oval deformation before buckling in the case of curved pipe is larger than that of the straight pipe. The tendency of the effect of imperfection on buckling strength in the case of curved pipe is almost same as in the case of straight pipe.

Chapter V

Buckling Strength of Pipe under Bending and External Pressure

5.1 Introduction

Offshore pipelines will be subjected to a wide range of loads, such as: bending moment, tension and external pressure. In the previous chapter, the buckling strength of pipe under bending has been investigated, not only for perfect pipe, but also for imperfect pipe. However, a comprehensive study on buckling strength of pipe due to combination loads, bending moment and external pressure has not been found.

In this Chapter, the buckling strength of pipe under the combination of bending moment and external pressure will be investigated by nonlinear *FEA*, considering the effect of a cross sectional oval deformation by changing the variables of pipes, that is *D/t* varying from about 50 to 200 and *L/D* varying from about 2.5 to 40. Moreover the buckling strength of curved pipes *(D/t* = 200*)* have been investigated by changing *R/D* from 50 to 200. Not only elastic buckling but also elasto-plastic buckling will investigated.

In this study, the series of calculations of buckling and collapse strength of straight and curved pipe under bending and external pressure are performed by utilizing nonlinear *FE* software.

5.2 Procedure of Calculation for Estimating Nonlinear Buckling Strength of Pipe under Bending and External Pressure

5.2.1 Parameters for calculation

In the calculation of straight pipe, the ratio of pipe length to diameter *(L/D)* and the ratio of diameter to thickness *(D/t)* are taken as the calculation parameters. *L/D* varies from 2.5 to 40, in which the diameter is changing from 1000 to 4000 mm. And *D/t* varies from 50 to 200. Where, *D* is the pipe diameter, *t* is the wall thickness, and *L* is the pipe length.

In the calculation of a curved pipe, the pipe diameter is originally fixed to 4000 mm and the thickness is fixed to 20 mm. *L/D* varies from 2.5 to 30 by changing the pipe length. *R/D* varies from 50 to 200. Where, *R* is radius of curvature in curved pipe as shown in Figure 3-2.

As well as for pipe under bending, in calculation of the elasto-plastic analysis for pipe under combination of bending moment and external pressure, the yield stress of material assumed to be 621 MPa which is the yield stress of material API X80. The elasto-prefect material is choosed in the numerical analysis. It means strength hardening after yielding has not been considered.

5.2.2 Model for calculation and calculation program

The full length models of straight and curved pipes are used in *FEA.* The nonlinear buckling calculations of pipe under bending and external pressure are performed. General purpose *FE* software MSC Marc is used for nonlinear buckling analysis in which the cross sectional oval deformation before buckling is taken into account.

The quadrilateral 4 node element (No.75) is used. The calculating region is divided into 36 elements in circumferential direction. The element number is basically 120 and more elements are used to maintain the calculation accuracy in the case of the long cylinder. The mesh convergence study had already been carried out in chapter III.

5.2.3 Boundary conditions and loading conditions

The *(X, Y, Z)* coordinates are used. The rigid body elements *(RBE)* are inserted at both end sections in order to connect the centre of the circle and the points on the circle as shown in Figure 5-1. The bending moment is loaded at the centre of the circle at both ends. The Rigid Body Elements *(RBE)* prevent the oval deformation of both ends section, and keep the section in plane under rotational deformation by bending moment. In MSC Marc, a rigid link for either small deformation or large deformation can be implemented by using tying or *RBE*. The external pressures are loaded uniformly at the surface of the pipe as shown in Figure 5-2.

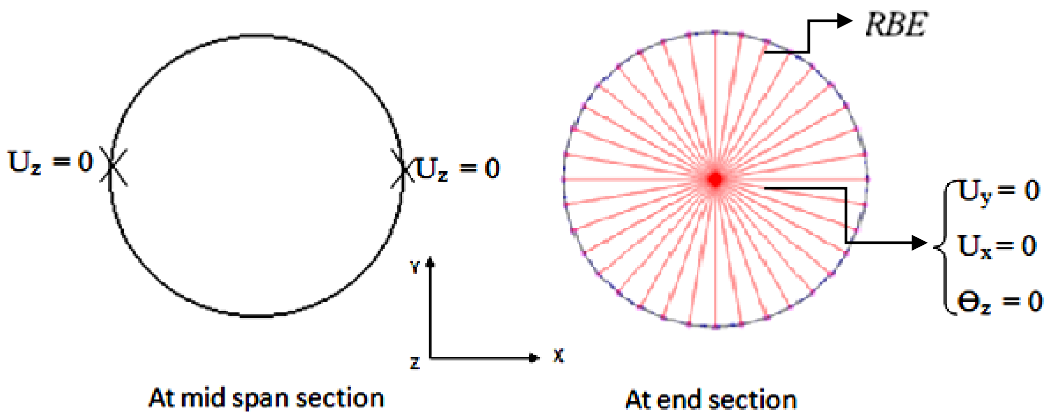

Figure 5-1. Boundary conditions of pipe under combined loading of bending and external pressure

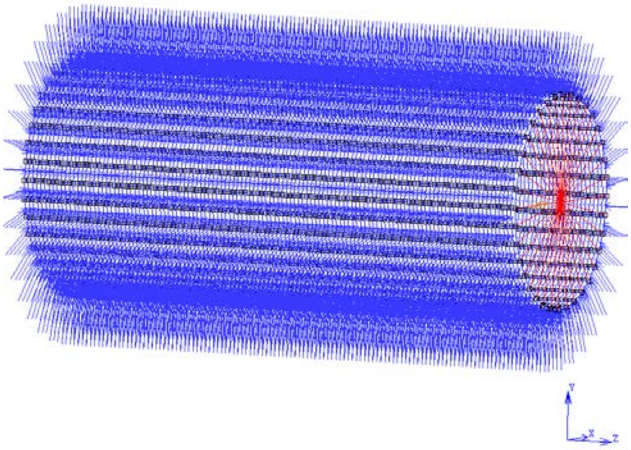

Figure 5-2. The applied load vector of uniform external pressure

5.3 The Numerical Results on Nonlinear Buckling Strength of Straight Pipe under Bending and External Pressure

Figure 5-3 shows the relationships between non-dimensional pressure and length of pipe when the pipe behaves elastically. The vertical axis shows the non-dimensional pressure *(P/Pcr)*, where the critical pressure for the pipe with infinite length is shown in Eq. (5. 1). The horizontal axis is length of pipe.

$$P_{cr} = \frac{E'}{4}\left(\frac{t}{R}\right)^3 \quad (5.\ 1)$$

Where, $E' = \frac{E}{(1-v^2)}$

(As shown in section (1.2.3) for the buckling strength of pipe under external pressure)

As with the straight pipe under bending moment, the buckling strength for a shorter pipe under external pressure is larger than a long pipe. In a short pipe, the effect of the constraint at both ends of pipe is greater than in longer pipes. The buckling strength for the straight pipe subjected to external pressure will be reduced with increasing *L/D* and become constant for the long pipe. The critical pressure will increase when *D/t* decreases.

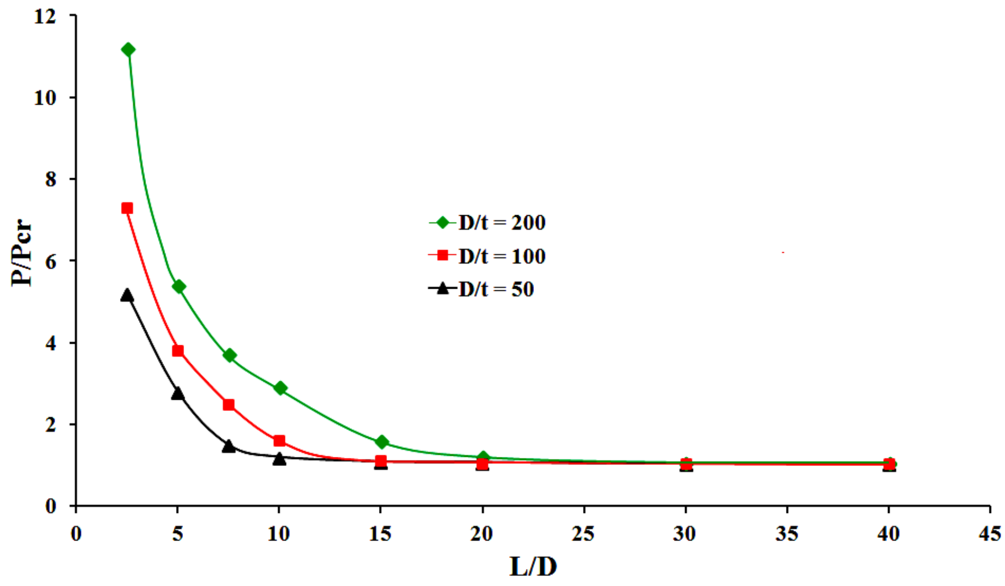

Figure 5-3. Relationship between non-dimensional pressure and *L/D* for straight pipe (*D/t* = 50~200) in elastic analysis.

Figure 5-4 shows the moment - pressure interaction curves of buckling for straight pipes in elastic analysis. The vertical axis shows the non-dimensional pressure *(P/Pcr)*, while the horizontal axis shows the non-dimensional moment *(M/Mcr1)*. Where, M_{cr1} is the critical bending moment of a cylinder under axial compression as shown in Eq (1. 25). The tendency of the interaction curve on buckling strength under combined loading of bending and external pressure is same for every value of *D/t*.

In actual offshore pipelines, a pipe with $D/t \geqq 35$ and $\sigma_Y = 621$MPa will usually be utilized. In those cases, it is confirmed that the buckling of pipe under external pressure occurs in the elastic region.

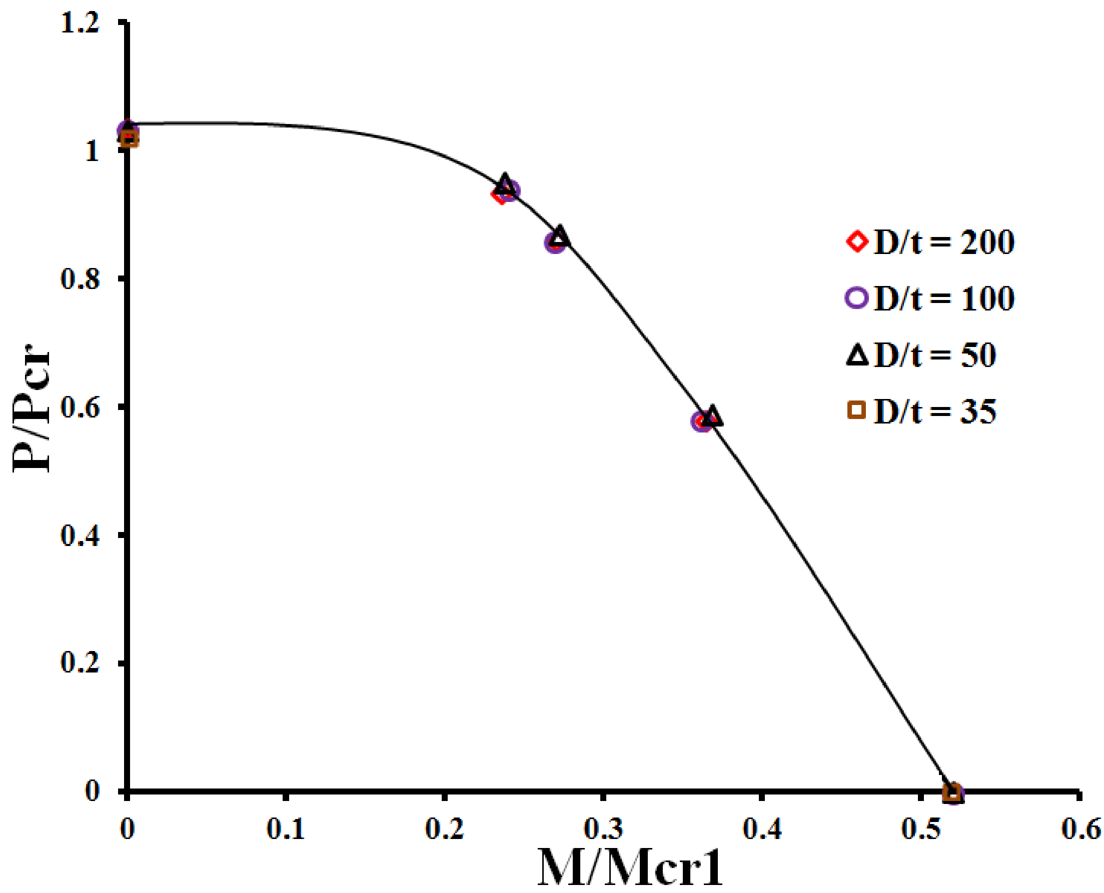

Figure 5-4. Moment - pressure interaction stability for straight pipe in elastic analysis (*L/D* = 30)

Figure 5-5 shows the moment - pressure interaction curves of buckling for straight pipes, considering the yielding effect of material when the yield strength of material is 621 MPa. The dotted curves are numerical result in elasto-plastic analysis. In this figure, the elastic numerical results are also plotted with solid curves. The maximum buckling strength considering yielding effect is smaller than that of elastic calculation especially for the pipe with small value of *D/t.* Therefore, under combined loading of bending and external pressure, pipes with small values of *D/t* will buckle more plastically than those with large *D/t* values

Under the external pressure, the buckling strength obtained by elasto-plastic calculation is same as that obtained by elastic calculation as shown in Figure 5-4 and 5-5. This means that pipes with $D/t \geq 35$ will buckle elastically under the external pressure.

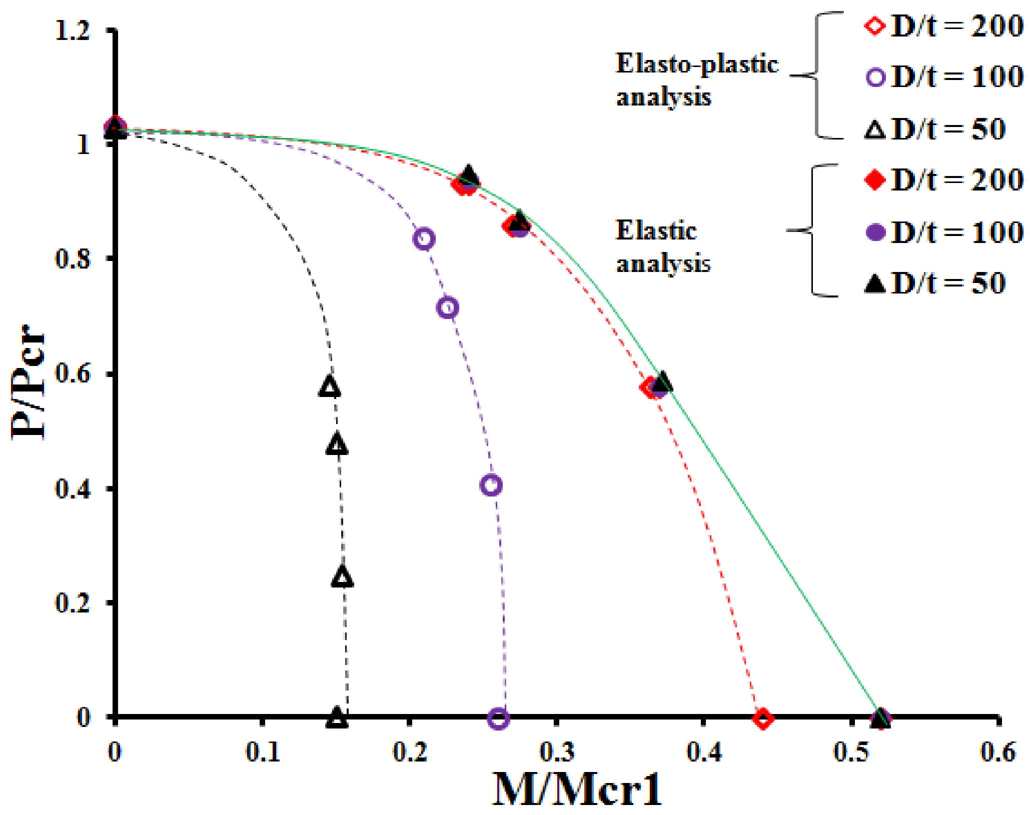

Figure 5-5. Moment - pressure interaction stability for straight pipe in elasto-plastic analysis (*L/D* = 30)

To investigate the yielding effect on the buckling strength of pipe under pure bending and external pressure, the non-dimensional parameter (β) as shown in Eq (5. 2) is considered.

$$\beta = (D/t)(\sigma_Y / E) \tag{5.2}$$

This parameter is proportionate to the ratio of the linear buckling moment to initial yielding moment. If the ratio of the linear buckling pressure to initial yielding pressure, $\alpha = (P_{cr}/P_Y)$ is proportionate to $(D/t)^2(\sigma_Y/E)$. But buckling under external pressure will take place elastically if $D/t \geq 35$. Therefore, the non-dimensional parameter $\beta = (D/t)\ (\sigma_Y/E)$ can be seen as the parameter under the combined loading of bending and pressure. The elasto-plastic buckling strength is examined by changing the yield stress and the diameter.

Figure 5-6 shows the moment - pressure interaction curves of buckling for straight pipes in elasto-plastic analysis. The curves with hollow diamond, hollow circle, and hollow triangle markers are the numerical results by D/t = 200, 100, 50 and σ_Y = 621, where β equals to 0.6, 0.3 and 0.15 respectively. Moreover, the solid diamond marker represents the numerical results for D/t = 100 and σ_Y = 1260, β equals to 0.6. The solid circle and solid triangle makers meanwhile, are the numerical results for D/t = 200 and σ_Y = 315 MPa and 157.5MPa, where β equals to 0.3 and 0.15. When the value of β is large, it means the pipe buckles elastically. And when the value of β is small, the pipe buckles in the elasto-plastic region. The buckling strength of pipe in the elasto-plastic range under the combined loading of bending and pressure can be estimated using the non-dimensional parameter β, because the buckling strength of pipe with different D/t and σ_Y/E and the same β of pipe are same shown in Figure 5-6.

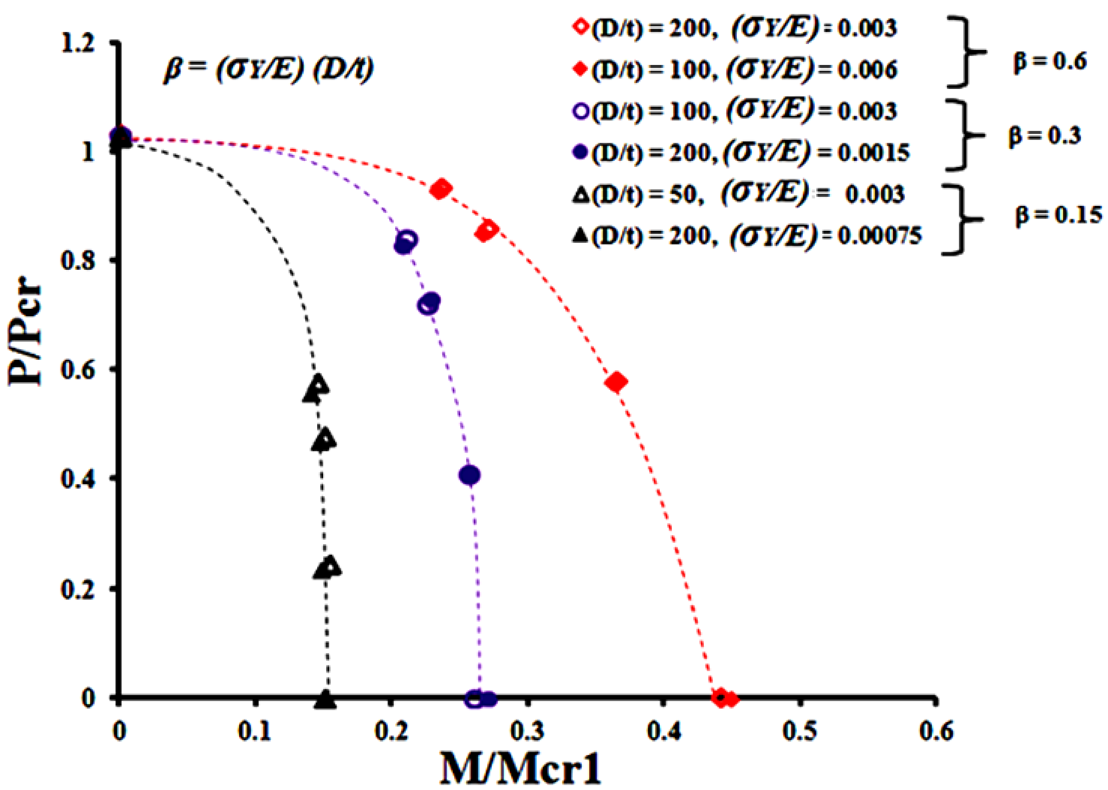

Figure 5-6. Moment - pressure interaction stability for straight pipe in elasto-plastic analysis by using parameter β (L/D = 30)

5.4 The Numerical Results on Nonlinear Buckling Strength of Curved Pipe under Bending and External Pressure

Figure 5-7 shows the relationship between non-dimensional pressure and *L/D* for curved pipe (*D/t* = 200) and *R/D* varying from 50 to 200 by elastic analysis. As well as the straight pipe, the buckling strength of curved pipe will be decreased with increasing *L/D* and become constant on the long pipe. For a curved pipe under external pressure, the effects of constraint at both ends of pipe are large on short pipe. For a curved pipe under external pressure with same *D/t* and different *R/D*, the values of buckling strength are almost same for each same value of *L/D*, or the differences is not large. This is in contrast with a curved pipe under bending as shown in Figure 3-18. The buckling strength of pipe under bending will decrease with decreasing of *R/D* due to the oval deformation at cross section. But, under the external pressure, the oval deformation is not dominant before buckling.

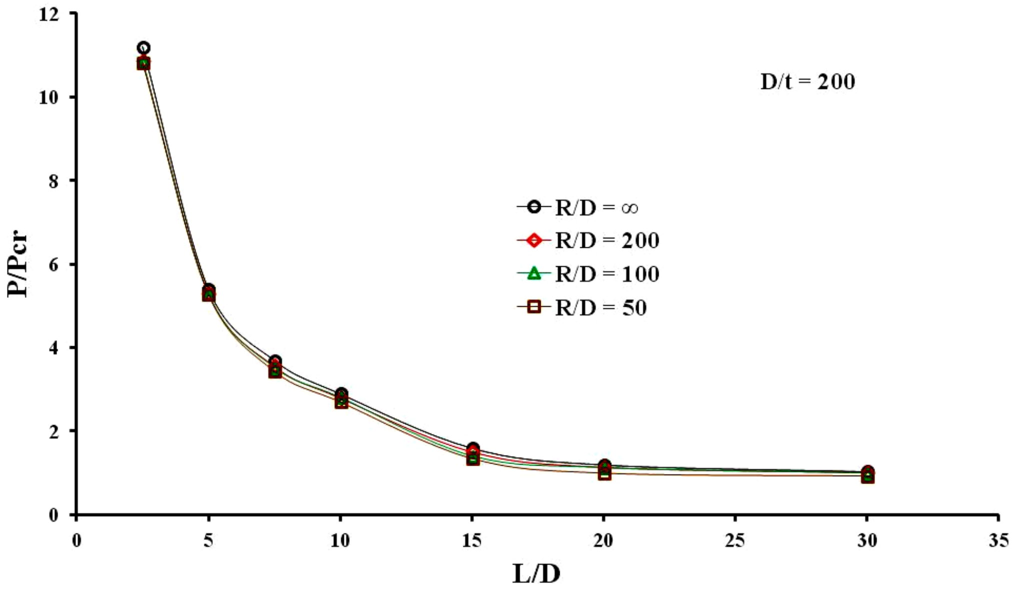

Figure 5-7. Relationship between non-dimensional pressure and *L/D* for curved pipe (*D/t* = 200) in elastic analysis.

Figure 5-8 shows the moment - pressure interaction curves of buckling for curved pipe in elastic analysis. The vertical axis shows the non-dimensional pressure *(P/Pcr)*, while the horizontal axis shows the non-dimensional moment *(M/Mcr1)*. The buckling strength will decrease with decreasing values of *R/D*.

Figure 5-9 shows the moment - pressure interaction stability for curved pipe in elasto-plastic analysis when the yield strength of material is 621 *MPa*. The dotted curves are numerical result in elasto-plastic analysis. In this figure, the elastic numerical results are also plotted with solid curves. The pipes with small values of *R/D* buckle more elastically than those with large values of *R/D*. Therefore, the buckling strength obtained in elato-plastic analysis is almost same as that obtained in elastic analysis for pipes with small *R/D* values. But, the elasto-plastic buckling strength of pipes with large values of *R/D* is smaller than the *elastic* buckling strength because of yielding of the material.

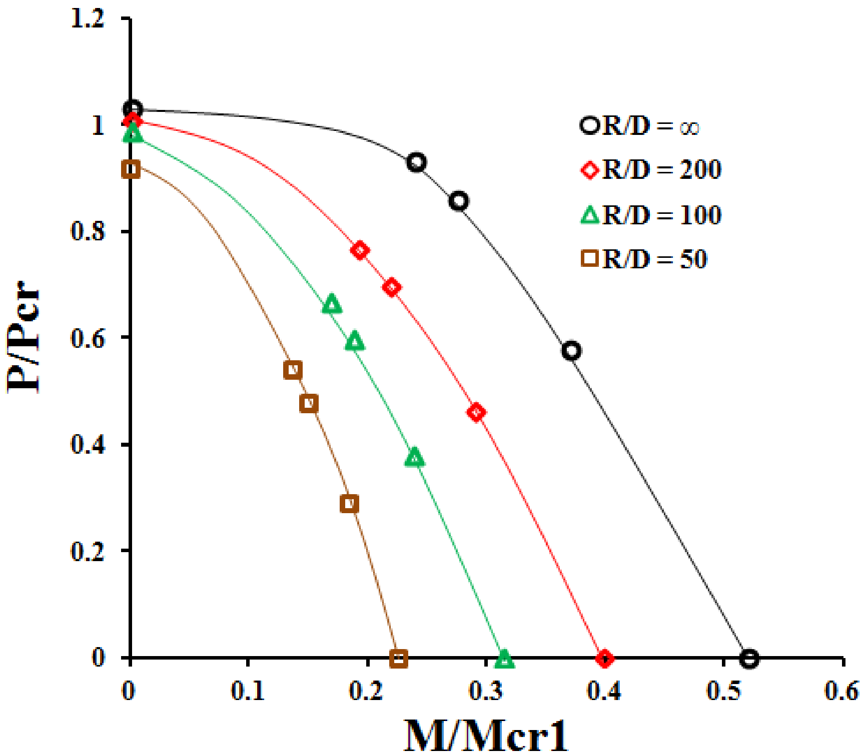

Figure 5-8. Moment - pressure interaction stability for curved pipe in elastic analysis (*L/D* = 30)

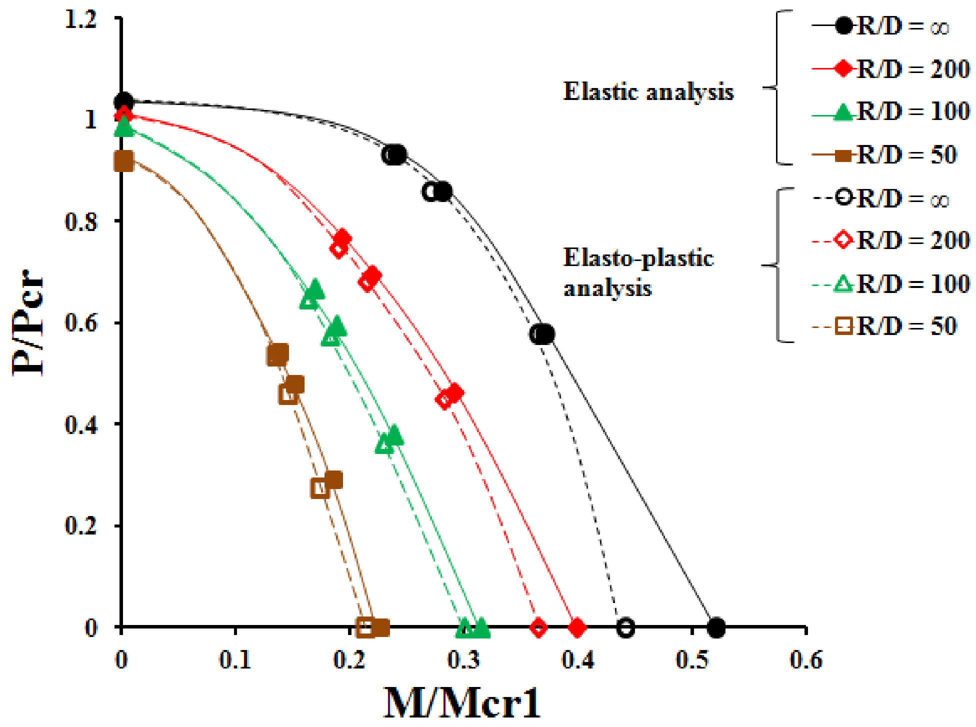

Figure 5-9. Moment - pressure interaction stability for curved pipe in elasto-plastic analysis (L/D = 30)

5.5 Conclusions

In this study, the calculations of buckling and collapse strength of straight and curved pipes under combination loads, that is, bending and external pressure are performed utilizing nonlinear *FE* software.

The following findings are elucidated by the numerical calculations. In elastic analysis, the reductions of buckling strength are due to external pressure by increasing L/D and become constant on the long pipes. The effect of constraint at both ends in the shorter pipes is larger than in the longer pipes.

In elastic analysis, the tendency of the interaction curve on buckling strength for straight pipe under combined loading of bending and external pressure was the same for every value of D/t.

For straight pipes with $D/t \geqq 35$ and $\sigma_Y = 621$MPa under external pressure, the buckling strength occurs in the elastic region. Therefore, although the ratio of linear buckling pressure to initial yielding pressure, $\alpha = (P_{cr}/P_Y)$ is proportionate to $(D/t)^2(\sigma_Y/E)$, the non-dimensional parameter (β) ,which is proportionate to $(D/t)(\sigma_Y/E)$ is considered to investigate the yielding effect on the buckling strength of pipe under combined loading of bending and external pressure as well as under bending. Using the non-dimensional parameter β, the buckling strength of pipe in elasto-plastic range under the combined loading of bending and pressure can be estimated.

For a curved pipe under external pressure with the same *D/t* and different *R/D*, the values of buckling strength were almost same for each same value of *L/D*. This is in contrast to a curved pipe under bending. This is because the buckling strength of pipe under bending will decrease with decreasing *R/D* values due to the oval deformation at cross section. But, under the external pressure, the oval deformation is not dominant before buckling.

The pipe with small values of *R/D* buckles more elastically than the pipe with large values of *R/D*. Therefore, the buckling strength obtained in elasto-plastic analysis is almost the same as that obtained in elastic analysis for the pipe with small *R/D*. But, the elasto-plastic buckling strength of pipes with large values of *R/D* is smaller than the elastic buckling strength because of yielding of material.

Chapter VI

Conclusions

6.1 Summary

Offshore pipelines are needed to transport oil or gas from subsea wells to production facility platforms, and then transporting oil or gas from production facility platforms to shore. Buckling and collapse are the important failure modes not only for the laying condition, but also in operating condition. The pipeline will be subjected to a wide range of loads, such as bending moment, tension and external pressure. Thus, it is required to analyse the buckling strength of pipe under various kinds of loads.

In this dissertation, the buckling strength of pipes under pure bending and under combined loading, that is, bending and external pressure, was examined.

In Chapter I, the purpose of this research was explained and the previous researches for the buckling strength of pipe under bending moments were reviewed.

In Chapter II, the linear buckling strength for pipe under bending was investigated by linear *FEA*. The eigenvalue calculations under bending load was performed for various length, radiuses and thicknesses of pipe. The linear bucking strength was compared with the previously proposed formula which was derived from the buckling strength of pipe under axial compression. From the numerical results, the critical bending moment M_{cr2} in linear calculation can be expressed as follows. It is shown that the linear buckling moment M_{cr2} is approximately 1.1 times M_{cr1}, where M_{cr1} is the critical bending moment when the critical buckling stress of a cylinder under bending is same as the buckling stress of a cylinder under axial compression.

In actual pipe, the oval deformation of cross section takes place before buckling, and the buckling moment is reduced due to this deformation. Therefore, the linear buckling moment does not present the exact strength of pipe under bending. But, it can be the rough standard of the buckling moment of pipe. In the following chapter, the exact buckling moments are examined by considering the pre-buckling oval deformation, and are compared with the linear buckling moment M_{cr2} or the buckling moment M_{cr1} to clarify the effect of pre-buckling oval deformation on the buckling moments.

In Chapter III, the parametric calculations of buckling and collapse strength of straight and curved pipe under bending were performed by utilizing non-linear *FE* software. The followings were clarified by the numerical calculations.

The region of buckling is limited at the compressive side in the vicinity of mid span because the magnitude of oval deformation is large at mid span.

In a short pipe, the oval deformation before buckling is small due to the restriction of sectional deformation at both ends. Therefore, the reduction of buckling strength due to oval deformation is smaller in shorter pipes than longer pipes.

For enough long pipes, the maximum moment converges to one value. In elastic analysis, the maximum moment for long pipes, considering oval deformation can be represented as follows:

$$M_{\max} = 0.52 M_{cr1} = 0.314 \pi E r t^2$$

In elato-plastic analysis, the buckling moment is almost constant regardless of the pipe length, because the maximum bending moment is limited by yielding if the pipes have the same value of *D/t*.

The non-dimensional parameter β, which is proportion to (M_{cr}/M_Y) is proposed. The parameter of $\beta = (D/t)\ (\sigma_Y/E)$ is possible to be the parameter which represents the yielding effect on buckling strength of pipe under bending. When β is small, the pipe buckles plastically. Using Figure 3-13~3-20 and this parameter, the buckling moment can be predicted without *FEA*.

In the case of the curved pipe, the buckling moment is smaller than the straight pipe, because the oval deformation is larger than straight pipe. The oval deformation increases when *R/D* decreases. This is because that the axial stresses in bending have larger component of vertical direction in the pipe with smaller *R/D* than the pipe with larger *R/D*.

In Chapter IV, the parametric calculations of buckling and collapse strength of straight and curved pipes with initial imperfection under bending were performed by utilizing nonlinear *FE* software. The followings were clarified by the numerical calculation.

The buckling strength reduces more by the imperfection of the buckling mode than the oval mode. The reduction of buckling strength due to imperfection is larger in shorter pipes than in longer pipes. It is because the effect of oval deformation on the buckling strength becomes larger than the effect of imperfection in the case of longer pipe. The buckling moment decreases with increasing imperfection, and the buckling moment becomes constant when the large imperfection exists.

The effect of imperfection on buckling moment in plastic range is smaller than in elastic range. As well as the perfect pipe, the parameter of $\beta = (D/t)\ (\sigma_Y/E)$ is possible to be the parameter which represents the yielding effect on buckling strength of pipe under bending for the case of imperfect pipe.

The tendency of the effect of imperfection on buckling strength in the case of curved pipe is almost same as that in the case of straight pipe.

In Chapter V, the calculations of buckling and collapse strength of straight and curved pipes under combination load, that is, bending and external pressure were performed by utilizing nonlinear *FE* software. The followings were clarified by the numerical calculation.

The interaction curve on buckling strength for straight pipe and curved pipe under combined loading of bending and external pressure was shown.

For straight pipe with *D/t* $\geqq$ 35 and σ_Y = 621MPa under external pressure, the buckling strength occurs on elastic region. Therefore, although the ratio of linear buckling pressure to initial yielding pressure $\alpha = (P_{cr}/P_Y)$ is proportion to $(D/t)^2(\sigma_Y/E)$, the non-dimensional parameter $\beta=(M_{cr}/M_Y)$, which is proportion to $(D/t)(\sigma_Y/E)$, can be the parameter which represents the yielding effect on the buckling strength of pipe under combined loading of bending and external pressure. Using the non-dimensional parameter β, the buckling strength of pipe in elasto-plastic range can be estimated.

For a curved pipe with same value of *D/t*, the buckling strength under combined loading decreases with decreasing *R/D*. This result is same as under bending.

It is expected that the designers can estimate the buckling strength of straight and curved pipe under bending and the combined loading of bending and external pressure, not only in elastic range but also in elasto-plastic range, without *FEA* utilizing the results shown in this paper.

6.2 Recommendation for Future Work

Buckling and collapse of offshore pipelines could be occurring due to the influence of combination loads. In this dissertation, the buckling strength of pipe under combination load bending and external pressure has been investigated; not only for perfect pipes, but also for pipes with initial imperfections.

In the long period of operation, the pipe is vulnerable to attack by internal and external corrosion. If a water pipeline was to leak, it could be a problem but it usually would not harm the environment to any great extent. However, if a petroleum or gas pipeline leaks, it can be an environmental disaster of great proportion. Furthermore, effect of corrosion on buckling strength could be considered. When pipes suffer corrosion, certainly, it would reduce pipe thickness. Therefore, it is clear that investigation is needed as to how great the effect of corrosion on the buckling strength of pipes might be.

In addition, the pipe connection system that is commonly used with welded joints or flanges needs to be reviewed. The buckling strength of pipe will be influenced by the condition of the pipe joints, especially in connections made by welding. Therefore, it needs to investigate the effect of welded pipe in terms of its buckling strength.

And also, in the case of pipelines on the seabed, the effects of the elastic support of sea bottom soil, the force from stream of sea, enforced displacement by the shape of sea bed can be considered for further research.

References

Axelrad, E. (1978). Flexible shell-theory and buckling of toroidal shells and tubes. *Ingenieur-Archiv* 47, pp. 95—104.

Axelrad, E. (1987). *Theory of Flexible Shells.* Amsterdam: North-Holland.

Baker, E.H., et al. (1968). *Shell Analysis Manual*. NASA CR-912, Apr.

Bantlin, A. (1910). Formänderung und beanspruchung federnder ausgleichrohre. *VDI-Z.*54. pp. 43-49.

Boyle, J.T. (1981). The finite bending of curved pipe. *Int. J. Of Solids and Structures* Vol. 17, pp. 515 – 529.

Boussaa, Dj., Van, K.D, Labbe, P & Tang, H.T. (1996). Finite pure bending of curved pipes. *J. Computer & structures,* Vol 60, No 6, pp. 1003-1012.

Brazier, L.G. (1927). On the flexure of thin cylindrical shells and other thin sections. *Proc. Royal. Society*. Series. A 116, pp. 104–114.

Chen, W.F., Sohal, I.*S.* (1988). Cylindrical members in offshore structure. *Thin-Walled Structures,* Volume 6, Issue 3, pp.153-285.

Chwalla, V.E. (1933). Reine Biegung Schlanker, Dünnwandiger Rohre Mit Gerader Achse. *Zeitschrift für Angewandte Mathematik und Mechanik* , Band 13, Heft 1.

Corona, E., Kyriakides, S. (1988). On the collapse of inelastic tubes under combined bending and pressure. *Int, J. of Solids and Structures***,** Vol 24, No 5, pp 505 – 535.

Donnell, L.H. (1934). A new theory for the buckling of thin cylinders under axial compression and bending. *Trans. ASME,* Vol. 56, pp. 795 – 806.

Donnell, L. H. (1976). *Beams, Plates and Shells.* McGraw-Hill, NewYork.

Fabian, O. (1977). Collapse of cylindrical, elastic tubes under combined bending, pressure and axial loads. *Int. J. Solid Structures*, Vol. 13, pp. 1257-1270.

Flügge, W. (1960). Stress in shells. *Springer-Verlag, OHG., Berlin*, pp. 208-218,407-432.

Fung, Y.C., Sechler, E.E. (1957). Buckling of thin walled circular cylinders under axial compression and internal pressure. *J. Aeronaut. Sci,* Vol. 24, pp. 351 – 356.

Gellin, S. (1980). The plastic buckling of long cylinder shells under pure bending. *Int. J. Solids Struct,* Vol. 16, pp. 397 – 407.

Gerard, G., Becker, H. (1957). *Handbook of Structural Stability: Part 3. Buckling of Curved Plate and Shells.* NACA Tech. Note No. 3783, Aug.

Gerard, G. (1957). Plastic stability theory of thin shells. *J. Aeronaut. Sci,* Vol. 24, No.4, p.269.

Ghazijahani, T.G., Showkati, H. (2013). Experiments on cylindrical shells under pure bending and external pressure. *J. of Constructional Steel Research,* 88, pp. 109–12.

Guo, B.,Song, S., Chacko, J., & Ghalambor, A. (2005). *Offshore Pipelines.* Elsevier Inc.

Hartono Yudo,. Yoshikawa, T. (2012). Mechanical behaviour of pipe under pure bending load. *Proceedings of the 26th Asian Technical Exchange and Advisory Meeting on Marine Structures,* JAPAN, TEAM, pp. 359 -364.

Hartono Yudo,. Yoshikawa, T. (2014). Buckling phenomenon for straight and curved pipe under pure bending. *J. of Marine Sci and Tech,* DOI: 10.1007/s00773-014-0254-5.

Houliara, S., Karamanos, S. A. (2006). Buckling and post-buckling of long pressurized elastic thin-walled tubes under in-plane bending. *Int. J.of Non-Linear Mechanics* 41, pp. 491 – 511.

Hauch, S., Bai, Y. (1999). Bending moment capacity of pipe. *Offshore Mechanical and Arctic Engineering,* PL-99 – 5033.

Hunt, G. W., Lord, G. J., & Champneys, A. R. (1999). Homoclinic and heteroclinic orbits underlying the post-buckling of axially-compressed cylindrical shells. *J. Comput. Meth. Appl. Mech. Eng.* 170,239–251 (doi:10.1016/S0045-7825(98)00197-2).

Igland, R.T., Moan, T (2000). Reliability analysis of pipelines during laying, considering ultimate strength under combined loads. *J. of Offshore Mechanics and Arctic Engineering.* Vol 122, pp. 40-46.

Jialing, Y., Reid, S.R. (1997). Approximate estimation of hardening-softening behaviour of circular pipes subjected to pure bending. *The Chinese Society of Theoretical and Applied Mechanics, Chinese Journal of Mechanics Press, Beijing,* China .Vol.13, No.3.

Ju, G.T., Kyriakides, S. (1992). Bifurcation and localization instabilities in cylindrical shells under bending, part II predictions. *Int. J. Solids Struct,* Vol. 29, pp. 1143–117.

Khurram, W. M., Ahmer, W. M,. Andrew, P. B, & Andreas, A. A. (2005). Longitudinally inhomogeneous deformation patterns in isotropic tubes under pure bending. *Proc. R. Soc. A* 2006 462, 817- 838. (doi : 10.1098/rspa.2005.1596).

Kyriakides, S., Corona, E. (2007). *Mechanics of Offshore Pipelines. Volume 1. Buckling and Collapse***,** Elsevier.

Levyakov, S.V. (2013). Evaluation of Reissner's equations of finite pure bending of curved elastic tubes. *J. of Applied Mechanics*. Vol 81.

Lo, H., Crate, H., & Schwartz, E.B. (1951). *Buckling of Thin Walled Cylinders Under Axial Compression and Internal Pressure*. NASA Rep. No. 1027(formerly 2021).

Mina, K. (2012). Installation of steel pipelines and flexible pipelines in sideway current, Master's Thesis, University of Stavanger, Norway.

Mungan, I. (1974). Buckling Stress States of Cylindrical Shells. *ASCE Struct. Div*, Vol 100, No. ST11, pp. 2289-2306.

Odland, J. (1978). *Buckling Resistance of Unstiffened and Stiffened Circular Cylindrical Shell Structures.* Norweigian Maritime Research, Vol. 6, No.3.

Reddy, B.D. (1979). An experimental study of the plastic buckling of circular cylindrical shells in pure bending. *Int. J. Solids Struct*. 15, pp. 669-683.

Reissner, E. (1949). On the bending of curved thin-walled tubes. *Proc. National Acad. Sci*. (U.S.) 35, pp. 204-208.

Reissner, E. (1981). On finite pure bending of curved tubes. *Int. J. Solids Struct*, 17(9), pp. 839–844.

Seide, P., Weingarten, V. I. (1961). On the buckling of circular cylindrical shells under pure bending. *Transaction. ASME, J. Appl. Mech.* Vol.28, pp. 112–116.

Southwell, R. V. (1913). On the general theory of elastic stability", *Philosophical Trans,* 213A, pp. 187-244.

SUPERB. (1996). *Buckling and Collapse Limit State.* December 1996.

Timoshenko, S., Gere, J. (1961). *Theory of Elastic Stability*, 2nd Edition, McGraw-Hill International Book Company.

Timoshenko, S., Woinowsky, S., & Krieger. (1959). *Theory of Plates and Shells,* 2nd Edition, McGraw-Hill International Book Company.

Tokugawa, T. (1929). Model experiments on the elastic stability of closed and cross-stiffened circular cylinders under uniform external pressure. *Proc. of the World Engineering Congress, Tokyo,* No.651, pp. 249-79.

Von Mises, R. (1914). Der kritische Aubendruck zylindrischer Rohre (The critical external pressure of cylindrical tubes). *VDI-Zeitschrift,* Vol. 58, pp. 750–755.

Website: http:// www.lib.utexas.edu/maps/indonesia.html. Accessed date 14/7/2014.

Website: http://www.offshore-technology.com/projects/natuna/. Accessed date 14/7/2014.

Website: http://file.scirp.org/Html/9-2000136_23279.htm.Accessed date 14/7/2014.

Zhang, L.C., Yu, T.X. (1987). An investigation of the Brazier effect of a cylindrical tube under pure elastic-plastic bending. *Int. J. Pres. Ves. & Piping*, Vol.30, pp. 77-86.